UCSF
UC San Francisco Electronic Theses and Dissertations

Title
Bending, structural and thermal characterization of NiTi ortodontic wires

Permalink
https://escholarship.org/uc/item/9m65d62f

Author
Quo, Stacey Dagmar

Publication Date
1994

Peer reviewed|Thesis/dissertation

eScholarship.org Powered by the California Digital Library
University of California

Bending, Structural and Thermal Characterization of NiTi Orthodontic Wires

by

Stacey Dagmar Quo, DDS

THESIS

Submitted in partial satisfaction of the requirements for the degree of

MASTER OF SCIENCE

in

Oral Biology

in the

GRADUATE DIVISION

of the

UNIVERSITY OF CALIFORNIA

San Francisco

Bending, Structural and Thermal Characterization of NiTi Orthodontic Wires

Stacey D. Quo, DDS

in partial fulfillment of the requirements for a
Master of Science Degree in Oral Biology
University of California, San Francisco

Committee Members:
Sally J. Marshall, Ph.D.
Grayson W. Marshall, D.D.S., M.P.H., Ph.D.
Alan R. Pelton, Ph.D.
Sheldon Baumrind, D.D.S., M.S.

Table of Contents

Acknowledgements iii

List of Figures iv

List of Tables vi

ABSTRACT 1

1. STATEMENT OF THE PROBLEM 2

2. SPECIFIC AIMS 4

3. BACKGROUND 5

3.1. Martensitic Transformation 5

3.2. Formation Mechanisms 7

3.2.1. *Shape Memory* 10
3.2.2. *Superelasticity* 11

3.3. R-Phase 12

3.4. Metallurgy 14
3.4.1. *Chemical Composition* 14
3.4.2. *Transformation Temperatures* 16
3.4.3. *Phase Description* 17
3.4.4. *Microstructure* 18

3.5. Mechanical Properties 19

3.6. Processing Conditions 20

3.7. Experimental Design 21

3.8. Experimental Techniques for Structural Characterization 24

3.8.1. *Scanning Electron Microscopy* 24
3.8.2. *Energy Dispersive X-ray Spectroscopy* 24
3.8.3. *X-ray Diffraction* 25

4. MATERIALS & METHODS 26

4.1. Annealing Conditions 27

4.2. Deformation Bending 27

4.3. Determination of Chemical Composition of As received NiTi archwires. 28

4.4. Determination of Transformation Temperatures 29

4.5. Characterization of Mechanical Behavior 31

4.6. Characterization of Microstructural Changes during Phase Transformation 33

4.7. X-ray Diffraction and Phase Identification 35

4.7.1. *Specimen Preparation* 35
4.7.2. *Data Analysis* 37

5. RESULTS **38**
5.1. Chemical Composition 38
5.2. Transformation Temperatures 39
5.3. Mechanical Properties 43
5.4. Microstructural Analysis 52
5.5. X-ray Diffraction 59

6. DISCUSSION **73**
6.1. Wire Characterization 73
6.2. Extent of Transformation 78
6.3. Variability 82
6.4. Clinical Applications 86

7. SUMMARY **90**

8. FUTURE STUDIES **92**

9. REFERENCES **93**

Acknowledgements

This work is the culmination of the efforts of many. My committee has been instrumental in the success of this project. My advisors and mentors, Drs. Bill and Sally Marshall, have generously allowed me to pursue this project, and have been my database of knowledge. Dr. Alan Pelton from Nitinol Devices and Components, has fostered this project for me through his generosity in instruction and guidance. I am grateful for his interest and teachings.

The assistance and technical support of Andreas Wick and Larry Watanabe cannot be acknowledged enough times. I also want to acknowledge Nitinol Devices and Components for allowing the use of their facilities to execute the material testing, and the Ormco Corp., Unitek Corp. and Reliance Products for their donation of materials.

Much gratitude to Dr. Faro Farz-nia, Ormco Corp., for the many enlightening discussions and reference materials. My conversations with Dr. Farz-nia helped shape the initial direction of this project. There are several others that deserve recognition from whose discussions have also been helpful : Drs. Sheldon Baumrind, Charles Burstone, Keith Melton, Shuichi Miyazaki, Fujio Muira and Rohit Sachdeva.

As always, endless gratitude and dedication to my mother and father. Special recognition to my father who has spent countless hours in conversation and instruction with me in the fundamentals of mechanics of materials.

List of Figures

Figure #	*Title*	*Page*
Figure 3.1	Relationship of Property Change and Phase Content to Temperature.	7
Figure 3.2	Stress Strain Profile of the Shape Memory Effect.	10
Figure 3.3	Stress Strain Profile of the Superelastic Effect.	11
Figure 3.4	Relation of Transformation Temperature and Nickel Content.	15
Figure 3.5	Illustration of Orthodontic Application to correct malaligned tooth positions in 1st and 2nd order activations.	22
Figure 3.6	Deformation Mode in Bending.	23
Figure 4.1	Bend Configuration for Microstructure and Diffraction Examination.	27
Figure 4.2	Af Test Temperature Assembly.	30
Figure 4.3	Calculation of Af temperatures.	30
Figure 4.4	Diagrammatic Flowchart of Mechanical Testing Assembly.	31
Figure 4.5	Parameters of the 3-point Bend Test.	32
Figure 4.6	Illustration of Wire Orientation in Diffraction Specimen Holder.	36
Figure 4.7	Assembly for Temperature Controlled XRD Testing.	37
Figure 5.1	Relative at% Ni determination along the length of the Sentalloy SE wire.	38
Figure 5.2	Relative at% Ni determination along the length of the Nitinol SE wire.	39
Figure 5.3	Strain as a Function of Temperature for wires with a definite Af.	40
Figure 5.4	Strain as a Function of Temperature for wires showing R-phase interaction.	40
Figure 5.5	Relation of Transformation Temperature and Nickel Content as determined from the annealed wires.	41
Figure 5.6	Comparison of Load Deflection Properties of As-received wires, tested at 22°C.	45
Figure 5.7	Comparison of Load Deflection Properties of As-received wires, tested at 37°C.	46
Figure 5.8	Comparison of Load Deflection Properties of Annealed Wires.	47

UCSF LIBRARY

Figure 5.9	Load Deflection Properties of Sentalloy (SE).	48
Figure 5.10	Load Deflection Properties of Neosentalloy (SM).	49
Figure 5.11	Load Deflection Properties of Nitinol SE.	50
Figure 5.12	Load Deflection Properties of Nitinol (SM).	51
Figure 5.13	Micrographs of Sentalloy (SE) under deformation.	55
Figure 5.14	Micrographs of Neosentalloy (SM) under deformation.	56
Figure 5.15	Micrographs of Nitinol SE under deformation.	57
Figure 5.16	Micrographs of Nitinol (SM) under deformation.	58
Figure 5.17	Integrated Intensity of (110) peak vs. Deformation (Bend Angle) Nitinol SE.	61
Figure 5.18	Integrated Intensity of (110) peak vs. Deformation (Bend Angle) Neosentalloy (SM).	61
Figure 5.19	Integrated Intensity of (110) peak of the Undeformed Annealed and As-received wires at 42.1 - 42.4° 2θ.	62
Figure 5.20	FWHM as a function of the amount of deformation in the as-received wires tested at 37°C.	64
Figure 5.21	FWHM as a function of the amount of deformation in the annealed specimens.	64
Figure 5.22	XRD of Sentalloy (SE) As-received wires under deformation.	65
Figure 5.23	XRD of Sentalloy (SE) Annealed wires under deformation.	66
Figure 5.24	XRD of Neosentalloy (SM) As-received wires under deformation.	67
Figure 5.25	XRD of Neosentalloy (SM) Annealed wires under deformation.	68
Figure 5.26	XRD of Nitinol SE As-received wires under deformation.	69
Figure 5.27	XRD of Nitinol SE Annealed wires under deformation.	70
Figure 5.28	XRD of Nitinol (SM) As-received wires under deformation.	71
Figure 5.29	XRD of Nitinol (SM) Annealed wires under deformation.	72
Figure 6.1	Mechanical Performance for Suggested Use.	88

UCSF LIBRARY

List of Tables

Table #	*Title*	*Page*
Table 3.1	Property Changes Associated with the Shape Memory Transformation.	17
Table 4.1	NiTi Orthodontic Archwires.	26
Table 4.2	Etching Times.	34
Table 5.1	Summary of Chemical Composition, Transformation Temperature and Mechanical Properties.	42

UCSF LIBRARY

Bending, Structural and Thermal Characterization of NiTi Orthodontic Wires

ABSTRACT

This study provided a quantitative and qualitative characterization of superelastic and shape memory NiTi orthodontic arch wires. Superelasticity and shape memory result from the martensitic transformation in nickel-titanium. Orthodontic applications utilize the force delivery from the phase transformation to straighten malaligned teeth. The extent of the transformation as a function of deformation was evaluated. Variability in mechanical performance between superelastic and shape memory wires was also assessed. Differences between commercially available supplies of NiTi wires may lie in the material composition and/or the production method.[1-6] To understand these manipulations, the structural and mechanical aspects, and the austenite to martensite transformation of the two wire types, wires in the as-received state and after heat treatment were investigated in bending using x-ray diffraction and scanning electron microscopy. Relative amounts of austenite during the transformation were examined for three levels of deformation. Relative amounts of Ni and Ti using x-ray spectroscopy techniques and the transformation temperature for Af were determined for each wire. Comparisons of wire performance after heat treatment and in the as-received condition demonstrated processing effects and provided insight into the nature of the transformation.

UCSF LIBRARY

1. STATEMENT OF THE PROBLEM

The clinical practice of orthodontics has changed with the introduction of nickel titanium (NiTi) shape memory alloys. Because of the unique properties of shape memory and pseudoelasticity (superelasticity), these wires afford the practitioner the advantage of applying a constant load over a long period of time to move teeth, without having to see the patient as frequently for adjustments. As such, nickel titanium wires have been routinely employed in clinical practice and the market for these wires has exploded over the last two decades. Several orthodontic companies now supply nickel titanium archwires and the practitioner is flooded with a myriad of 'nickel titanium' wires to choose, in a variety of sizes, with a variety of costs.

However the problem lies in the variable clinical performance of these wires. The complex metallurgy of this alloy partially accounts for the inconsistent behavior. Not only do the wires from different manufacturers exhibit different properties, but wires from the same lot of the same manufacturer show variance in their properties. These differences have been shown to be clinically significant.[7] Since the biology of tooth movement and alveolar bone modeling/remodeling is not understood, there are no standard guidelines for optimal and efficient tooth movement. The principles of force delivery proposed in the late 1950's[8,9] still guide the orthodontist today. The definitive properties for the orthodontist are formability/ductility and a large capacity for energy storage. Other properties such as constant force delivery and low force levels are thought to be desirable. These conditions of a constant low stress are thought to be the most favorable conditions for tooth movement, which makes nickel titanium wires ideal in theory for the rate of force application. For the manufacturers, it becomes a formidable task to develop materials without defined mechanical parameters. Consequently manufacturers are left with somewhat tentative guidelines for product specifications based on what that particular company believes to be the most favorable.[10]

USC LIBRARY

It is difficult to characterize the behavior of NiTi, since the mechanical properties of NiTi are largely effected by the mode of testing. Studies show that NiTi performs differently in compression, tension and torsion.[1,11-14] As NiTi is a very elastic material, it is able to recover strains of up to 8%, as determined in tensile tests.[1,11,15] However in orthodontics, modes of pure tension or pure compression are rarely encountered. Deformations are generally in bending, which is partly a combination of compression and tension. Even in bending, the stress-strain profile varies according to the loading conditions. Cantilever, 3-point bend and 6-point bend tests of NiTi do not yield the same results.[14] There remains a need to characterize the mechanical performance of NiTi under clinically simulated conditions.

UCSF LIBRARY

2. SPECIFIC AIMS

The goal of this study was to characterize the transformation in the NiTi orthodontic wires under simulated clinical conditions and relate this to the variability commonly seen in the wire performance in the clinical setting. While there are numerous brands of NiTi wires on the market, a need for product optimization and improvement exists. It was a secondary objective to identify the differences among wires so that the variability could be explained and to further differentiate the parameters between superelastic wires and shape memory wires.

This study was limited to the examination of the structural changes produced by bending in the shape memory and superelastic type orthodontic wires from two different manufacturers. NiTi wires are generally incorporated in the initial months of a patient's orthodontic treatment. Usually the clinician employs a series of four to five different wires from the beginning to the end of treatment. With the application of the newer generation of wires, the same treatment goals can be achieved using fewer wires and less frequent arch wire adjustments. Understanding the force delivery, and subsequently the deformation behavior during the force delivery stage (or reverse transformation) of the NiTi wires is paramount for optimal wire selection. It is hoped that this work will contribute to the body of information in the elucidation of the utility and behavior of NiTi shape memory alloys.

The clinical implications of this study include addressing the following :

1. What is the clinical limit of shape memory ?
2. What is the distinction between wires ?
3. What guidelines should the clinician use in product selection ?
4. What are the applications of shape memory and superelastic principles ?

UCSF LIBRARY

3. BACKGROUND

The shape memory phenomenon is not solely associated with nickel titanium alloys. It was first identified by Chang and Read[16] in Au-Cd structures, and experienced a resurgence attributable to Buehler in NiTi structures. William Buehler, working as a metallurgist for the Naval Ordinance Laboratory, fabricated the alloy NiTi in 1958 and named it Nitinol for the chemical symbols of its components and the acronym of his lab.[17] He recognized the atomic rearrangement in the alloy based on the variable acoustic emission the alloy exhibited at different temperatures. From this realization the scientific investigation of NiTi was spawned and potential uses for the material have been steadily increasing. While many other alloys display the shape memory effect (SME), NiTi has clearly been the most utilized because of its biocompatibility, low stress-strain profile, corrosion resistance and temperature sensitivity.

The shape memory applications are far reaching, from industrial to medical applications. The first application of NiTi shape memory materials began in pipe couplings for hydraulic systems in aircraft engines.[17] The automobile industry has utilized the shape memory alloys for purposes of ventilation and climate control while the medical field has incorporated these alloys in the design of prostheses and implants. George Andreasen brought the potential application to orthodontics in 1969,[18] with the first clinical trial reported in May, 1972.[19] The initial application Andreasen described employed the shape memory property. Today, most clinicians utilize NiTi wires for their superelastic property. Because the remarkable properties of pseudoelasticity, or superelasticity (SE), and shape memory (SM) have created a market for these wires, these properties deserve definition.

3.1 Martensitic Transformation

Shape memory and superelasticity are closely related terms, such that SE is thought to be a subset of SM. The SM and SE properties of NiTi are attributed to the martensitic type phase transformation as a result of applied stress and/or temperature. The martensitic transformation is a

UCSF LIBRARY

crystallographic solid state displacive or diffusionless transformation in which a new phase is formed through atomic rearrangements, but the same chemical composition of the original matrix is retained.[20] The atoms do not shift independently, but undergo a type of shearing deformation.[15] On a microscopic level, this shearing deformation has components in a parallel and perpendicular direction to the habit plane.[21] The perpendicular lattice deformation is a Bain strain composed of several atomic shuffles[1] that collectively comprise the volume change associated with the structural transformation. The parallel lattice invariant shear is an accomodation for the volume change via twinning mechanisms. The key premise to this transformation is the singular relationship between the parent and martensite phase lattices.[5] For NiTi, this will only occur if the parent austenitic phase is ordered. Consequently, the martensitic phase must also be ordered, as there is a direct lattice correspondence between the parent and martensitic structures.

The nature of both the parent and transformed phases in NiTi have been extensively studied. The matrix, or the parent phase called austenite, has been identified in NiTi as a β-phase B2 CsCl-like simple cubic structure. The Ti atom may sit in the center of the Ni simple cubic lattice, so the structure is essentially two interpenetrating ordered simple cubic lattices. It is of higher symmetry and exists as the stabilized compound at higher temperatures. At lower temperatures, the α phase martensitic structure is stabilized, which is of lower symmetry and is generally thought to be a monoclinic[22] distortion of an orthorhombic B19 cell, thus noted B19'.[23]

The transformations are governed by the start and finish temperatures of the phase transformation. These will be noted as follows:

Ms	Temperature at which martensite starts to form
Mf	Temperature at which martensite has completely formed, or finished
Md	Temperature above which martensite cannot be stress induced
As	Temperature at which austenite starts to form
Af	Temperature at which austenite has completely formed, or finished
Td	Temperature at which the specimen is deformed

Where $Mf < Ms < As < Af < Md$.

The relationship between these temperatures is best depicted in Figure 3.1.

Figure 3.1. Relationship of Property Change and Phase Content to Temperature adapted from *Engineering Aspects of Shape Memory Alloys*. [15]

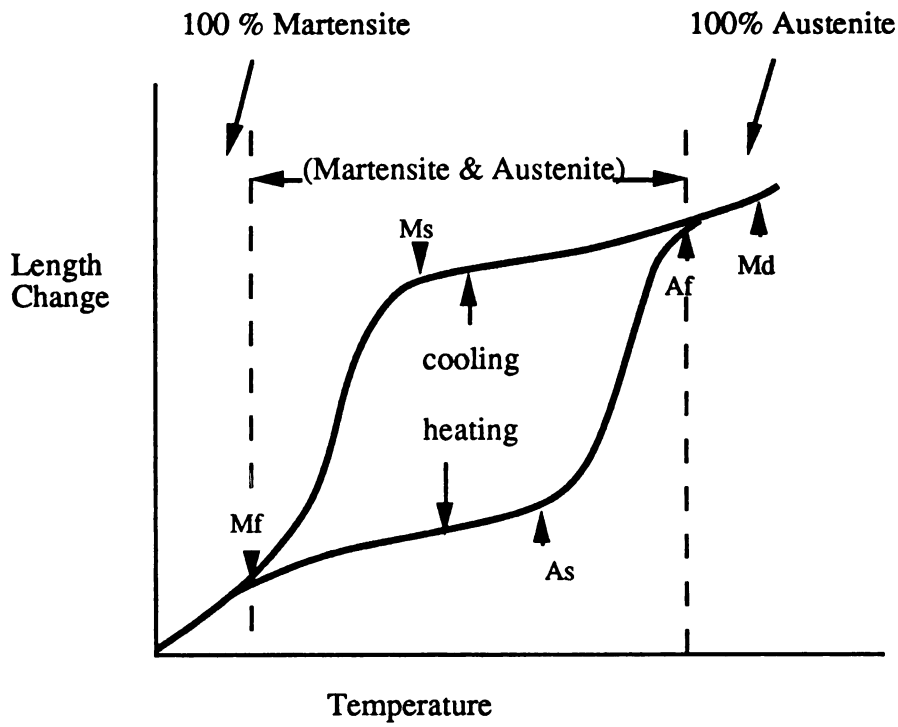

UCSF LIBRARY

Depending on the temperature, the material will either be completely martensite (when Td < Mf), austenite (Td > Md), or a mixture of the two phases (Mf < Td < Af). Understanding the temperature dependence and the influence of applied stress on this alloy is critical to understanding the material behavior. Since martensite can be thermally or mechanically induced, the mechanisms of martensite formation will vary according to the method of induction.

3.2 Formation mechanisms

Thermal martensite forms from the parent phase through a thermoelastic process when the parent phase is cooled below Ms. However, in a polycrystalline structure, at temperatures between Af and Mf, the structure is a mixture of both the parent phase of austenite and martensite. If the specimen is cooled from a region where both phases exist (between Af and Mf), through the

process of nucleation, new martensite plates will form and the existing martensite variants will swell in response to decreased temperatures. The individual variants will change in size and shape and many different variants will coexist. Wasilewski [5] and Wayman [24] noted 24 possible variants of thermal martensite that may result when austenite is cooled between Ms and Mf. Some variants will grow at the expense of others, but due to a process of self-accommodation of the existing variants, no macroscopic net shape or volume change is observed as the specimen is cooled from Af to Mf.[15] Surface relief effects may be evident. The twin boundary motion within the martensite plates, which approximates pure shear deformation, accounts for the accommodation. The mobile twin boundaries move in a twinning type of elastic behavior to produce other variants. Growth of the martensite crystals halts when the equilibrium between the thermal and elastic effects is reached.[25] The volume fraction of martensite increases as the temperature decreases from Ms to Mf. If the temperature is now increased to As, martensite becomes unstable and the structure will undergo the reverse transformation and crystallographically revert to austenite.

UCSF LIBRARY

This scenario becomes more complex if stress is added, because martensite can also be induced through stress. Martensite may be formed when stress is applied above Ms, but below Md. Because the transformation is stress induced and independent of temperature, it is called an isothermal transformation. It is important to differentiate what effects are observed when loads are applied to deform the specimen at different temperatures. When NiTi is elastically deformed below Mf, the specimen is completely martensite and will remain deformed even if the load is released, as there is no driving force for the deformed specimen to return to its parent phase. However, if the applied stress does not exceed the yield strength of martensite, the deformation can be accommodated through the migration of the twin interfaces, detwinning and coalescence of martensite variants. In the range between Ms and Mf, the specimen is not entirely martensite, but a mixture of martensite with some of the parent phase. The deformation mechanisms remain the same. If the material is deformed between Ms and As, additional deformation mechanisms include nucleation of new stress induced martensite (SIM). Martensite nucleation is assisted by internal

stress fields.[26] The material still will remain deformed at this temperature range. Between As and Md, if the specimen is deformed, then deformation proceeds by nucleation of SIM only. When the load is released and if the applied stress does not exceed the limit for plastic deformation of martensite, the alloy will return to the austenitic phase and exhibit some recovery. At Af<Td<Md, the material is completely austenitic and transforms into martensite through SIM only. Both thermally induced and stress induced transformations are reversible due in part to the mobility of the twin interfaces.[18]

Thermal martensite forms without any macroscopic shape change because the several martensite variants that may form will self-accommodate each other. Conversely, SIM will preferentially form a single variant in the direction of the applied stress. This creates a shape change when the material is under stress. There is a practical limit of recoverable deformations. Strains up to 8% have been reported to be recoverable upon either unloading or heating above Af.[27,28] So shape memory occurs within a defined stress and temperature range and is dependent on the heat processing, the number of cycles the specimen undergoes, the load, and the specimen's shape and dimensions.[25]

For thermal martensite, the progress of the forward or reverse transformation is controlled by the chemical driving force due to an increase/decrease in temperature, the elastic strain energy stored in a material during the forward transformation and released during the reverse transformation, and also due to the frictional force arising from the movement of interfaces and the creation of defects.[5,18,22] The stored elastic energy assists the chemical driving force gained by heating and enhances the reverse transformation, and actually hinders the forward transformation. The last martensite plate to form from the forward transformation is thought to be the last martensite plate to disappear on reversion to austenite.[29] However, equilibrium conditions are not likely to be present in orthodontic wires.

USSF LIBRARY

3.2.1 *Shape Memory*

The reversibility of the martensite transformation provides the basis for the shape memory effect. In essence, it is a shape recovery event initiated by temperature. If the material is deformed in the martensitic phase, then heated to above Af, it will return to its undeformed state. As another example, if an austenitic material is cooled to below Ms, then deformed, then heated to above As, the material 'remembers' its original shape as it returns to its austenitic parent phase. It is this actual transformation to the parent phase that restores the original shape. On a stress-strain diagram (Fig. 3.2, below), the residual strain is recovered only after heating, even if the stress is removed. Unloading begins when the stress decreases, as seen in Figure 3.2, and there will be some strain recovery. The actual amount of this recovery, and the subsequent shape of the unloading curve is dictated by the relationship of Td to Af. Shape recovery begins at As and will only be completely realized when the material is heated to above Af in the reverse transformation.

Figure 3.2. Stress-Strain profile of the Shape Memory Effect. Td < Af. Adapted from *Shape Memory Alloys*. [25]

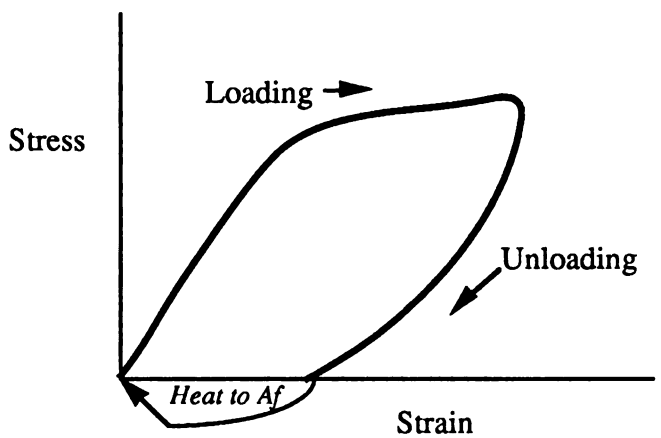

UCSF LIBRARY

3.2.2 *Superelasticity*

Pseudoelasticity, commonly referred to as superelasticity, is a type of shape memory. The term pseudoelasticity was derived from the elastic-like character of the material seen on unloading. It is not linear, which would describe elastic behavior, and thus it is called pseudoelastic, or superelastic.[28] The term superelasticity now commercially refers to a product with a flag shaped stress strain profile and a flat plateau upon unloading. SE is differentiated from SM in that it occurs only within a certain temperature range between As and Md, where the alloy is mostly austenitic. Within this range, when the material is deformed, martensite forms primarily due to the applied stress and secondarily due to the growth of existing martensite variants. As soon as the stress is removed, the martensite is no longer stress stabilized and reverts back to its austenitic parent phase and returns to its original shape. This is best illustrated in Fig. 3.3, below.

Figure 3.3. Stress Strain Profile of the Superelastic Effect.
Td > As. Adapted from *Engineering Aspects of Shape Memory Alloys*. [15]
A denotes the stress/strain region where stress induced martensite forms.

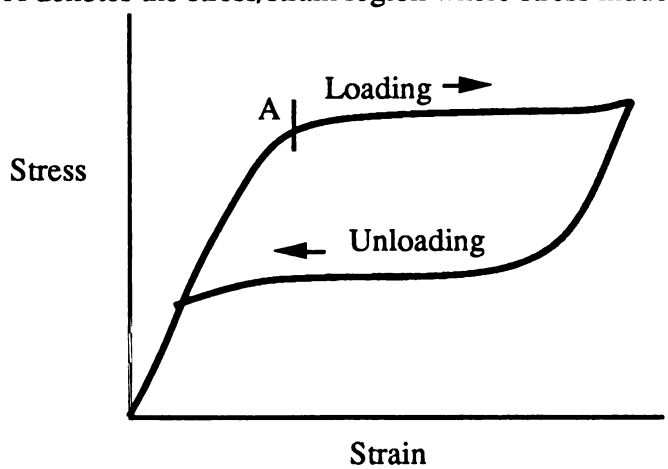

The figure shows that as the material is deformed in loading, martensite forms at a specific stress level (region marked A, Fig. 3.3) and then the stress reaches a plateau. For optimal superelasticity, Td > Af and the material will be completely austenitic in its initial state. Complete shape recovery is expected, since martensite is thermally unstable above Af. It should be evident that temperature plays a critical role in any application using shape memory alloys.

UCSF LIBRARY

3.3 R-Phase

During the forward transformation, another intermediate phase, the R-phase, was identified by Dautovich and Purdy.[30] This phase was thought to exist as a premartensitic instability, but has been designated as a completely different phase from martensite within the last decade.[31-33] It has a rhombohedral structure and its own associated start and finish temperatures, Rs, Rf. The transformation can progress as B2 --> R --> B19' (A --> R --> M), while the reverse transformation is from B19' --> R --> B2 (M --> R --> A).[34] The effects of the R-phase on the mechanical performance show that superelasticity and shape memory are associated within the R-phase transformation in both the forward and reverse directions. This isolated transformation has utility in many industrial applications where a small thermal or stress hysteresis is indicated.[35] Processing conditions to fully express the R-phase have been developed and it is at the expense of martensite transformation that this occurs. This R-phase can be controlled by its thermomechanical treatment, either by aging or annealing immediately after cold work at temperatures between 673 and 573°K.[36] The R-phase in orthodontic wires has been detected,[37] and should be evident in the characterization of the wire.

UCSF LIBRARY

In orthodontics, the forward transformation occurs upon loading, or ligating the arch wire into the bracket. The reverse transformation of martensite to austenite usually receives less attention, but is more clinically relevant than the forward transformation. In thermoelastic martensite, the martensite crystals shrink as the temperature increases. In contrast, the stress induced martensite (or isothermal martensite) displays a different reversion whereby the austenite crystals nucleate and grow within the martensite. The plateau seen upon unloading (Fig. 3.3) is a result of the transformation from SIM back to austenite.

In the clinical application of shape memory in orthodontics, the situation is a little more complicated because of concurrent stress and temperature factors. Shape memory orthodontic wires are formed into an arch shape by the manufacturer and are reported as martensite in their as-received condition

at ambient temperature. The wires are relatively easy to engage into malaligned brackets because as martensite, the wires can sustain large deformations at low loads. As the wire is heated in the mouth, the transformation to austenite occurs. This should create a recovery stress[38] large enough to initiate tooth movement. However, this recovery stress may not be constant as the strain is recovered, but may decrease as strain decreases and increase as the surrounding temperature increases, i.e. as the wire is heated to equilibrium with intraoral temperatures. The recovery stress may not be constant during normal ingestion and deglutition with the fluctuating oral temperatures. However, the material should display complete shape recovery provided that the total strain does not exceed 8%, the recovery stress is adequate, and intraoral temperature is less than Md.

The superelastic orthodontic wires will clinically achieve the same result, i.e. tooth movement. These SE wires (Af < 37°C) are austenitic at ambient temperatures and transform to martensite upon loading, which commences when the wire is ligated to the tooth. This imposes a certain amount of force on the tooth and in response to this stress, the tooth will move. Since the tooth has moved, the load applied to the tooth decreases from the load the clinician used to engage the wire to the bracket, and unloading of the wire begins. Unloading causes the martensite (SIM) to revert back to austenite. At this point, the force delivery mechanism diverges from the SM application, because the load, or recovery stress, will be constant as the strain is decreased[38] along the unloading plateau (Fig. 3.3). The deformed wire returns to its initial shape and brings the tooth into alignment. In this situation both the forward and reverse transformations occur, but do not depend on going from ambient to mouth temperature since no thermal martensite is involved.

In summary, it is the reverse transformation of martensite to austenite that creates force generation for tooth movement. These conditions of a constant low stress are thought to be the most favorable conditions for tooth movement,[8,9] which makes the nickel-titanium wires ideal in theory for the rate of force application.

UCSF LIBRARY

3.4 Metallurgy

The NiTi compound is an equiatomic, substitutional, ordered alloy at ambient temperatures.[15,32] Nickel imparts strength and high temperature,[25] and it improves the formability, weldability and strength attainable by cold work. Titanium itself is noted for its high meting point (1668°C), low density and corrosion resistance. Because it is lightweight and temperature resistant, titanium alloys are widely used in the space industry.[39] Titanium based products are now widely available, and in the biomedical field, titanium alloy products are employed due to their corrosion resistance and biocompatibility.

3.4.1 *Chemical Composition*

It is well established that the chemical composition greatly affects the behavior and physical performance of NiTi. While several factors affect the transformation temperature, the most critical factor is the chemical composition of the alloy.[40-41] Slight compositional changes, on the order of one tenth to one hundredth of a percent can markedly affect the transformation temperatures and thus affect the mechanical properties.[11] Most NiTi compounds contain Ni in the range of 48 to 51 at%.[23] Generally the nickel titanium archwires are nearly equiatomic nickel and titanium (stoichiometric composition). These compositions yield lower transformation temperatures suitable for medical and dental applications. If not stoichiometric NiTi, then other phases or precipitates form which may depress or maintain the transformation temperatures, depending on whether the alloy is nickel or titanium rich.[2]

Ms shows a strong dependence on composition, particularly on the Ni rich side. Ni rich alloys have been defined as Ni >50.7at%.[42] These Ni rich alloys exhibit a lower Ms, and a decreased capacity for shape recovery when the nickel content approaches 60 at%. If the application requires lower Ms temperatures, then Ni rich alloys are used. Due to the differences in solubility, precipitates readily form that destabilize the matrix.[39] On the other hand, Ti rich alloys usually

UCSF LIBRARY

have little effect in altering the transformation temperatures. The Ti rich precipitates that form leave the matrix unchanged.[15] This relationship is depicted in Figure 3.4.

Figure 3.4. Relation of Transformation Temperature and Nickel Content, adapted from SMST Proceedings.[23]

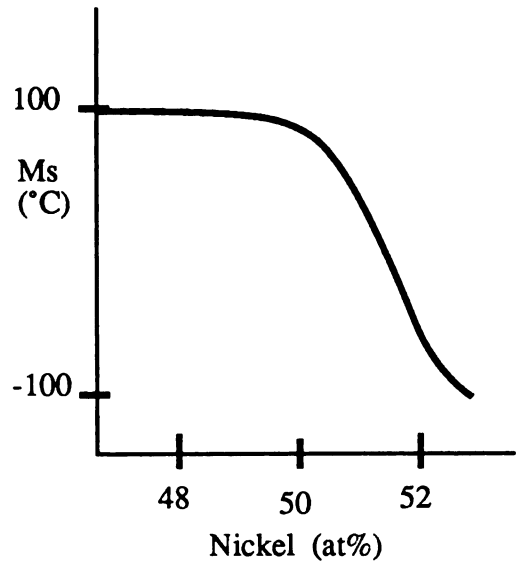

UCSF LIBRARY

Alloying can increase the yield strength of the material or achieve superelasticity at lower temperatures. In early studies, Wasilewski[43] identified that alloying trace amounts of Co, Cr, Mn, Fe or Cu lowered the forward transformation temperature and increased the range of start and finish phase temperatures (Ms - Mf and As - Af), when compared to the behavior of stoichiometric NiTi. He attributed this spreading out of the transformation range to the introduction of solute atoms into the lattice. It has since been an established technique to use these elements to change the transformation temperatures.

Unintentional impurities that are incorporated into the alloy during processing create problems because NiTi is such a composition sensitive material. Carbon, nitrogen, oxygen and hydrogen all depress the Ms temperature and thus affect the mechanical performance. Carbides, nitrides, oxides and hydrides are byproducts of these gaseous impurities reacting with NiTi and may cause

embrittlement in the alloy. Since many industries manufacture NiTi using graphite crucibles, it is generally impossible to avoid carbon contamination during melting such that carbon may constitute 0.2 - 0.6 at% of the alloy.[40] Carbon reacts with NiTi to form another carbon containing phase, and may also precipitate TiC. When carbides form, the effective Ni concentration increases so the Ms decreases. Fukanubo postulated that carbon in the solid solution leaves a residual strain that lowers Ms.[25] Similarly, titanium has an extremely high affinity for oxygen and as a result, the Ni concentration in the matrix increases if the alloy is contaminated with oxygen. Although unintentional, oxygen will always be found in NiTi alloys. Surface oxides of TiO_2 form on the external surface,[34] while most of the oxygen in the matrix forms internal precipitates of Ti_4Ni_2O.[23,25] As mentioned earlier, the NiTi alloy is particularly sensitive to compositional variation. This specificity lies within a tenth of a percent, which in manufacturing, is such a narrow range that precise compositional control is difficult.

UCSF LIBRARY

The properties of NiTi alloys are largely determined by their compositions and the methods of processing. Consistent mechanical behavior is dependent on manufacturing practices. Quality control becomes a matter of cost. The need to adhere to tightly controlled manufacturing specifications and product tolerances to produce devices with reproducible and predictable properties has been recognized.[1,10]

3.4.2 *Transformation Temperatures*

In theory any of the changes that accompany the SM transformation, as listed in Table 3.1, could be used to determine the transformation temperatures. There are four major easily reproduced and reliable methods to determine transformation temperatures, based on the changes of electrical resistance, latent heat of transformation, strain and stress as a function of temperature.[39] Because most chemical analyses to determine composition are not sensitive enough to detect differences of a tenth of a percent, the transformation temperature commonly is used to determine the amount of Ni and Ti in the alloy. Since the transition temperature range is affected by composition, the mode of

deformation and the thermomechanical history, the composition or thermal history of the material can be estimated indirectly by measuring its transformation temperature.

Table 3.1. Property Changes Associated with the SM Transformation adapted from *Engineering Aspects of Shape Memory Alloys*. [44]

Feel	Acoustic Emission
Ring	Electrical Resistance
Bend	Magnetic Properties
Color	EMF
Roughness	Thermoelectric Power
Hardness	Hall Coefficient
Expansion	Heat Capacity
Yield Strength	Latent Heat of Transformation
Young's Modulus	Thermal Conductivity
Damping	Lattice Spacing
Internal Friction	

UCSF LIBRARY

3.4.3 *Phase Description*

Metals are produced as a conglomerate mass of crystals or grains. The arrangement and interaction of these individual grains determine the final properties. In wire fabrication, the structure of the polycrystalline mass is heavily oriented due to the forming of the wire itself (processing will be discussed later).[21,39,45] The individual grains are generally oriented in the direction of drawing along the long axis of the wire. This preferred orientation, or texture, of the individual grains will impart certain macroscopic properties which may or may not be desirable.

X-ray diffraction is used to study various structural aspects of crystals.[45] For the study of polycrystalline structures such as wires, it may be used for qualitative determination of the crystal quality and orientation as well as phase content analysis. In wire form, the crystals are so heavily oriented, that much of the diffraction work describes the orientation that results from processing. To determine processing effects, the wires are often heat treated under various conditions and analyzed for differences in phase contents.

The nature of the austenite to martensite phase transformation is of particular relevance to orthodontics. In the early studies on NiTi, Buehler[2] noted NiTi existed as a CsCl type cubic intermetallic compound. Depending on the actual composition around the equiatomic point, it can exist as a single phase or as a component of a two phase system, with the other phase as Ti_2Ni or $TiNi_3$. His studies in the 1960's showed that altering the phases present in stoichiometric NiTi alloys results in dramatic behavior changes. Austenite has clearly been identified as a cubic B2 structure, similar to CsCl.[46] The martensitic structure in NiTi is considered to be a monoclinic distortion of the B19' structure.[47,48] Determination of the martensite structure is difficult since the grain size of NiTi (25 μm)[49] is small and there are several variants from which martensite may form. Recent work on single crystals of NiTi provides convincing data that the martensitic crystal structure has the lattice parameters of a = 2.898 Å, b = 4.108 Å, c = 4.646 Å, ß = 97.78°.[47]

UCSF LIBRARY

3.4.4 *Microstructure*

An evaluation of the microstructural changes accompanying the phase changes help elucidate the deformation mechanism. Microstructural analysis is also used to determine grain size, but in NiTi systems, the grains are very small (≈ 25 μm) and not easily detected. In NiTi systems, smaller grain size structures actually suppress the formation of stress induced martensite. Similarly, polycrystalline materials have less pronounced pseudoelastic properties than single crystals. Single crystals exhibit the SM by the preferential orientation of only one martensitic variant, whereas polycrystalline materials have several variants forming in different regions of any grain. Adjacent grains will impose constraints and stress concentrations that must be overcome in order to display the entire superelastic effect. Although the literature is replete with microstructural studies on shape memory alloys such as CuZnAl and CuAlNi, and even NiTiCu, there is little information on Ni-Ti even though the transformations have been well described. Because the wire has preferred orientation, optical microscopy of as-received wires often reveals little about the microstructure.

Ideally it would be of interest to capture the microstructural changes in Ni-Ti occurring during the forward and reverse transformations under the effects of temperature and applied stress. Martensite forms through a twinning type of mechanism and is easily distinguished because it is heavily twinned. Twins are a type of crystal defect that are characteristically identified. Saburi, et. al[42] have described the microstructure of NiTiCu during transformation using transmission electron microscopy. The transformation was thermally induced in the microscope by controlling the intensity of the incident electron beam. They examined a NiTi specimen that was mostly martensite at room temperature (Ms = 30°C, Mf = 20°C). The microstructure of the as-received NiTi undeformed wires at room temperature has been qualitatively described by Lee, et. al.[3] They found an even dispersion of a few nonmetallic inclusions and holes in the NiTi matrix, and twin patterns. The inclusions were thought to be titanium carbonitrides and nickel titanium oxides.

3.5 Mechanical Properties

While several studies have examined the loading behavior, the aspect that is perhaps more significant for clinical orthodontic application is the unloading characteristics of the wire. Table 3.1 lists those measurable changes seen in shape memory alloys. Among those relevant for orthodontic applications are bend, roughness, yield strength, and modulus. Tensile tests, cantilever tests, and 3-point bend testing conditions attempt to simulate clinical conditions. Numerous studies using tensile and three point bend have been performed on the different brands of NiTi currently available.[1,50] In a recent study comparing 20 different brands of NiTi archwires in 3-point bend tests at 37°C, noticeably different stress/strain curves were shown from among the various suppliers.[6] Slight variation is expected among the different brands as there is really no defined or ideal stress/strain curve established for wire performance in orthodontics.[1,10] The range of variability suggests that the nature of the metallurgy remains somewhat elusive at this time due to the sensitivity of the metal in processing.

It has been well established that the SE property is greatly affected and dependent on test temperature. For biomedical applications, testing should be conducted at body/intraoral temperature, since the unloading stiffness may double between room temperature and mouth temperature.[28]

3.6 Processing Conditions

Shape memory and superelasticity can be imparted in NiTi through its processing techniques. The structural and mechanical properties of NiTi are affected by its manufacturing processes as exemplified by the shifting of the transformation temperatures. Microstructural analysis, Af temperatures, phase differences and mechanical property testing help determine the processing effects on the material structure.

Manufacturing NiTi into small diameter wires creates a highly strained material with a small grain size and a preferred orientation of the individual grains. Further processing will increase or decrease the defects that inherently exist in a polycrystalline material.[51] These defects, e.g. twins, dislocations, stacking faults, create barriers to motion and act as sources of internal stress/strain. These stress fields facilitate martensite formation and decrease Ms. Plastic deformation of the matrix, impurities, and the presence of other phases will also increase the internal strain and have similar effects on the martensitic transformation. However, at a certain threshold, the introduction of more dislocations may create so much internal strain that Ms increases.

Annealing and cold work are generally used in conjunction with each other in processing, and actually have contrary effects. The effects due to annealing will vary according to the time and temperature of the anneal. High temperature annealing will tend to increase the Ms, and increase the ductility, while decreasing the yield strength.[28] The proper combination of cold work, annealing, aging or solution treating can enhance the SE or SM properties in NiTi. Shape memory properties are superior in alloys processed at intermediate temperatures of 400 - 500°C,[25] while

cold work without any subsequent heat treatment will obliterate the SE martensite plateau.[15] Between the austenitic yield strength plateau and the martensitic yield strength plateau, there is generally a 20 - 40°C hysteresis.

3.7 Experimental Design

There were three areas that this study investigated.

i) The principal objective was to describe the stress induced transformation under simulated clinical conditions to gain an understanding of the *in vitro* load delivery of NiTi. The extent of transformation was assessed from a microstructural description, supplemented with phase analysis. In orthodontics, NiTi wires have been useful over large ranges of activations. The amount of transformation that occurs through this activation in the clinical setting is unknown but of considerable interest. In clinical application, the reverse transformation is of particular interest, but experimentally was found too difficult to isolate. Therefore loading, or the forward transformation, was studied.

Before the transformation could be examined, a description or characterization of the NiTi wires had to be established at the structural level. Understanding the structure, and the subsequent manipulation of the structure, provides insight into the behavior and performance of any material. While there are several different levels at which a material's structure can be assessed, ranging from the atomic level to a macroscopic level, for our purposes, we were interested in examination at the microstructural level. X-ray diffraction, scanning electron microscopy and energy dispersive x-ray spectroscopy are complementary experimental techniques used to gather structural information about materials. These techniques and their limitations will be reviewed in Section 3.8.

UCSF LIBRARY

Because the internal structure will govern the material performance, it will be reflected in the material's mechanical properties. However in NiTi alloys, the mechanical properties differ, depending on the mode of deformation. The tensile, torsional and compressive properties are markedly different, indicating that different amounts (and mechanisms) of the transformation occur in different deformation modes. Orthodontic applications utilize the material in bending. Thus there is great interest in characterizing NiTi in bending, but no appropriate test of how bending is defined. In orthodontics, the clinical situation is illustrated in Figure 3.5.

Figure 3.5. Illustration of Orthodontic Application to correct malaligned tooth positions.

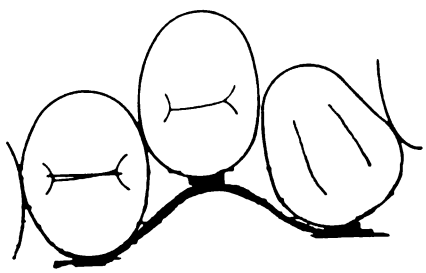

UCSF LIBRARY

The bending application becomes evident. The complications of examining the NiTi material under bending are illustrated in Figure 3.6. When a NiTi wire is bent, the outer fibers of the wire are in tension, while the inner fibers are in compression. Since the deformation mechanisms differ in tension and compression, characterization of the entire wire in bending is problematic. 3-point bending tests and cantilever type tests simulate the clinical application.

Figure 3.6. Deformation Mode in Bending

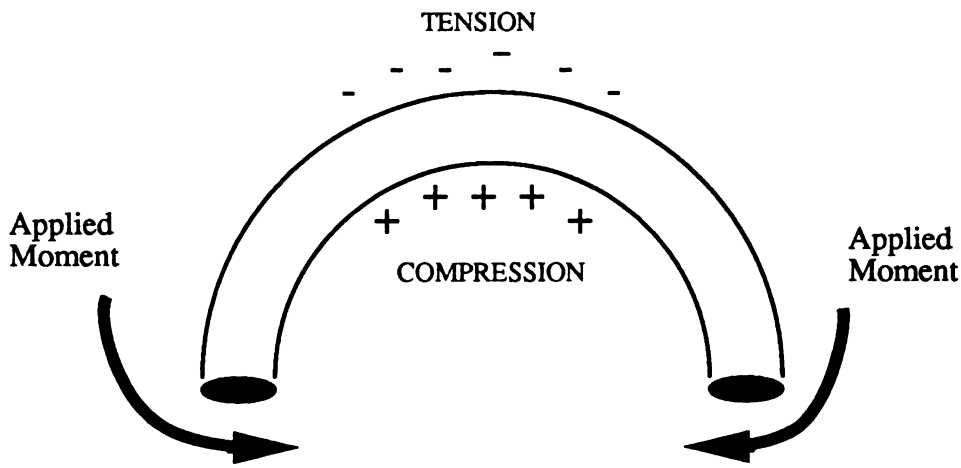

It was important to evaluate the wires in a test configuration that simulated its clinical application but also permitted the evaluation of its structural properties in the same configuration. The preparation of the specimen or the space restraints of the sample holder often present physical limitations in specimen analysis. A bending configuration was devised that satisfied the requirements of simulating the bending in orthodontics while also allowing examination of its structural properties. Much of the sample preparation and testing parameters were dictated by the physical limitations of the testing apparatus. Given the size of the wire, the load and the amount of deflection studied, the 3-point bend configuration was the closest approximation to the desired bending.

ii.) To derive any useful parameters for comparison of the data, it was necessary to define what properties were relevant for orthodontics. Since there are no accepted standards for comparison in NiTi, this study suggested clinically useful guidelines for characterization of the wires.

iii.)As a tertiary component to this study, the variability among different NiTi wires was explored. Ultimately this variability is the clinical manifestation of what is unknown about the transformation. Part of the variability stems from the different types of NiTi wires (SM and SE)

USC LIBRARY

available to the clinician. Comparisons of mechanical properties, Af temperatures, microstructure and phase analysis of the as-received wires and annealed wires helped to identify the variability among wires.

3.8 Experimental Techniques for Structural Characterization

3.8.1 *Scanning Electron Microscopy*

Scanning electron microscopy (SEM) allows investigation of a material on a microstructural level. It provides information about the surface topography, individual grain size and shape, and various phases on the exposed surface.[52] An electron beam is used as the energy source to generate a signal from a specimen. The electron beam is accelerated through a vacuum column and scanned across the sample. Different phases, grains and regions of the sample result in different electron signal intensities emanating from the surface based on differences in topography and/or compositional characteristics. The resulting signal at each step of the scan is converted to a certain viewing brightness on a cathode ray tube producing an image on the screen.

USC LIBRARY

3.8.2 *Energy Dispersive X-ray Spectroscopy*

The chemical compositions of different materials can be compared using techniques of energy dispersive x-ray spectroscopy (EDS, EDX or EDXS). Briefly, this technique utilizes the unique relation of the atomic number of an element as a function of the energy or wavelength of its characteristic x-rays.[52] X-rays are produced by electron bombardment of a target in an SEM in the same process as dental x-rays are generated. However, at sufficiently high energies, characteristic x-rays from the elements of the target are emitted. The x-rays of all energies are collected simultaneously in a Si semiconductor crystal detector. The energy of each x-ray is determined by the number of electron hole pairs created during ionization of the crystal detector. The number of each x-ray type can be counted and used to determine composition on a semi-quantitative basis.

3.8.3 *X-ray Diffraction*

Diffraction is another technique to study the structural aspects of a specimen. Depending on the type of diffraction method, a material can be studied at the atomic level, the crystal level, or on a more macroscopic level, to examine a texture. All techniques of diffraction are based on the principle of Bragg's Law, where x-rays of known wavelength are used to determine the structural parameters.[45] In a crystalline structure, the atoms have a certain periodicity that will scatter an incident x-ray beam at a certain angular deflection proportional to distance between the atoms themselves and the planes of atoms. For this study, the diffractometer technique was employed to investigate the crystal quality and orientation and phase relationships.

USSF LIBRARY

4. MATERIALS and METHODS

0.018" x 0.025" superelastic and shape memory wires from two different companies, Unitek (Monrovia, CA) and GAC (Central Islip, NY) were examined. These are listed in Table 4.1.

Table 4.1. NiTi Orthodontic Archwires

Wire	Type	Grade	Brand
Sentalloy	Superelastic	Medium	GAC
Neosentalloy	Shape Memory	F-200	GAC
Nitinol SE	Superelastic		Unitek
Nitinol	Shape Memory		Unitek

The two different Unitek and GAC wires were chosen based on their reported clinical differences and transformational differences. As shape memory wires, the Nitinol and the Neosentalloy wires are reported as martensitic in the as-received state. These were compared to the superelastic Nitinol SE and Sentalloy wires that are supposedly austenitic at ambient temperatures and the martensitic transformation is stress induced. The GAC wires were available in a variety of force levels. For uniform comparison, the Sentalloy Medium and Neosentalloy F-200 were chosen. Both wire types are reported to deliver medium forces of ≈ 200g.

For all tests, sections of 30mm lengths of 0.018" x 0.025" cross section were cut from the posterior straight section of orthodontic arch wires. Ideally, all samples should be perfectly straight in the posterior section, but since there was variability in the arch form and size, some sections were not entirely straight, as was more evident in the GAC wires, Sentalloy (SE) and Neosentalloy (SM). 30mm segment lengths were chosen, as a result of the limitations of the testing apparatus and specimen preparation. When the arch wires were cut, the ends were deformed under such heavy forces that plastic deformation ensued at the cut section. Since the primary objective of this study was to examine the wires in bending, a 30mm segment provided enough undistorted length to study the phases and microstructure at the area of maximum bending.

USC LIBRARY

4.1 Annealing conditions

Heat treatment was performed at 750°C using an air furnace. The wires were heated for 15 minutes at temperature, then air cooled on the bench top. Annealing conditions have marked effects of the final material performance. Under these annealing conditions, recrystallization and grain growth should occur,[23] so that much of the prior processing or heat treatment effects can be removed from the material.

4.2 Deformation Bending

A bending configuration was devised that simulated the bending in orthodontics while also allowing evaluation of the structural properties. The wires were held in bending by holding the legs of the wire in a fixed holder. The bend angle was approximately determined by measuring the angle formed by the intersection of tangents drawn to the legs of the wire (Figure 4.1). By altering d, the distance between the legs of the span (Figure 4.1), the bend angle changed. Two states of bending, 45° and 75°, were examined, along with the straight undeformed section, 180°. For x-ray diffraction, the wires were aligned tightly adjacent to each other, as will be described in part F of this section. For microstructural analysis, the wires were maintained in this bend angle by placing a layer of dual curing resin over the wire and allowing it to set. The specific preparation will be discussed in greater detail in part 4.7 of this section.

Figure 4.1. Bend Configuration for Diffraction and Microstructural Examination. Measured Bend Angle = γ. d = 22 mm (45° bend angle), & 14mm (75° bend angle).

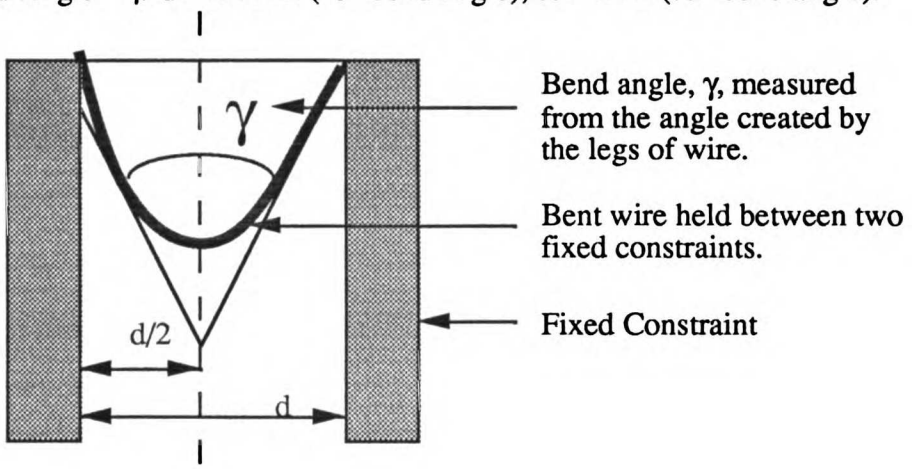

UCSF LIBRARY

4.3 Determination of Chemical Composition of As-received NiTi archwires.

Variability within and between wires may be due to compositional differences. Three samples of each wire type were analyzed for differences in chemical composition utilizing SEM equipped with an EDS System (Kevex, Delta Class IV, Quantum Detector, San Carlos, CA.). The x-ray spectra of all energies were collected and compared to the theoretical values for Ni and Ti x-ray peak positions versus energy. Five random areas in the center of the wire, away from the cut ends, were scanned for each wire in the SEM. The samples were prepared in a similar manner as for microstructural analysis (part 4.6 of this section), but were not etched; the specimens were embedded in a low temperature curing resin, and metallographically polished to a 0.03 micrometer finish. Homogeneity was assessed for each wire, as well as relative differences between each wire. Using parametric methods, the five scans for each wire were analyzed to determine if differences in composition exist within each wire. To determine differences between the wire types, the 15 scans for each wire type were averaged and the means and standard deviations were compared using ANOVA tests.

Operating conditions for detection :

accelerating voltage	20KeV
beam-sample incidence angle	90 degrees
X-ray emergence angle	24.4 degrees
X-ray - window incidence angle	9.4 degrees
scanning time	60 sec
counting rate	3000-5000 cps
magnification	250X
ZAF corrected	

If an element exists in trace amounts, a certain minimum percent material may be detected.[52] This detection limit depends on the operating conditions, which peaks are present, the signal to noise ratio and the location of the peak intensity relative to the other peaks that are present. Most EDS studies assume that a spectral peak from an element must contain enough counts to exceed two standard deviations of the background for detection, thus giving 5% probability of the peak being undetectable. Based on this assumption and the particular elements in a sample, the minimum detectability limit will vary from 0.1 to about 2%.

UCSF LIBRARY

Due to the strong affinity of Ti for oxygen, hydrogen and carbon, internal oxides, hydrides and nitrides will be present. EDS analysis is unable to accurately quantify the presence of these elements, partly due to the physical limitations of the boron nitride window on the Si(Li) detector and the inaccuracies in the ZAF factors for these elements. This is important to remember in data interpretation because these elements and their associated products are probably present in significant amounts and will greatly affect the final properties and material performance.

4.4 Determination of Transformation Temperatures

The Af temperature is not only a measure of the chemical composition of the wire, but it also reflects its manufacturing history. The austenitic finish temperatures were determined by thermally cycling the specimen under a load. This technique provided the best approximation of the Af temperature of the as-received wire. Other methods of determining transformation temperatures require sample preparation, and as such, the prepared sample may not represent the actual material. The apparatus is depicted in Figure 4.2. 30mm sections were deformed at subzero temperatures under a constant 15g load in a 3-point bend configuration within a temperature controlled bath. The entire testing apparatus was immersed in an alcohol bath set over a temperature controlled stirrer/heating plate. Liquid nitrogen was the coolant used to reach subzero temperatures. A stirring bar in the bath ensured consistent temperatures throughout the bath. Gradually the temperature of the heating plate was increased, and the deformation recovery as a function of temperature was plotted. Unloading of the wire was measured using the LVDT such that the data were transmitted to a chart recorder (Soltec X-Y Recorder VP-64155) as a simultaneous recording of displacement and temperature. A thermocouple, attached to the test assembly and placed inside the bath near the specimen, provided a constant digital readout of the bath temperature (Omega Digicator). Two samples for each wire type were tested and a third sample was tested if discrepancies existed in the other two trials.

UCSF LIBRARY

Figure 4.2. Af Temperature Test Equipment. Liquid nitrogen was used to reach subzero temperatures (°C).

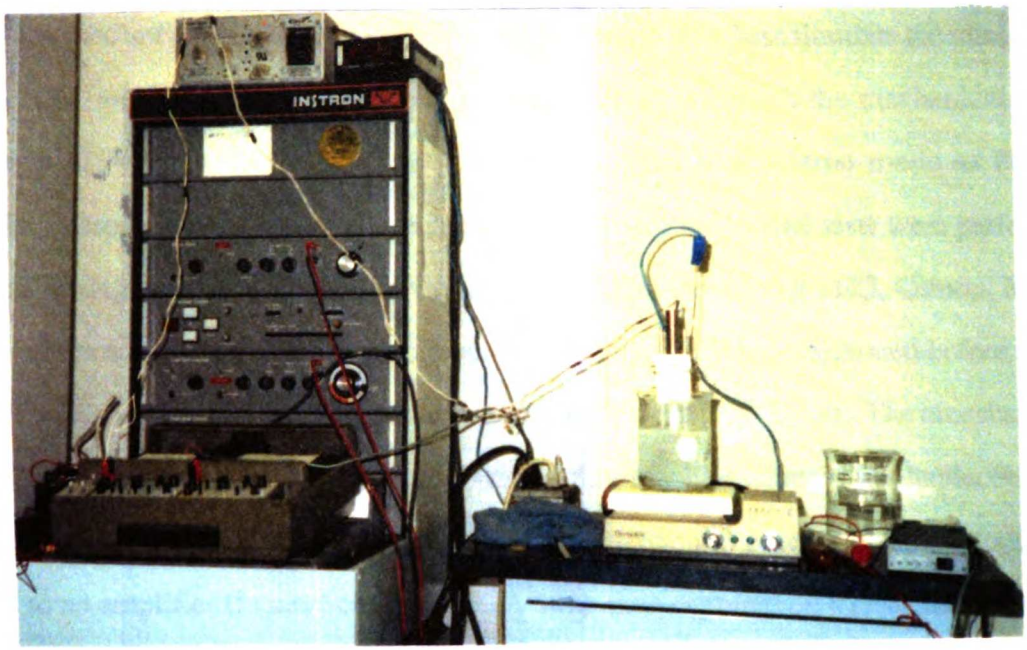

The Af temperature was determined as the point where there was no longer any recovery as the temperature was increased. This point was measured by the intersection of tangents as shown in the figure below.[39]

Figure 4.3. Calculation of Af Temperatures.

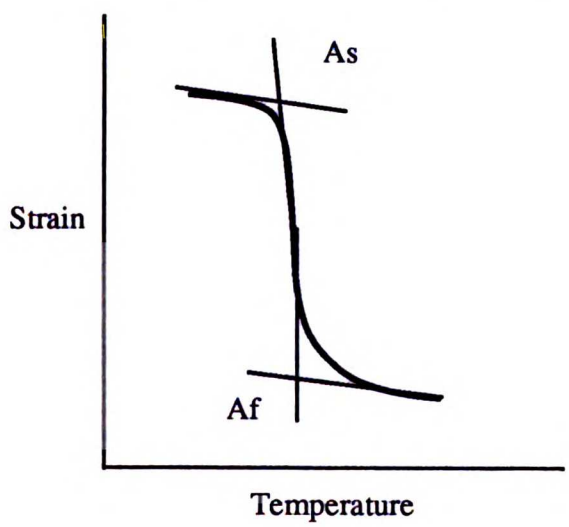

UCSF LIBRARY

4.5 Characterization of Mechanical Behavior

Differences in processing, transformation temperatures, and composition between wires will be reflected in the mechanical performance of the wires. Bending tests best simulate the clinical use of orthodontic arch wires and were performed to systematically establish the mechanical property differences in different wire types. The wires were loaded in the same mode as they were examined for microstructure and phase content analysis. Three point bend tests were performed on a mechanical testing machine (Instron Universal Testing Machine, Model 1123, Canton, Mass). A sample size of three was used for each wire type. A 1000g load cell was calibrated before and after each test. The load range was similar to that in tooth movement (100-700g). The crosshead speed was 0.5 mm/min. An LVDT was connected to the testing machine to measure displacement as a function of potential. The load was also measured as a function of potential. The voltage output was relayed to an amplifier (Lucas Schaevitz, ATA 101) then captured on a chart recorder (Soltec X-Y Recorder, VP-64155). Data were generated as load versus potential. The entire apparatus, depicted in Figure 4.4, was calibrated before and after each test.

USSF LIBRARY

Figure 4.4. Diagrammatic Flowchart of Mechanical Testing Assembly

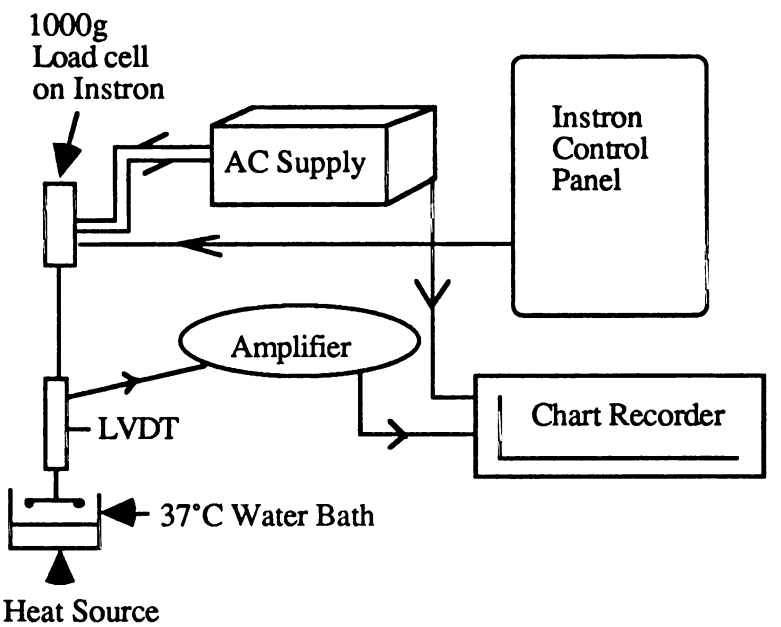

The span between the segments was 15mm, and designed as shown in Figure 4.5.

Figure 4.5. Parameters of the 3-point Bend Test.

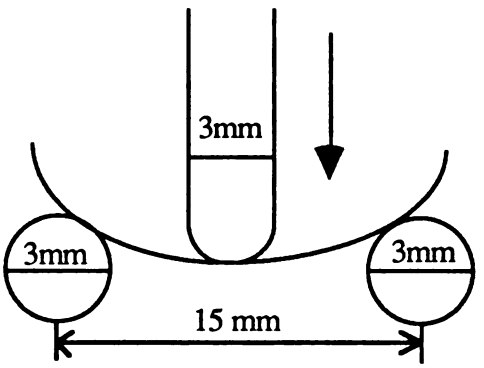

The end spans were wrapped in Teflon tape to prevent drag at the end points. The tape was replaced after each specimen. The upper member applying the load was an aluminum rod 3mm in diameter. The tip was rounded and polished to avoid nicking the wire and to minimize stress concentration from a point application. The unit was also zeroed to discount the weight of the aluminum rod. The wire was oriented so that the load was applied across the 0.025" cross-section, and each specimen was preloaded 0.02v.

Since the material is temperature activated, it was critical that all material testing occur at approximately 37°C. Most mechanical performance studies in the orthodontic literature were performed at ambient temperatures.[53,54] If tested at room temperature, the results and thus the clinical implications must be interpreted carefully.[55] As the Af temperatures are close to body temperature or ambient temperatures, the mechanical testing is only accurate for those temperatures that best simulate clinical conditions, i. e. intraoral temperatures of approximately 37°C. All as-received samples were tested at 37°C and 22°C so that the differences due to test temperature could be ascertained and eliminated. The annealed wires were tested at 22°C. In order to execute testing at 37°C, the testing apparatus was immersed in an alcohol bath over a temperature controlled

USSR LIBRARY

heating plate. A thermocouple, placed inside the bath near the specimen, provided a constant digital readout of the bath temperature. Test temperatures were maintained at 37°C ± 1°C.

There are currently no guidelines to assess optimal shape memory or superelastic conditions in orthodontics. In typical materials, the modulus of elasticity will define the limits for usage. However, for shape memory alloys, the modulus changes with temperature[56] and the crystallographic phase and test method.[16] The mechanical properties differ when NiTi is tested in compression and tension.[57] So as a basis for comparison, parameters were chosen that clinically best characterize the wire's mechanical performance. These parameters should give a good indication of performance and a numerical basis for comparison between wire types so that clear delineations in behavior at the 95% confidence level can be determined. Although there is much speculation as to what and how these parameters are defined,[6] the following variables were selected as the most significant :

length and height of the loading plateau
length and height of the unloading plateau
load drop during hysteresis loop
unrecovered/residual deformation

While the moduli of the austenitic and martensitic phases are important parameters, there is too much variability in how these numbers are calculated. Instead, those values that could be reliably determined were compared. The data were analyzed using parametric statistics, 1-way ANOVA to indicate if there were differences between the wires, and multiple comparison t-tests with Bonferroni corrections to locate those differences.

USC LIBRARY

4.6 Characterization of Microstructural Changes during Phase Transformation

To assess the structural changes that occur during deformation, each wire type in the as-received state was examined in 2 states of deformation, 45° and 75° bends, and in the undeformed state, 180°. The samples were deformed in bending and this bend was held while embedding the wire in resin. 30mm sections of each wire type were embedded in a special resin (Reliance™ Dual Cure

Resin) that cured without significant heat evolution. This was of critical importance since the usual curing resins are highly exothermic and in temperature sensitive specimens, this itself may induce transformation in the bent samples. The fully annealed wires were examined in straight sections only. It was not possible to conduct this part of the study at 37°C due to the physical limitations of introducing a heating element into the sample chamber of the SEM.

The specimen polishing preparation was based on standard methods.[39] Samples were ground under the following grits: 180, 240, 400, 600, 800, 1200. The friction that develops between the specimen and the sandpaper may also induce a thermal transformation while the pressure from polishing may also induce a stress assisted transformation, as well as create a cold worked specimen. Precautions were taken to minimize these possibilities. Light pressure was employed, and grinding was done under cool running water to reduce the friction that develops between the sandpaper and the specimen during grinding. The 1200 grit finished samples were metallographically polished starting with a 6 μm diamond paste, followed by an intermediate polish of 0.3 μm alumina slurry , and a final polish of 0.05 μm alumina slurry. Pressure decreased as polishing progressed.

USSF LIBRARY

After preliminary trials using different etchants and etching times, satisfactory etching protocols were outlined. Etching removes the oxidized surface layer and reveals the grain boundaries which are of higher energy and dissolve more readily. This chemical interaction creates lines across the structure which represent the grain boundaries. An etchant similar to Kroll's reagent[39] was used, 10ml HF, 5ml HNO_3, 85ml H_2O. The etching times varied among the different wires. This is outlined in Table 4.2.

Table 4.2		ETCHING TIMES	
		As-received wires	Annealed wires
Sentalloy	SE	1.25 hr.	15 min.
Neosentalloy	SM	1.25 hr.	10 min.
Nitinol SE	SE	20 min.	15 min.
Nitinol	SM	15 min.	15 min.

After initial pilot studies, the most revealing type of microscopy was found to be the backscattered electron SEM mode. The microstructures were examined at 500x, 1000x, and 2000x magnifications under an accelerating voltage of 20 kV. The specimens were examined at the approximate area of maximum bend. Because different mechanisms of transformation occur in tension and compression, the inner sections in compression and the outer sections in tension in the maximum bend area were examined. The entire area going from maximum tension to compression was scanned, and micrographs of the most representative areas were taken.

4.7 X-ray Diffraction and Phase Identification

X-ray diffraction allows the identification and determination of relative amounts of various phases present within an alloy. These determinations depend on comparison with JCPDS files, standards or calculations, all of which assume random orientation of grains. The texture present in wires reduces the usefulness of this technique. Without texture, the integrated intensities of the peaks are proportional to the volume fractions of the phases. Semi-quantitative judgments, such as more or less of a phase, can be made by comparing integrated intensities of peaks from specimens of similar texture.

UCSB LIBRARY

4.7.1 *Specimen Preparation*

As-received specimens and annealed specimens were examined for phase determination. The as-received wires were examined at 37°C ± 1°C in 2 bend states : 45° bend, 75° bend, and in the undeformed state (180°). The annealed wires were examined in the same 3 states. Five segments were used for each wire type. For the straight section, the wires were oriented parallel to the x-ray beam, with each segment in tight contact. This was held firmly to the specimen holder using transparent double stick tape. The bent sections were oriented so that the area of maximum bend was in the focal spot of the x-ray beam. For the bent specimens, the sections were cut in lengths of 30 mm, 29.5 mm, 29 mm, 28.5mm, 28 mm. The segments were cut progressively shorter so that the segments could be aligned adjacent to each other with no gaps between the wires. The x-

ray beam easily covered all 5 wires. An illustration of the wires held in the specimen holder is shown below, Figure 4.6.

Figure 4.6. Illustration of Wire Orientation in the Diffraction Specimen Holder

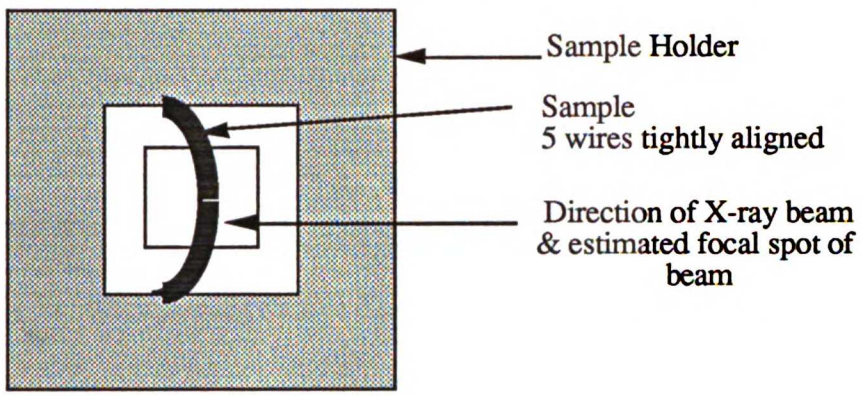

The wires were held in the sample holder with adhesive tape when needed. A Siemens D5000 diffractometer with a diffracted beam monochromator was used. CuKα ($\lambda = 1.54$ Å) radiation under the operating conditions of 40 kV excitation voltage, 30 mA tube current, a step scan of 0.05 degrees/step with a 0.5 sec/ step counting time. A 60 watt light bulb, placed into the chamber , was the heat source for testing at 37°C ± 1°C. The test assembly is depicted in Figure 4.7. The temperature was measured before and after each scan with a thermometer placed near the sample holder. The X-ray scan was started 5 minutes after the specimen was locked into the sample chamber to allow the specimen to reach 37°C.

The spot size of the x-ray beam is approximately 1 cm^2. Under the most optimal conditions, the entire spot size would be filled uniformly with the specimen. The wires were bent and oriented such that the beam was focused on the area of maximum bending. But in actuality, the beam scanned regions that probably consisted of the maximum bend area, and the adjacent areas of the wires under less deformation and some of the background of the specimen holder. The specimen holder was a LiF single crystal designed to minimize the background.

UCSF LIBRARY

Figure 4.7. Assembly for Temperature Controlled XRD Testing.

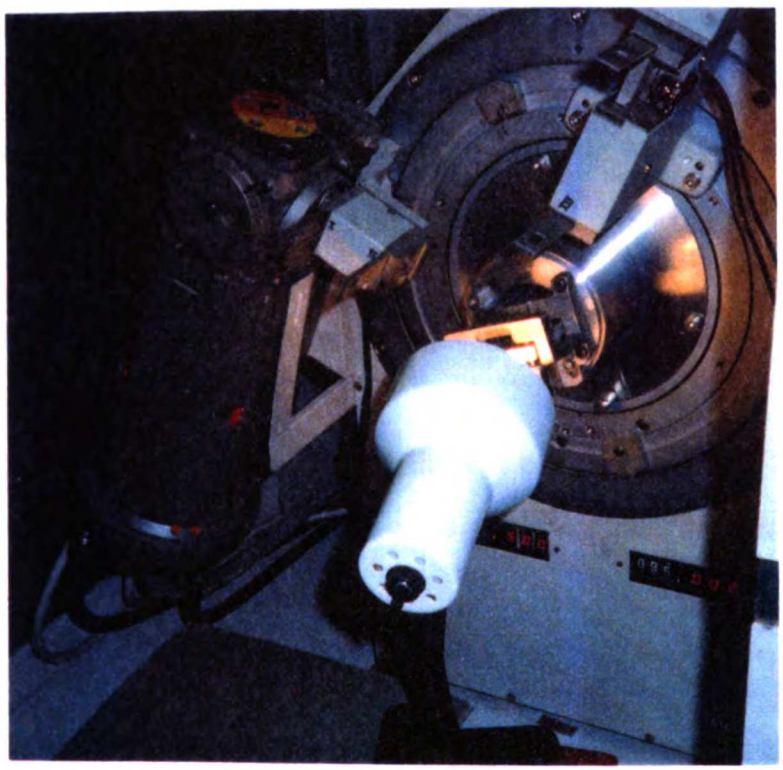

UCSF LIBRARY

4.7.2 *Data Analysis*

The x-ray diffractometer plots were analyzed by the computer directly using standards from the Joint Committee on Powder Diffraction Standards (JCPDS) for cubic austenite (18-899).[46] No JCPDS file exists for the martensite crystal structure determined by Kudoh et. al,[48] but the monoclinic martensite structure described by Otsuka[58](JCPDS 27-344) seemed to closely match some of the smaller peaks in the data. Thus only the likely presence or absence of martensite could be determined. This was complicated by the competing R-phase transformation, and its peak overlap. Data were generated as peak intensity (counts per second) versus angular position (2θ). It was expected that preferred orientation in the wires created slightly inaccurate peak intensities. Full width half maximum values and the integrated intensities of the most descriptive peaks were more useful and were calculated using DIFFRAC/AT Software, Socabim Sarc, Paris.

5. RESULTS

5.1 Chemical Composition

The data from EDS provides relative determinations of the amounts of Ni and Ti. Although other constituents may be present in trace amounts, EDS is not sensitive enough to detect small percentages reliably. The results are summarized in Table 5.1, categories 2 and 3, which lists the average of the 15 scans for each wire type (3 wires per sample, 5 spots randomly scanned in the center of each wire). The column under n represents the sample size.

Homogeneity within each wire was determined by comparing the at% Ni from each of the 5 scans along the wire using EDS. Some of the wires gave more variability in composition, as illustrated in Figure 5.1.

Figure 5.1. Relative at% Ni determination along the length of the Sentalloy SE wire, showing the greatest Ni variation in one sample.

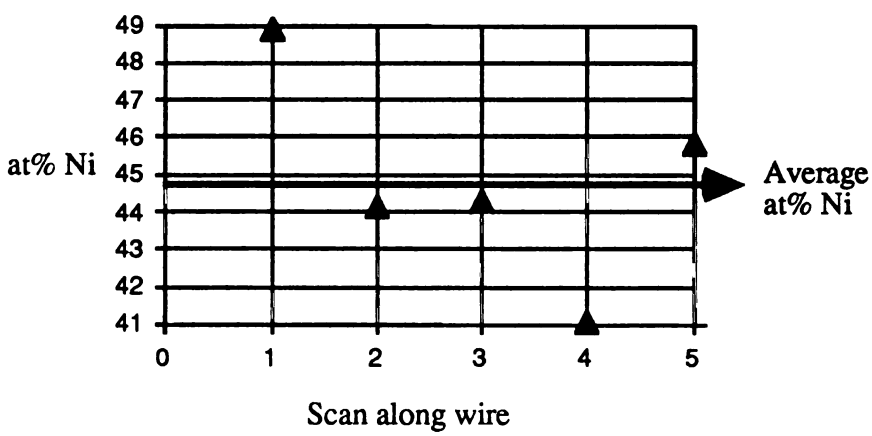

These histograms represent the wire with the least relative variability of the averaged 3 samples (Sentalloy SE) and the most variability (Nitinol SE), Figure 5.2. The variability shows deviations of up to 2 at%. It is expected that such deviations would not create significant mechanical and structural differences along the length of the wire, and are within the manufacturing tolerances for compositional control.

UNSW LIBRARY

Figure 5.2. Relative at% Ni determination along the length of the Nitinol SE wire, showing the least Ni variation in one sample

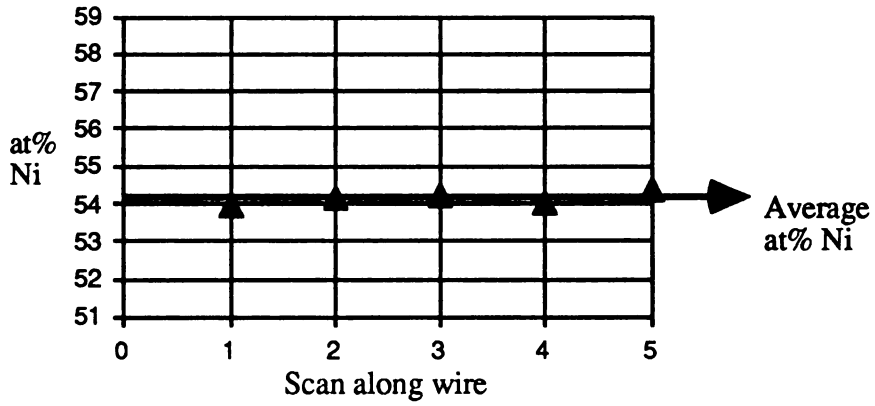

Trace amounts of cobalt and significant copper peaks were detected. Because of close proximity of Co and Cu to Ni in atomic number, the Co, Cu, and Ni peaks will be relatively close together. It is possible that these elements could exist in small percentages in the alloy, but their presence could not be confirmed under these operating conditions. Co is known to decrease the Ms, while Cu has stabilizing effects on the transformation by decreasing the hysteresis.[23] Since both of these effects are desirable for orthodontic applications, both elements are feasible additions.

UBC LIBRARY

5.2 Transformation Temperatures

The Af temperatures were measured, as shown in Table 5.1, categories 4 and 5. The SM wires of both brands had higher transformation temperatures than their SE counterparts in the as-received condition, as expected. While the transformation temperature could be reliably determined in 3 of the wire types, the Nitinol (SM) from Unitek showed considerable variability and so a third test was performed. The annealed SM wires had higher transformation temperatures (Af) than the annealed SE wires. The transformation temperature for the annealed SM type Nitinol was beyond the range of the testing scale. The difference between the annealed wire Af and the as-received Af for all wires was marked. For both brands of SE wire, the annealed Af was lower than the as-

received Af, while for the SM types, the annealed Af was above the as-received Af. This trend demonstrates the differences in processing to create SM and SE behavior in the wires.

In general, two types of strain profile curves emerged. Representative graphs are depicted in Figures 5.3 and 5.4. Figure 5.3 shows the sharp delineation of Af that was observed in the as-received and annealed Sentalloy (SE), as-received and annealed Neosentalloy (SM), and the annealed Nitinol SE wires. Figure 5.4 represents the as-received Nitinol SE and as-received and annealed Nitinol (SM) wires where the transformation temperatures were not as defined. Since the Af temperature was measured as the intersection of tangent drawn to the slope of the strain - temperature line, there was more variability in determination of Af in Fig. 5.4 simply because the slopes of the lines are not well defined. This variability is attributed to the coexistence of the R-phase.[59]

Figure 5.3. Strain as a Function of Temperature for wires with a definite Af.

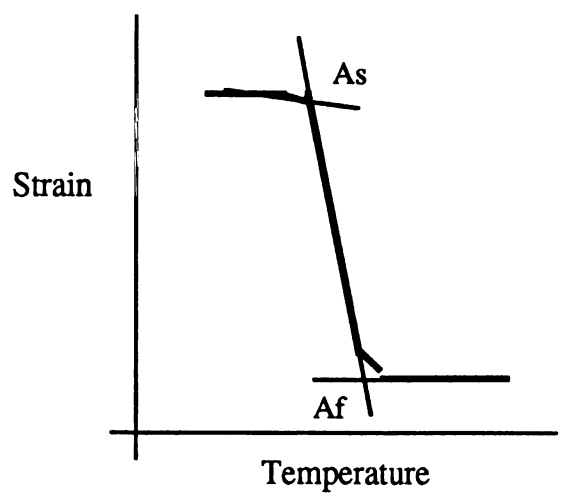

Figure 5.4. Strain as a Function of Temperature for wires showing R-phase interaction.

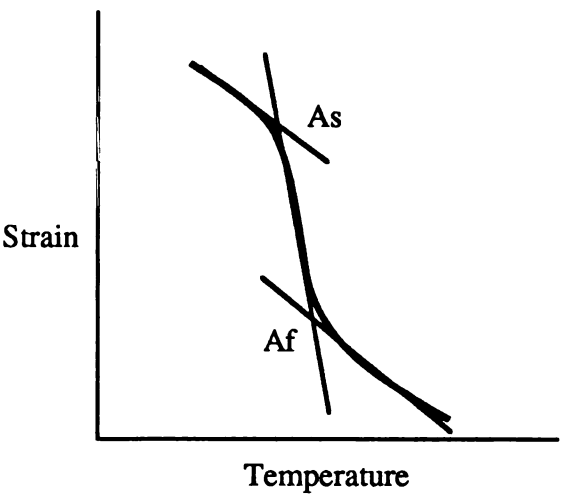

The Af temperatures of the wires after full anneal will directly indicate compositional differences. Since all the Af temperatures differ, the data show that all four wires have different chemical compositions (Table 5.1, category 5). In increasing Af temperature of the annealed wires,

Sentalloy (SE) < Nitinol SE < Neosentalloy (SM) < Nitinol (SM). This suggests that the lower Af temperature wires (Sentalloy (SE) and Nitinol SE) have a higher nickel content and the potential relation is depicted in Figure 5.5. It is also possible that the Af was lowered by intentionally alloying other elements into the Sentalloy (SE) and Nitinol SE wires. The EDS results, used as an adjunct to supplement the compositional determinations from the Af tests, are not in agreement with the Af tests of the annealed wires. The Af tests are a more reliable measure of nickel composition and will be used for relative composition determination

Figure 5.5. Relation of Transformation Temperature and Nickel Content as determined from the annealed wires.

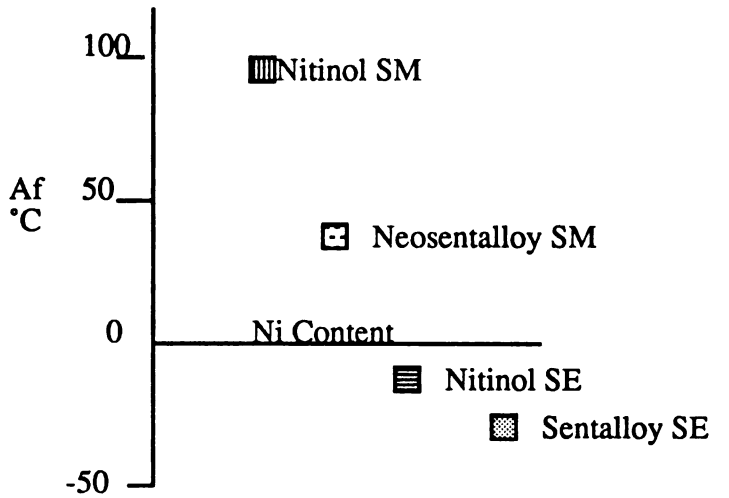

USNA LIBRARY

Table 5.1 : Summary of Chemical Composition, Transformation Temperature and Mechanical Properties

Property		n =	Sentalloy	Neo-sentalloy	Nitinol SE	Nitinol	p - value
1	Type		SE	SM	SE	SM	
2	at% Ni	15	47.4 ± 2.9	49.0 ± 0.6	54.0 ± 0.3	52.9 ± 1.7	$p < 0.01$
3	at% Ti	15	52.7 ± 2.9	51.0 ± 0.6	46.0 ± 0.3	47.1 ± 1.7	$p < 0.01$
4	Af (°C) As-received	2	23	26	16	29*	NS
5	Af (°C) Annealed	2	-15	31	-4	>95	$p < 0.01$
6	Loading Plateau (g) @ 22°C, As-received	3	340 ± 0	307 ± 8	521 ± 2	605 ± 22	$p < 0.01$
7	Loading Plateau (g) @ 37°C, As-received	3	463 ± 6	440 ± 10	617 ± 6	673 ± 38	$p < 0.01$
8	Unloading Plateau (g) @ 22°C, As-received	3	115 ± 13	119 ± 6	350 ± 2	420 ± 18	$p < 0.01$
9	Unloading Plateau (g) @37°C, As-received	3	173 ± 6	133 ± 6	400 ± 10	460 ± 0	$p < 0.01$
10	Hysteresis load drop (g) @ 22°C, As-received	3	203 ± 15	190 ± 4	181 ± 5	188 ± 21	n/a†
11	Hysteresis load drop (g) @ 37°C, As-received	3	279 ± 4	311 ± 8	220 ± 3	222 ± 33	n/a
12	Unrecovered Deformation (mm) @ 22°C, As-received	3	3	2	<1	<1	n/a
13	Unrecovered Deformation (mm) @ 37°C, As-received	3	<1	<1	<1	<1	n/a

*indicates the average of 3 tests, while all other reported temperatures are the average of 2 tests.
† n/a indicates not applicable.
NS indicates not significant

The data are graphically depicted in Figures 5.9 - 5.12 for each wire type, under the different test conditions.

USC LIBRARY

5.3 Mechanical Properties

As outlined, the five parameters that best describe the wire in clinical performance were defined as the heights and lengths of the loading and unloading plateaus, and the hysteresis load drop. The uncharacteristic yielding at larger strains is attributed to the design of the test, and not actual yielding of the specimen. So beyond the maximum height at loading and unloading, the data could not be used. Consequently the width of the loading and unloading plateaus were unable to be determined, but instead the maximum height of the plateaus were assessed, as listed in Table 5.1, categories 6 - 9. The data are illustrated in Figures 5.6 - 5.12. Each point on the graph represents the average of 3 data points. The variance for each test point was so minimal that it was not included on the graphs. The upper plateau depicts loading and represents the load levels necessary to insert the wire intraorally, while the height of the unloading plateau represents the load delivery during tooth movement.

The data (Table 5.1) and the figures indicated that all the wires in the as-received condition had different load deflection properties. ANOVA analysis indicated a significant difference ($p < 0.01$) between the loading levels of all the wires types, regardless of test temperature. Since there was so little variation in each data point, it was expected that these differences would be statistically significant. Furthermore, the unloading and hysteresis load drop differences between wire types were also significant, regardless of test temperature. These statistically significant differences indicated a true difference in mechanical behavior between the as-received wires. Multiple comparison tests using paired t-tests with Bonferroni corrections identified what groups demonstrated a significant difference. At 37°C for the loading and unloading plateaus, differences were found between all the wire types. The hysteresis load drop was significantly different between all groups except the Nitinol SE and Neosentalloy. It is important to recognize the statistically significant differences, and balance the results with the clinical significance of these differences.

UCSF LIBRARY

As the material is temperature sensitive, the data in Table 5.1 and Figures 5.2 and 5.3 show the sensitivity of the material properties to temperature. The difference in loading and unloading between the same wire tested at different temperatures is significant ($p<0.05$). There is on average a 100g difference in load delivery on loading and a 30g average difference on unloading when compared between room temperature and intraoral temperature. Deformation recovery improved in all of the wires tested at 37°C, as listed in categories 12 and 13 and Figure 5.7. This expected improvement was attributed to the complete reverse transformation to austenite at 37°C.

Figure 5.8 compares the mechanical performance of all the wires in the annealed state. All the wires display two inflection points where there is a small decrease in load at initial deflection under 1mm. This type of behavior is evident in all the wires, as-received and annealed, but it is more obvious in the annealed wires. It represents the plates of martensite (either existing if the Af temperature was greater than 22°C, or the nucleation of new plates if Af < 22°C) interacting with the dislocation tangle. This is a small effect and was evident in this study because of the testing parameters used to capture the low loads at small deflections.

UNSW LIBRARY

Figures 5.9 - 5.12 show the mechanical performance of each wire, when tested in 3-point bend under various conditions. The letters on the curves represent the corresponding structural and phases analyses studied at approximately the same amount of deformation. The consistent relationship depicted for all the wires showed that the loading and unloading plateaus were greater at 37°C than the 22°C, and as expected, the annealed wires of all wire types carried the lowest loading and unloading plateaus. Annealing changed the internal microstructure by decreasing the internal defects which led to lower yield strengths.

The hysteresis load drop is indicative of the different structures associated with the phase change.[42] Postulated as the frictional energy of twin boundary movement in martensite, clinically it represents

the load needed to tie the wire to the tooth. The hysteresis, listed as categories 10 and 11, Table 5.1, unexpectedly increased for all the wires when tested at 37°C compared to testing at 22°C.

Figure 5.6. Comparison of Load-deflection Properties of the As-received wires, tested at 22°C. n = 3 for each wire type. Upper curves represent loading, lower curves represent unloading. Range for Sentalloy, Neosentalloy and Nitinol SE data points = ± 8g. Range for Nitinol data points = ± 22g.

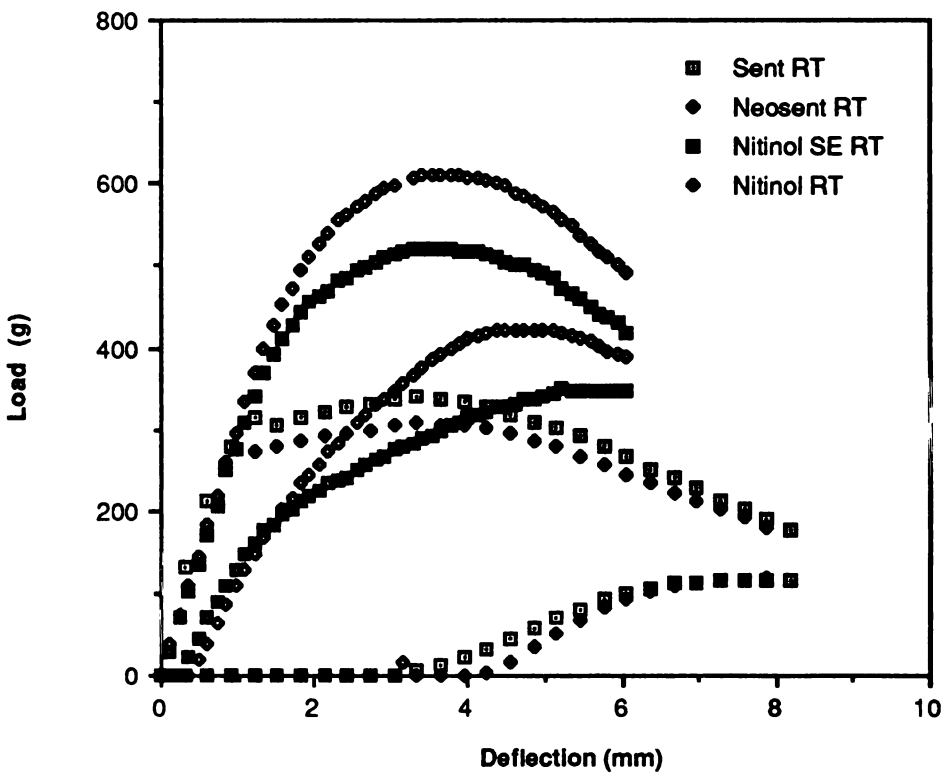

UCSF LIBRARY

Figure 5.7. Comparison of load-deflection properties of As-received wires, tested at 37°C. n = 3 for each wire type. Upper curves represent loading, lower curves represent unloading. Range for Sentalloy, Neosentalloy and Nitinol SE data points = ± 10g. Range for Nitinol data points = ± 38g.

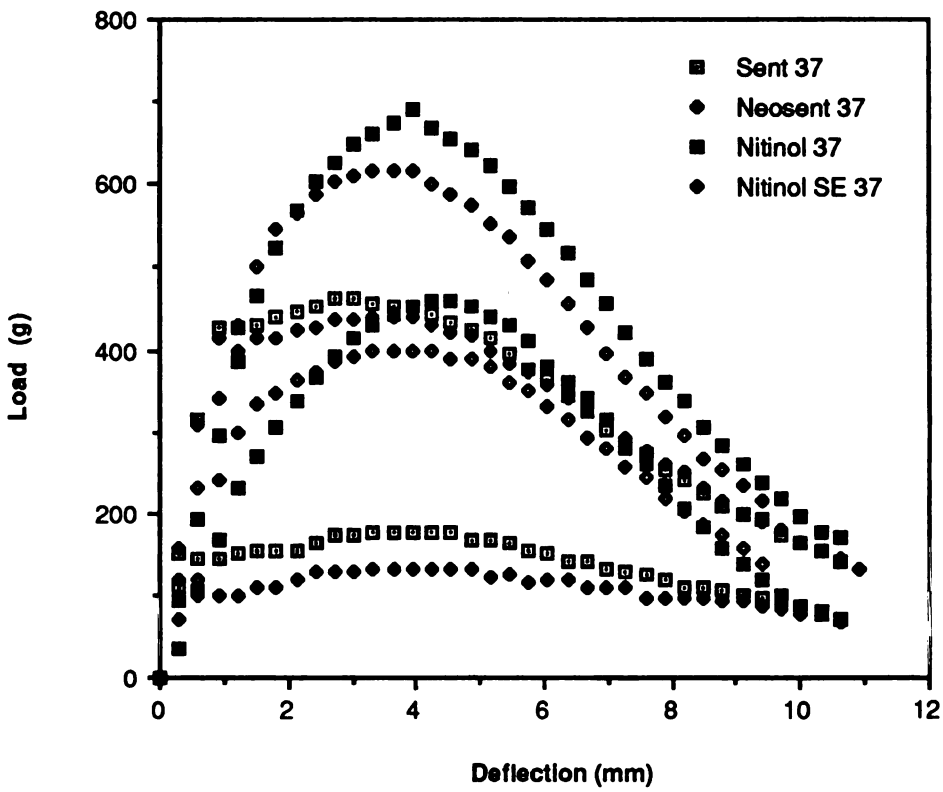

LIBRARY

Figure 5.8. Comparison of Load Deflection Properties of Annealed Wires. Td = 22°C, n=3 for each wire type. Upper curves represent loading, lower curves represent unloading.

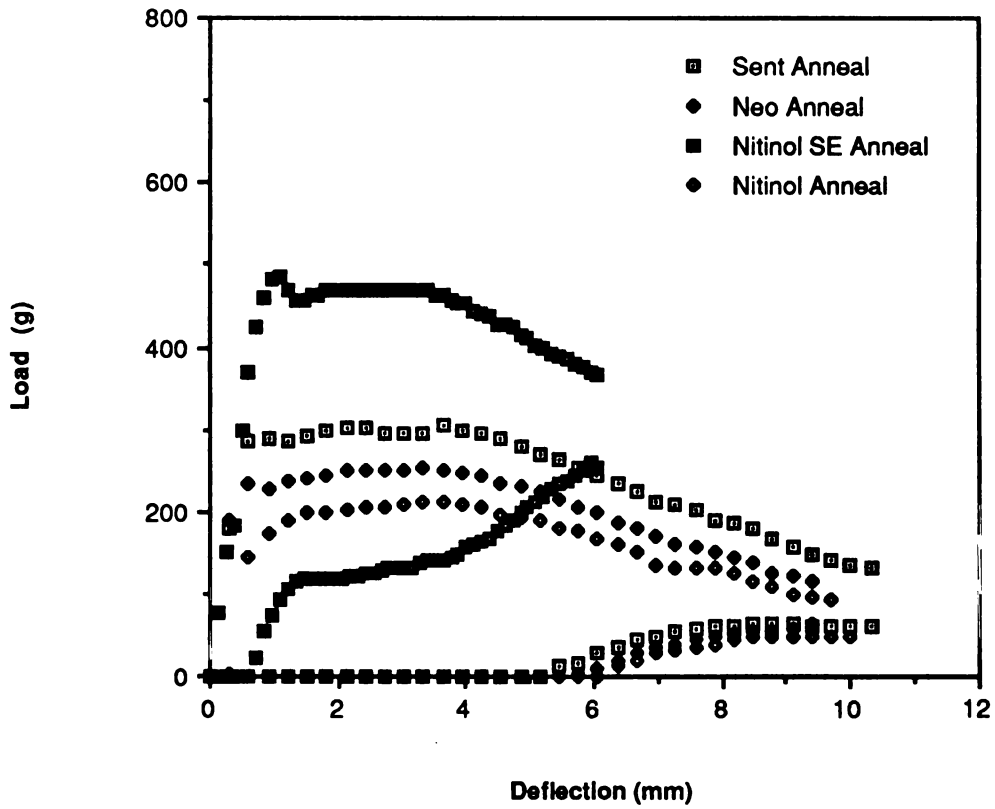

22g.

UCSF LIBRARY

Figure 5.9. Load-deflection Properties of Sentalloy (SE). Comparison of mechanical properties of the as-received wires, tested at different temperatures, and the annealed wires. n = 3 for each test. Upper curves represent loading, lower curves represent unloading. Points a, b, c represent the corresponding deformation in bending of 180°, 75°, 45°, respectively. Range for each data point = ± 13g.

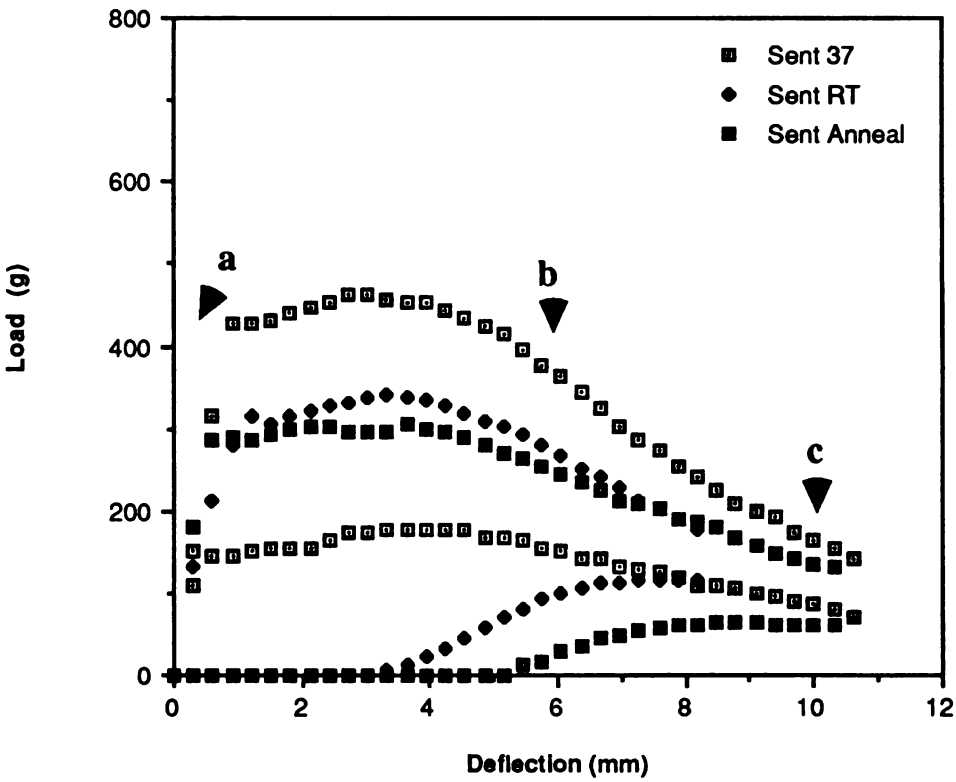

Figure 5.10. Load-deflection Properties of Neosentalloy (SM). Comparison of mechanical properties of the as-received wires, at different test temperatures, and the as-received wires. n = 3 for each test. Upper curves represent loading, lower curves represent unloading. Points a, b, c represent the corresponding deformation in bending of 180°, 75°, 45°, respectively. Range for each data point = ± 10g.

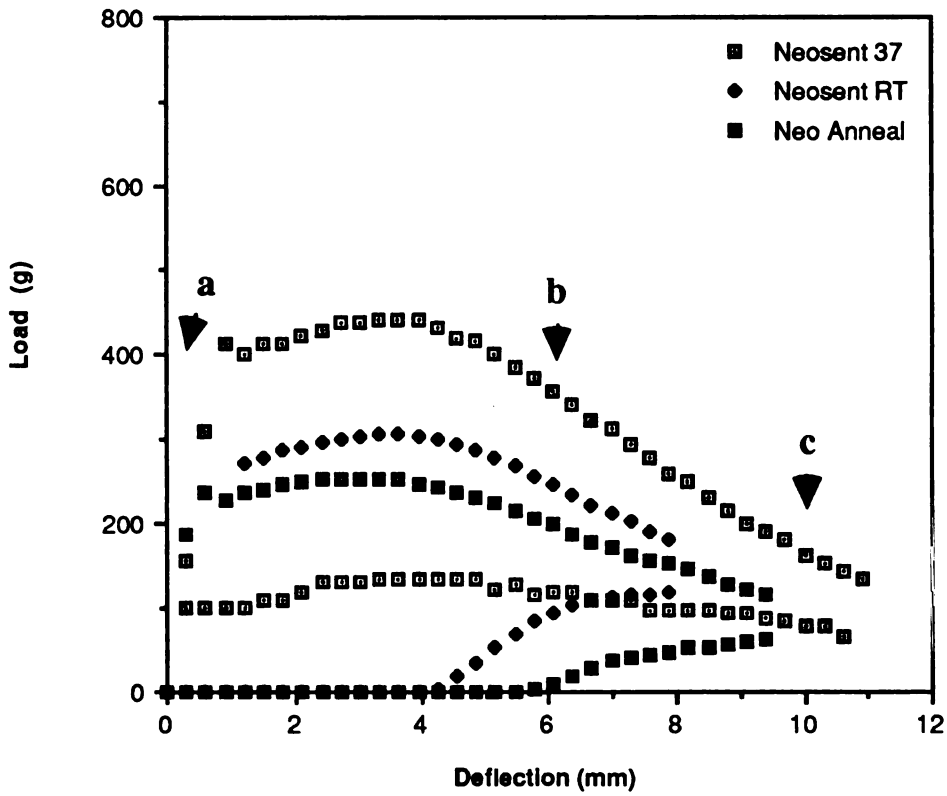

UCSF LIBRARY

Figure 5.11. Load-deflection Properties of Nitinol SE.
Comparison of mechanical properties of the as-received wires,
at different test temperatures, and the annealed wires. n = 3 for each test.
Upper curves represent loading, lower curves represent unloading.
Points a, b, c represent the corresponding deformation in bending of 180°, 75°,
45°, respectively. Range for each data point = ± 10g.

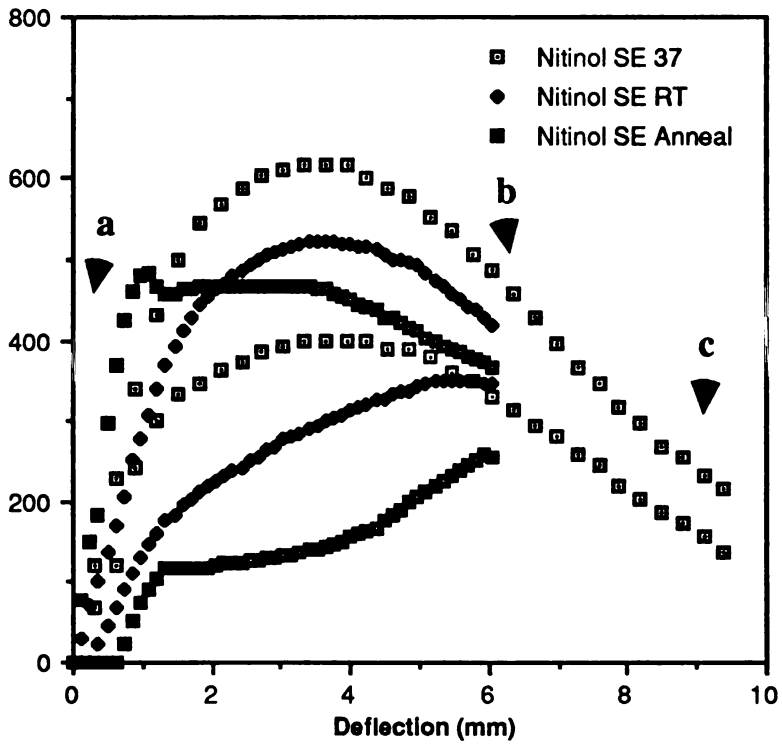

Figure 5.12. Load-deflection Properties of Nitinol (SM).
Comparison of mechanical properties of the as-received wires, at different test temperatures, and the annealed wires. n = 3 for each test. Upper curves represent loading, lower curves represent unloading. Points a, b, c represent the corresponding deformation in bending of 180°, 75°, 45°, respectively. Range for each data point = ± 38g.

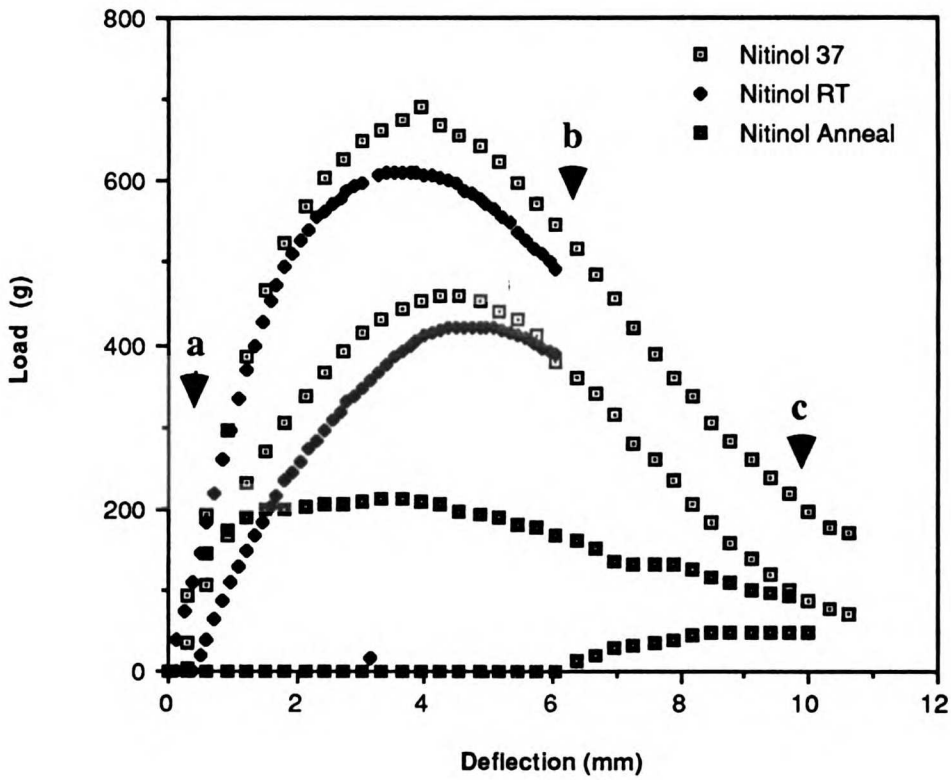

UOOT. LIBRARY

5.4 Microstructural Analysis

Each wire type was examined under SEM under two deformation states and as a straight section. The annealed sections were examined in straight sections only. Individual grains were difficult to detect using SEM. There were features common to all wire types, regardless of the amount of deformation. The voids seen in all specimens could have been dislocation etch pits (circular voids and elongated voids) or the result of etching out the internal oxides in the matrix (elongated voids). Some of the wires qualitatively appeared to contain more and larger voids than the others. The Nitinol (SM) wires appeared to have more internal defects than the other wires. If these voids were representative of some type of internal crystal defect, they would not be as prevalent in the annealed specimens, since annealing decreases the concentration of crystal defects. The direction of wire drawing is evident in all the wires, as it runs parallel to the direction of the voids. The white spots that appear on all the micrographs may be residual polishing compound, while the diamond shaped white deposits may be some chemical byproduct of the etchant reacting with the specimen. The inner and outer areas were examined separately, but no discernible differences in surface relief were found and so, for illustration, these inner and outer areas will not be separately designated. It was clear that the outer and inner areas of the wire were markedly different from the microstructure of the wire in the area of the central axis. This will be discussed in greater detail below.

For all wires, the corresponding mechanical properties are illustrated in Figs. 5.9 - 5.12. The points a, b, c on the load deflection plots correspond to the respective deformation on the micrographs labeled a, b, c. The Figures 5.13, a-d, depict the Sentalloy (SE) wire type in a progression from a straight section (Fig. 5.13a) to a bent section (Fig. 5.13b), to more of a bent section (Fig. 5.13c). This amount of deformation corresponds to the respective a, b, and c points on the load deflection diagram, Figure 5.5. Fig. 5.13d is the straight annealed section. The straight as-received (Af = 23°C, Td = 22°C) section (Fig. 5.13a) showed much surface relief. Fine striations which appear as twin bands were interspersed in the matrix. These twin bands

occurred at approximately 50 - 60 degrees to the direction of drawing in the wire. Under deformation, of approximately 75 degrees, the surface relief of the twin bands was more evident and consumed more of the matrix (Fig. 5.13b). These twin bands were again measured at 50-60 degrees to the drawing direction. Finally under greater deformation (Fig. 5.13c), the entire matrix was consumed with the herringbone twin structure that appeared to be martensite. These twin bands could either be martensite twins, or deformation twins. Verifying its crystallite structure-orientation using either transmission electron microscopy or selected area diffraction or powder diffraction techniques would define the nature of twin structures. This can be contrasted to the microstructure of the annealed Sentalloy (SM) specimen (Fig. 5.13d). Under our annealing conditions, the entire structure should convert to the parent phase, since Af = -15°C, Td = 22°C.

Similar structures were evident in the Neosentalloy (SM) wire (Fig. 5.14, a-c). The as-received specimen (Af = 26°C, Td = 22°C) showed surface relief and twin bands in a direction of 50-60 degrees to the drawing direction. As the strain on the specimen increased, the surface relief of the twin bands was more apparent. Fig. 5.14c does not follow this trend. The annealed Neosentalloy (Af = 31°C, Td = 22°C) microstructure differed from the Sentalloy annealed microstructure in that only a herringbone twin pattern was seen, and less of a grain structure was detected.

The Nitinol SE microstructures (Fig. 5.15, a-d) had noticeable surface relief. The annealed microstructure of the Nitinol SE (Af = -4°C, Td = 22°C) displayed a much more uniform grain structure than any of the other micrographs. Equiaxed grains that appear to be austenite were clearly outlined, similar to the structures seen in the annealed Sentalloy (SE) specimen (Fig. 5.13d). It is possible that they were either highly twinned or martensite has formed within the original austenite grains, or it may represent the R-phase.

The Nitinol (SM) as-received wires (Fig. 5.16, a-d) also showed surface relief (Af = 29°C, Td = 22°C), but the twin bands that were seen in the Sentalloy (SE) and Neosentalloy (SM) were not as

evident. This surface relief is in the form of broad lines across the surface measured at approximately 40-50 degrees to the drawing direction. These lines were seen on the outer and inner surfaces of all the wires regardless of the deformation state, and may represent variants of stress induced martensite.

POOR QUALITY

Figure 5.13, a-d. Micrographs of Sentalloy (SE) wire. a. As-received, straight section, 180° b. As-received, 75° bend, c. As-received, 45° bend, d. Annealed, straight section. Twin Bands (A), Herringbone twins (B), Equiaxed grains (C), and R-phase (R) are evident and marked in the micrographs. The micrographs are oriented to show the vertical drawing direction (long axis) of the wire.

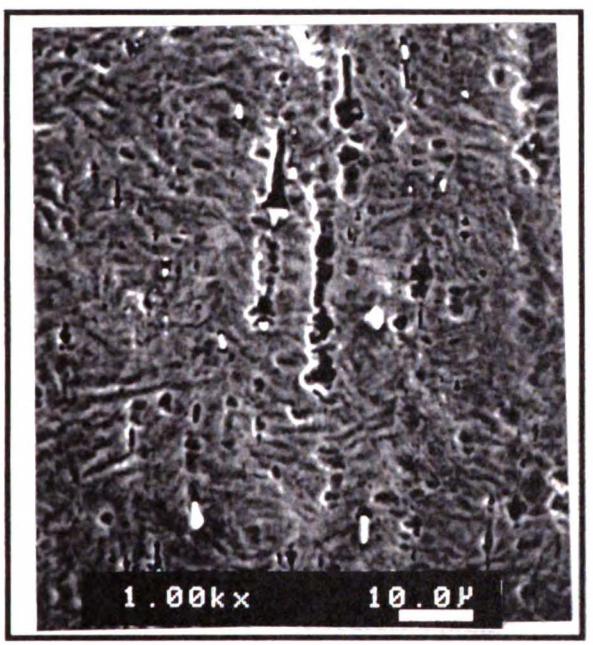

Fig. 5.13a

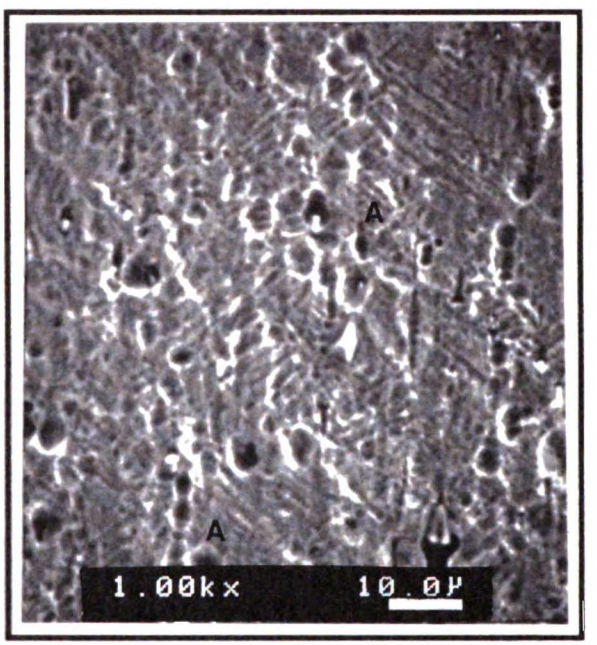

Fig. 5.13b

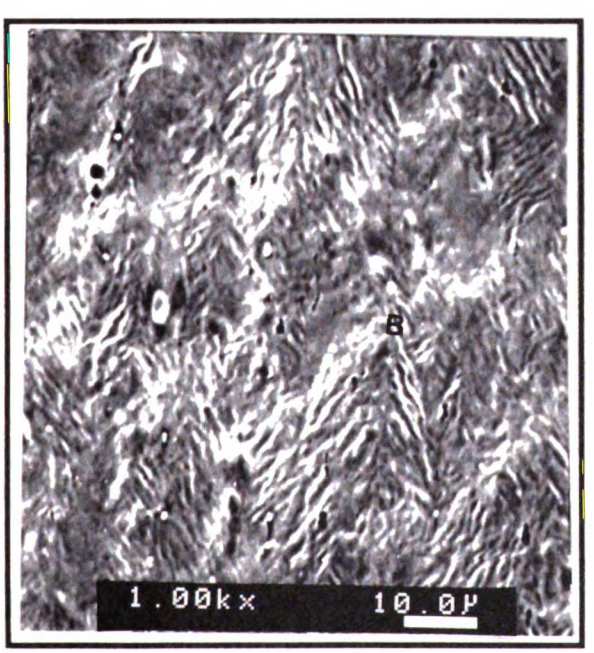

Fig. 5.13c

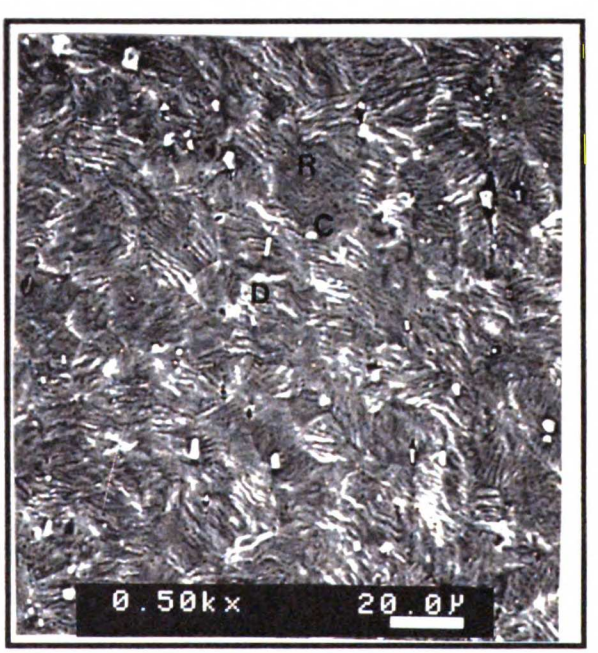

Fig. 5.13d

Figure 5.14, a-d. Micrographs of Neosentalloy (SM) wire. a. As-received, straight section, 180° b. As-received, 75° bend, c. As-received, 45° bend, d. Annealed, straight section. Twin Bands (A), Herringbone twins (B), Equiaxed grains (C), are evident and marked in the micrographs. The micrographs are oriented to show the vertical drawing direction (long axis) of the wire.

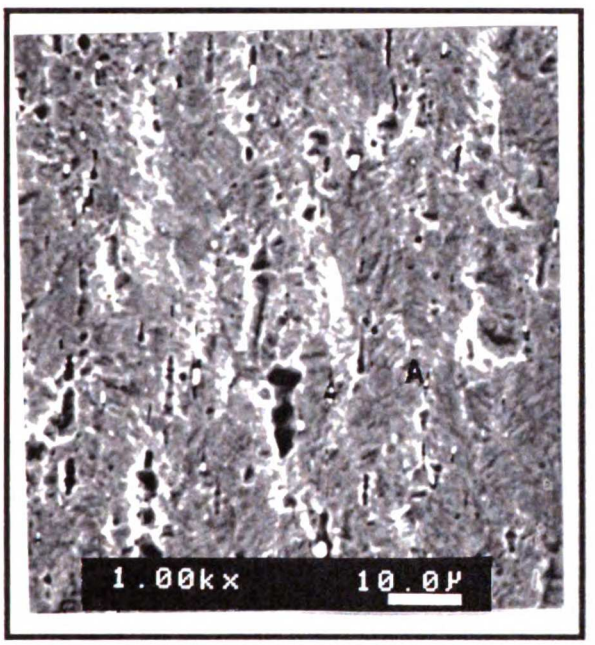

Fig. 5.14a

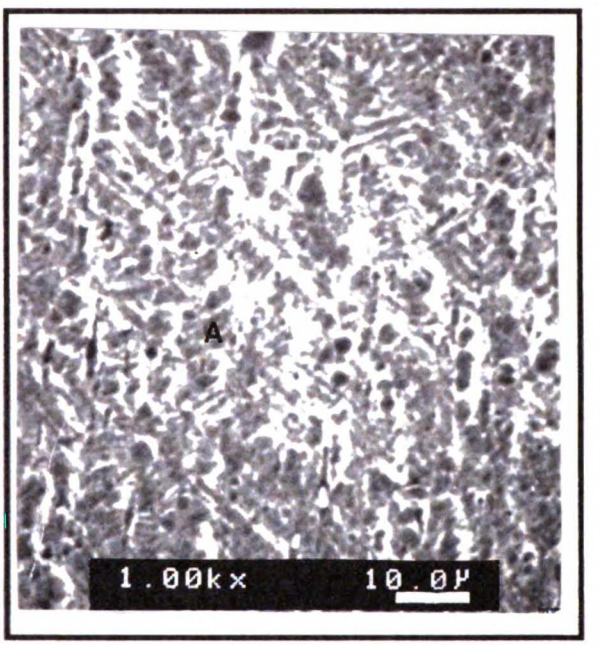

Fig. 5.14b

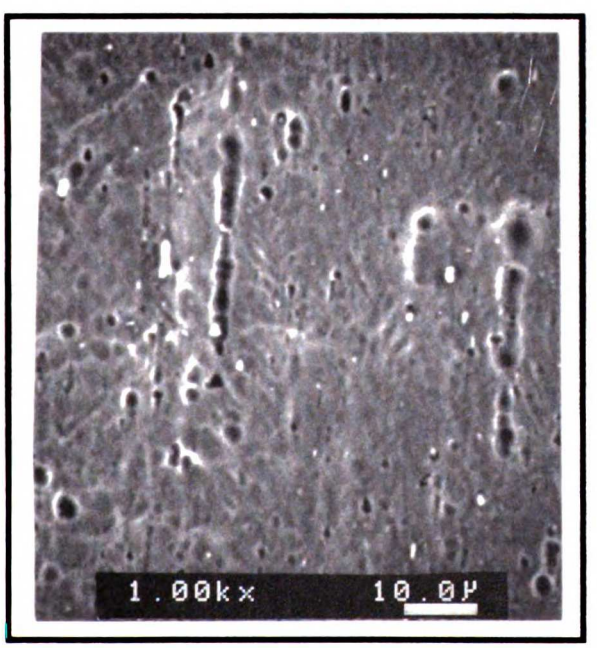

Fig. 5.14c

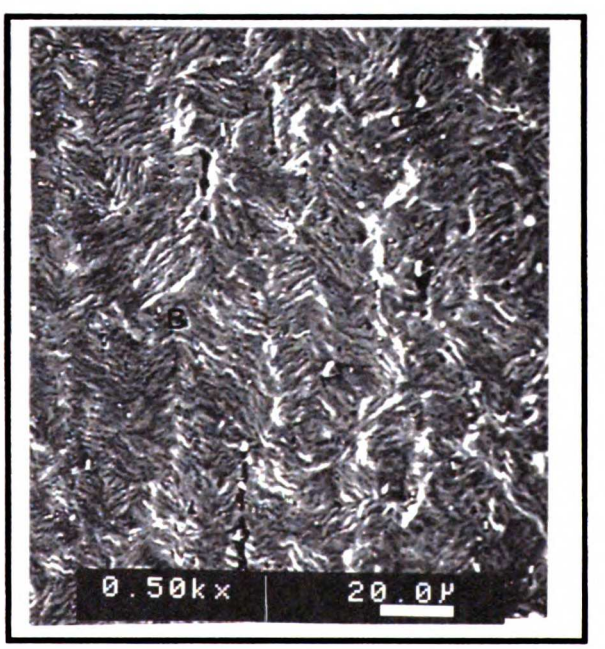

Fig. 5.14d

Figure 5.15, a-d. Micrographs of Nitinol SE wire. a. As-received, straight section, 180° b. As-received, 75° bend, c. As-received, 45° bend, d. Annealed, undeformed. Twin Bands (A), Herringbone twins (B), Equiaxed grains (C), and R-phase (R) are evident and marked in the micrographs. The micrographs are oriented to show the vertical drawing direction (long axis) of the wire.

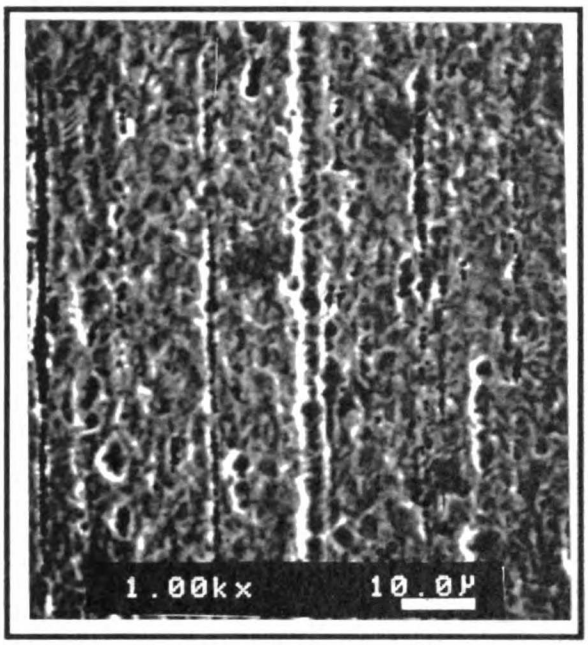

Fig. 5.15a

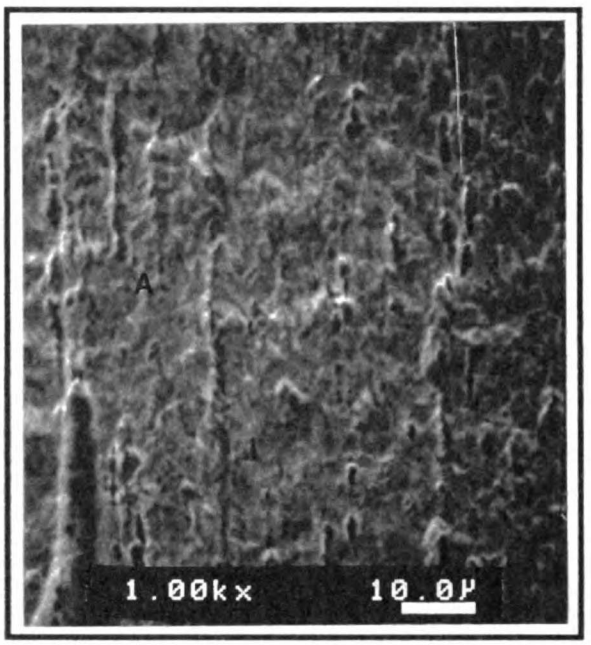

Fig. 5.15b

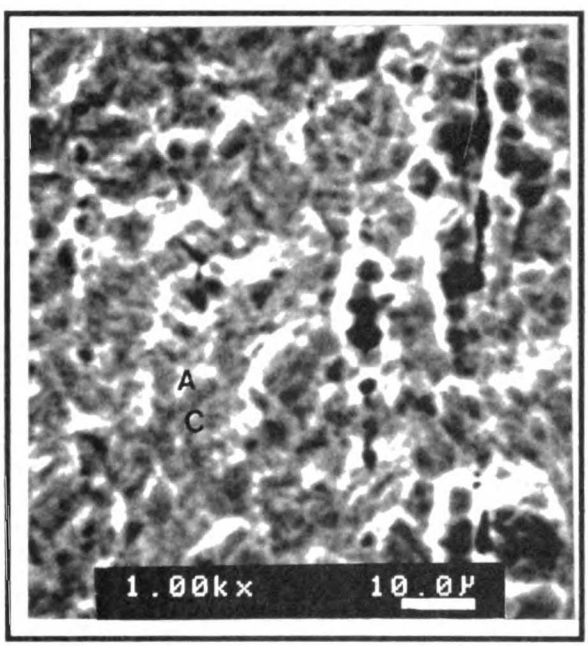

Fig. 5.15c

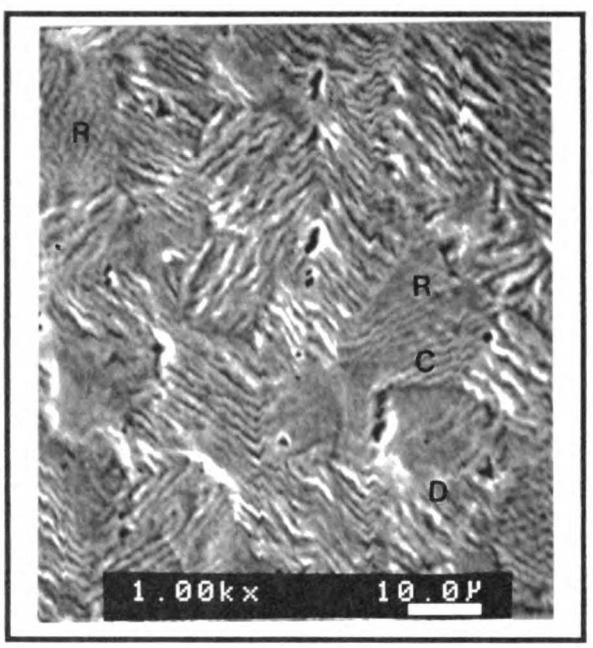

Fig. 5.15d

Figure 5.16, a-d. Micrographs of Nitinol (SM) wire. a. As-received, straight section, 180° b. As-received, 75° bend, c. As-received, 45° bend, d. Annealed, straight section. Twin Bands (A), Herringbone twins (B), Equiaxed grains (C), are evident and marked in the micrographs. The micrographs are oriented to show the vertical drawing direction (long axis) of the wire.

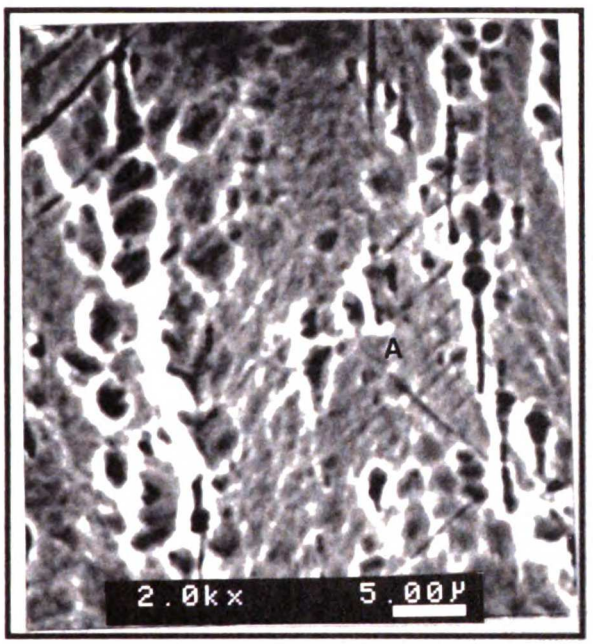

Fig. 5.16a

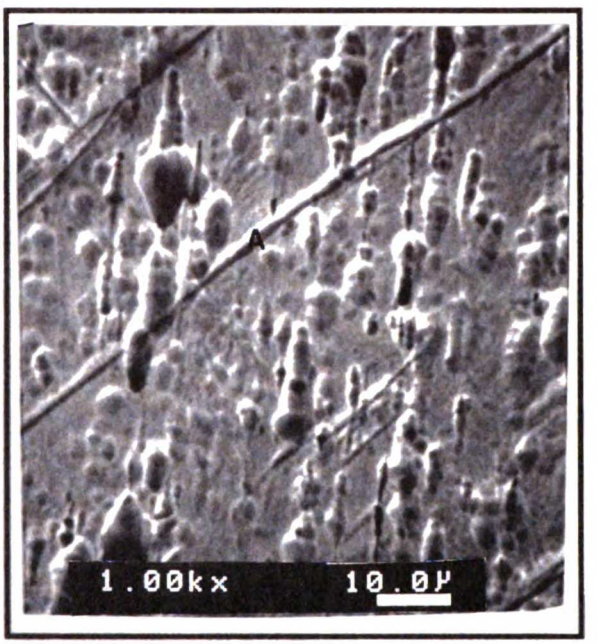

Fig. 5.16b

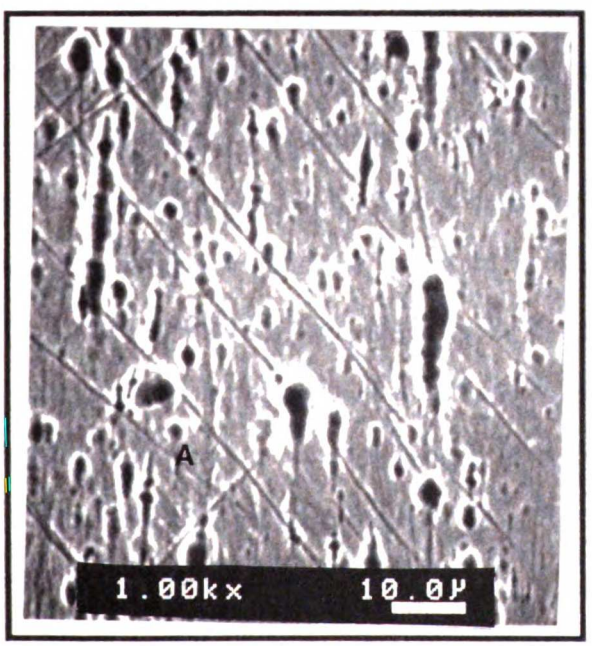

Fig. 5.16c

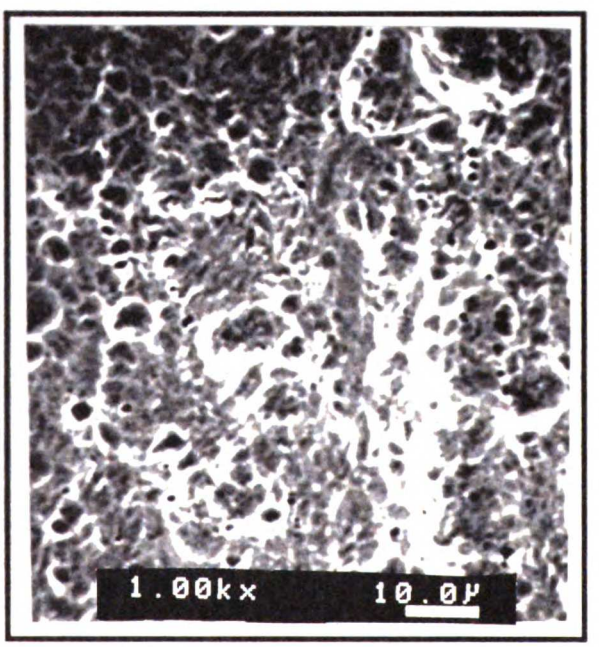

Fig. 5.16d

5.5 X-ray Diffraction

X-ray diffraction permitted the evaluation of phase differences among the wires. The diffraction plots for all wires are in Figures 5.22 - 5.29, a-c. Each series a-c represents the diffraction plots of the same wire at different levels of strain. Data were reported as the integrated intensity of the diffracted beam (in counts per second, cps). The number above each peak represents the calculated interplanar spacing. For all wires, discernible peaks were found near the 42° and 77° 2θ positions. The integrated intensities and the full width half-maximum (FWHM) of the strongest peaks were calculated using a computer peak fit program. The data were evaluated to describe several different types of relationships between the wires : difference in phases between the annealed and as-received wire, differences in phases of each wire under deformation. The calculated counting statistics were approximately 5% in peaks of 500 cps so the differences illustrated in the graphs may not be statistically significant.

As explained in the introduction, annealing relieves internal residual stress by allowing the dislocations to move so that portions of the matrix are actually dislocation free.[11,21,45] Depending on the conditions of annealing, internal residual stress can be completely eliminated. Since residual stress creates nonuniform strain in the matrix, the peak positions in diffraction will not change, but the peak intensity will decrease and the peaks will become broader. If uniform strain is present, the peak positions may shift, but the peak intensities and peak widths will not be affected. The FWHM provides adjunctive information to the integrated peak intensity because it provides information about the shape of the peak. Processing affects not only the relative amounts of the phases present, but also the sharpness or broadness of the peaks because it leads to a preferred orientation in a wire. The type of thermomechanical heat treatment may be inferred from the FWHM since different thermomechanical treatments affect crystal size and shape which is reflected in the peak shape.

From all the diffraction plots, the strongest peak at 42° corresponds to the (110) plane of cubic austenite, while the peak at 77° corresponds to the (211) plane. This strongly suggests that austenite is the principal phase, and is supported by direct comparison of the peaks with the JCPDS file for cubic austenite (18-899). Since the as-received wires were examined at 37°C, the wire should be entirely austenitic, as tests were conducted at temperatures greater than the Af for all the wires. If the composition were not equiatomic NiTi, then there would be other phases present. Additionally, the R-phase may exist at temperatures above Af. Thus broader peaks at the austenite positions could result from nonuniform strain or the presence of other phases.

The change in the integrated intensity of the largest peak was studied at different levels of strain. The variability in the results from the XRD work yield a standard deviation of approximately 5% of the integrated intensities. On the diffraction plots, the range of the integrated intensity calculated for the (110) peak was $\pm$ 40 cps. The differences among wires with similar integrated intensities may not be real. Both the shape memory and superelastic wires from both manufacturers showed an unexpected relationship. Representative graphs are shown in Figure 5.17 and 5.18. Since the largest peak corresponds to austenite, the intensity of this peak should decrease as the specimen is strained to produce SIM. Both the as-received and the annealed wires showed a decreased peak intensity at a 75° bend, but the intensity increased under greater strain at a 45° bend. The dip in intensity at the 75° bend may represent the R-phase that forms at intermediate strain. As mentioned earlier, the R-phase and martensite have peak positions near austenite, making quantification of either phase inconclusive due to peak overlap. The R-phase is a competing reaction for martensite. There definitely is a phase change occurring, but its exact nature cannot be determined from these results.

Figure 5.17. Integrated Intensity of (110) peak vs. Deformation (Bend Angle) Nitinol SE. 42.1 – 42.4 2θ

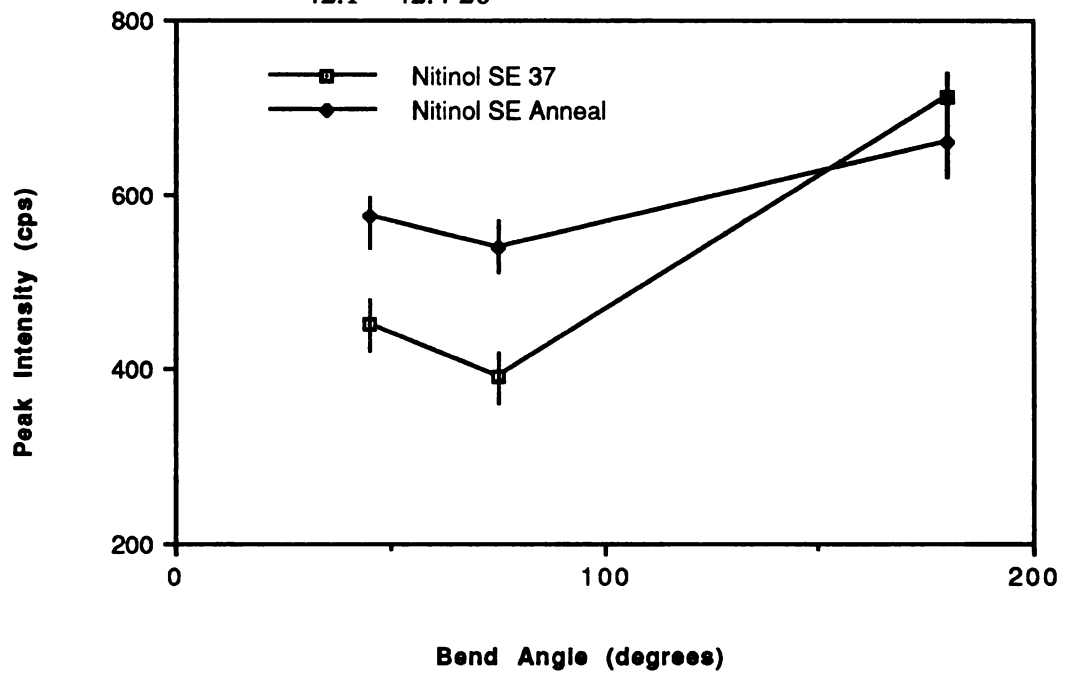

Figure 5.18. Integrated Intensity of (110) peak vs. Deformation (Bend Angle) Neosentalloy (SM). 42.1 – 42.4 2θ

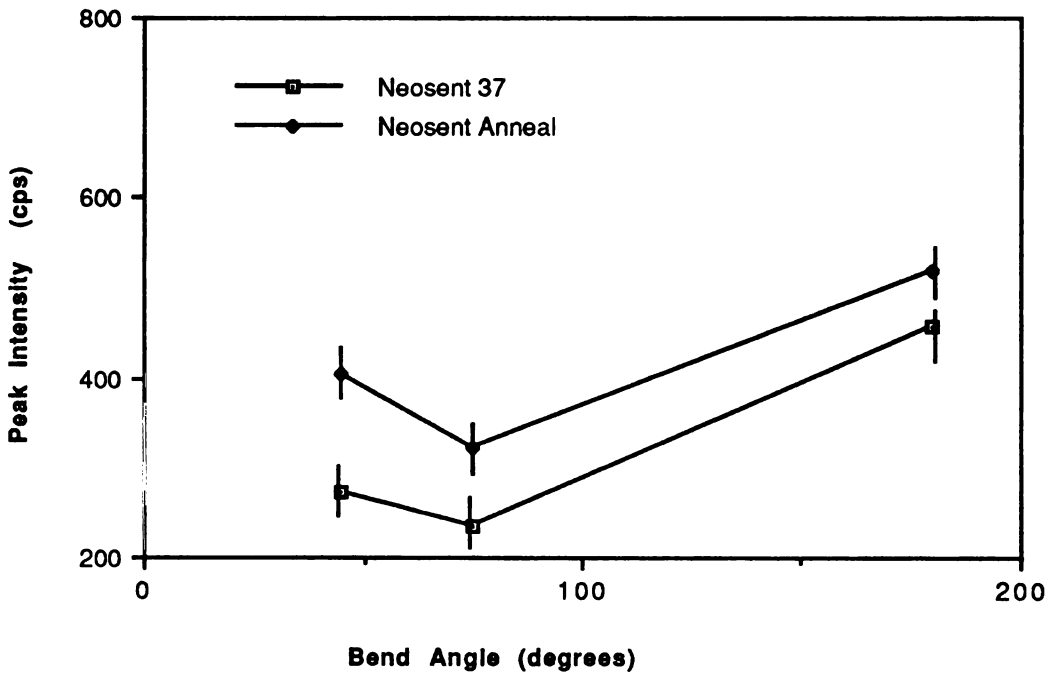

Comparison of the integrated intensities and the FWHM of the as-received wires to the annealed wires showed phase differences due to processing. In the straight section specimens, the intensity of the strongest peak differed between the as-received wires and the annealed wires. This relationship is depicted in Figure 5.19 below. The annealed shape memory type wires, Neosentalloy and Nitinol (Af > 22°C), had a lower peak intensity than in their straight as-received state, whereas the annealed superelastic type wires, Sentalloy and Nitinol SE (Af < 22°C), had a greater peak intensity as compared to the as-received straight section wires. As expected, the FWHM decreased in all the annealed specimens because annealing decreased the residual stress. There was little difference in the FWHM of the annealed and the as-received Sentalloy (SE) and Neosentalloy (SM) wires. Comparing the other two brands, the Nitinol SE and Nitinol (SM), had an increased FWHM for the as-received wires versus the annealed wires. This is probably the result of cold work or other processing of the alloy or secondarily due to other phases which may be present that have similar line intensities to create peak overlap and broadening of the diffraction peaks.

Figure 5.19. Integrated Intensity of (110) peak from the undeformed annealed and as-received wires at 42.1-42.4° 2θ. Range for each data point = ±50cps. FWHM values are listed above each column for each respective wire.

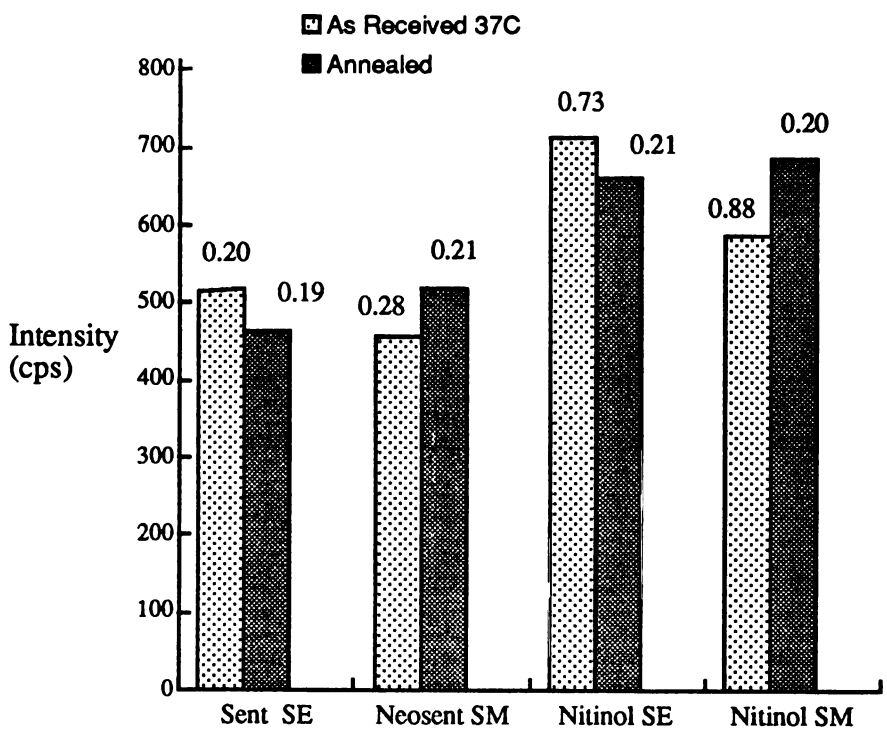

The FWHM values were calculated for all the annealed straight section specimens. The FWHM values were relatively the same for the strongest peak, near 42° 2θ, indicating that the effects of processing were removed and there was no line broadening due to potential peak overlap of other phases. Since the FWHM did not change in the as-received Sentalloy and Neosentalloy wires, probably there was little cold work in the as-received wires and the wires were completely austenitic in the as-received condition. The FWHM did change for the Nitinol (SM) and Nitinol SE wires. Since the undeformed wires should be completely austenitic at test temperature (Af<37°C), the larger FWHM of the as-received Nitinol (SM) and Nitinol SE wires versus the annealed wires was due primarily to cold work.

The FWHM of all wires, as-received and annealed, slightly increased as the wires were deformed. As an example, Figure 5.20 below illustrates this increase in the as-received wires tested at 37°C. There is a clear distinction between the FWHM of the Unitek brand, Nitinol SE and Nitinol SM, wires compared to the GAC brand wires, Sentalloy SE and Neosentalloy SM. Similarly, both brands have different patterns. The Nitinol SE and Nitinol SM as-received wires show an inflection point at intermediate bends, which is the exact opposite relationship of the peak intensity to the bend angle (or amount of deformation). Figure 5.21 shows the FWHM of the annealed wires under different states of deformation. In the undeformed state, all wires have similar FWHM values. This indicates that the annealing conditions affected all the wires in the same way, causing peak sharpening and possibly even larger grain sizes.

A final observation of the annealed plots for all the wires show additional peaks at various positions along the scan. These peaks are of lower intensity than the well defined peaks occurring at ≈ 42° and 77°. Comparison of the d spacings of these peaks suggests that these additional peaks are oxides. These peaks are consistent with titanium oxides or nickel titanium oxides.

Figure 5.20. FWHM as a function of the amount of deformation, of the as-received wires, tested at 37°C.

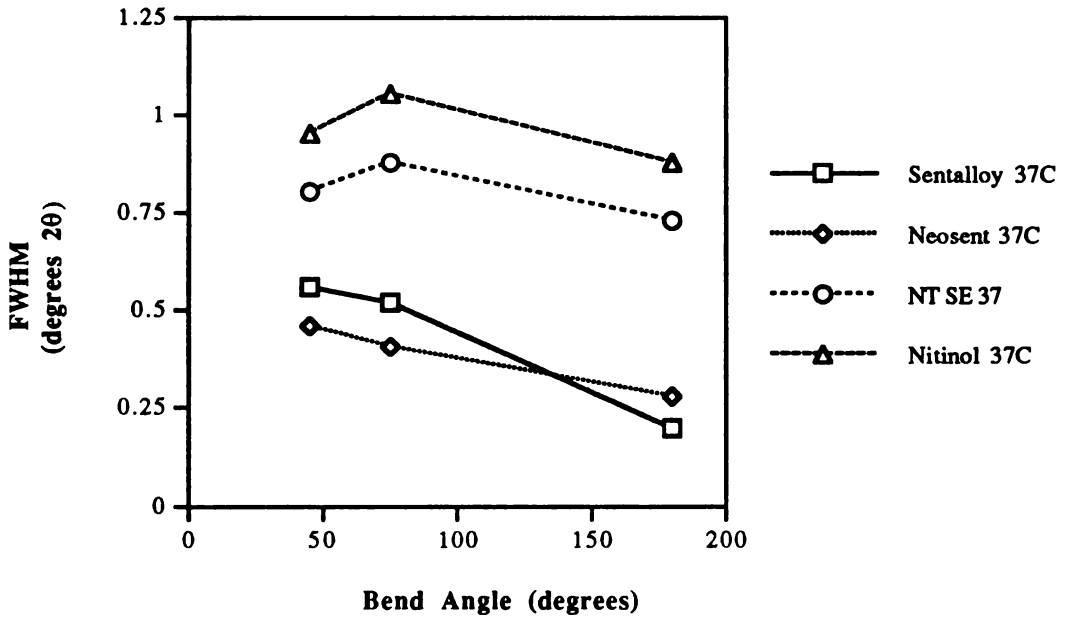

Figure 5.21. FWHM as a function of the amount of deformation in the annealed specimens

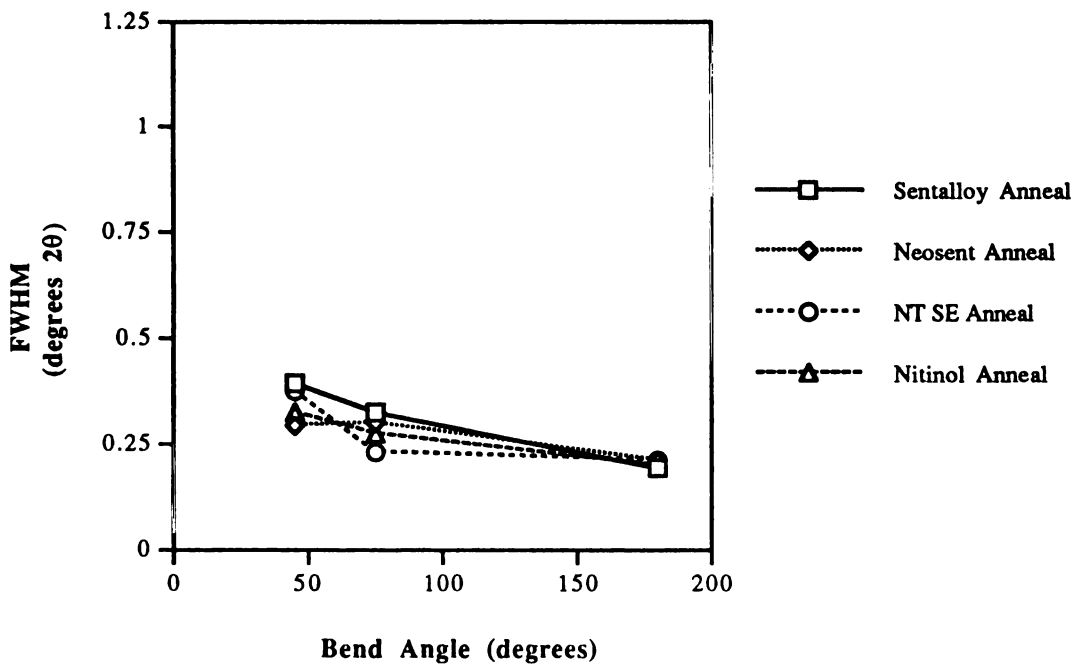

Figure 5.22, a-c. XRD patterns of Sentalloy (SE) as-received wires in
a. straight section 180°,
b. 75° bend,
c. 45° bend.
Temperature at 37°C.

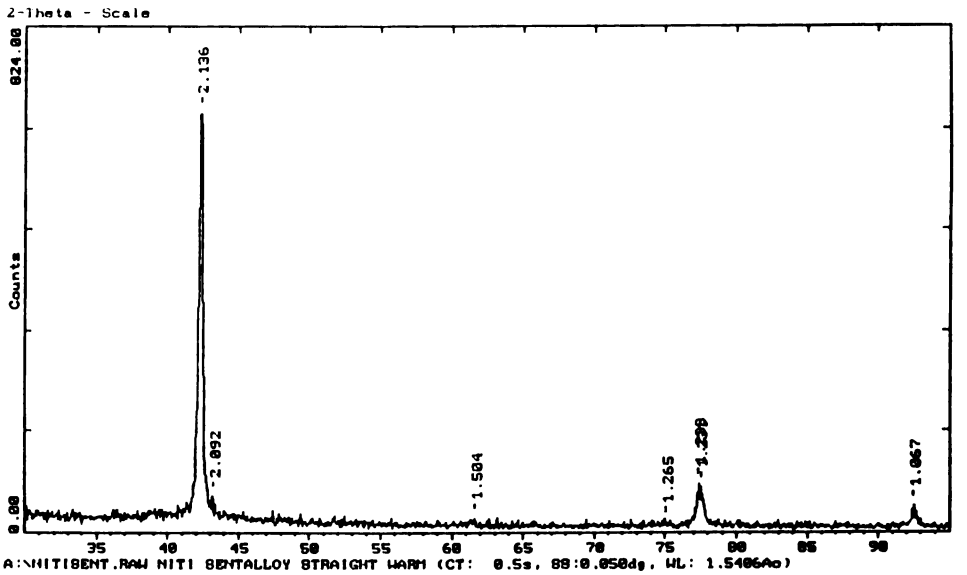

Fig. 5.22a

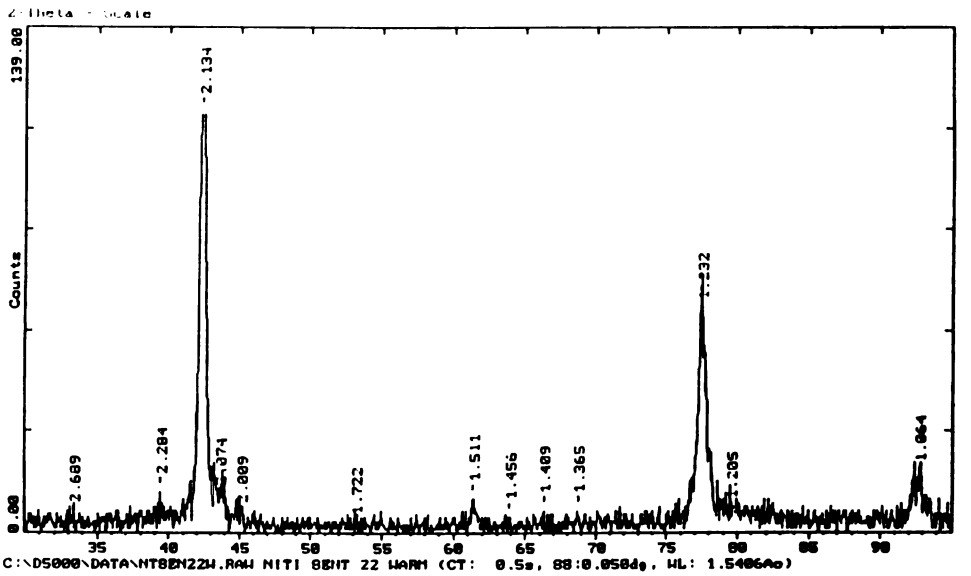

Fig. 5.22b

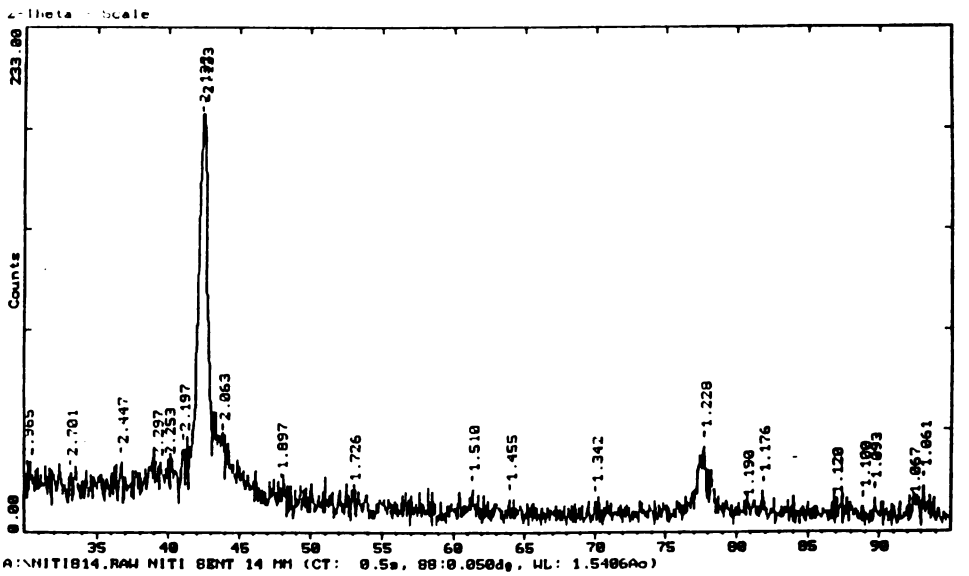

Fig. 5.22c

Figure 5.23, a-c. XRD patterns of Sentalloy (SE) annealed wires in
a. straight section, 180°,
b. 75° bend,
c. 45° bend.

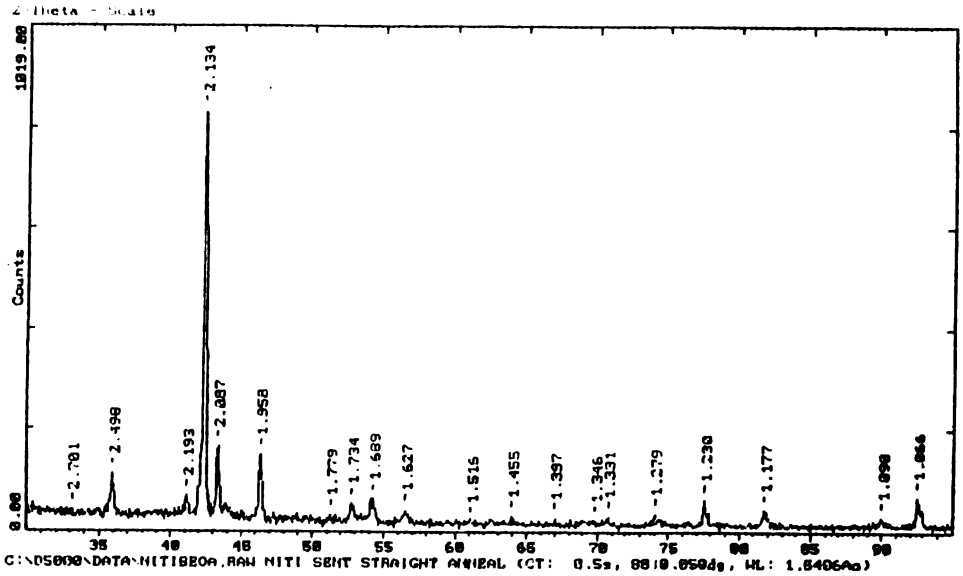

Fig. 5.23a

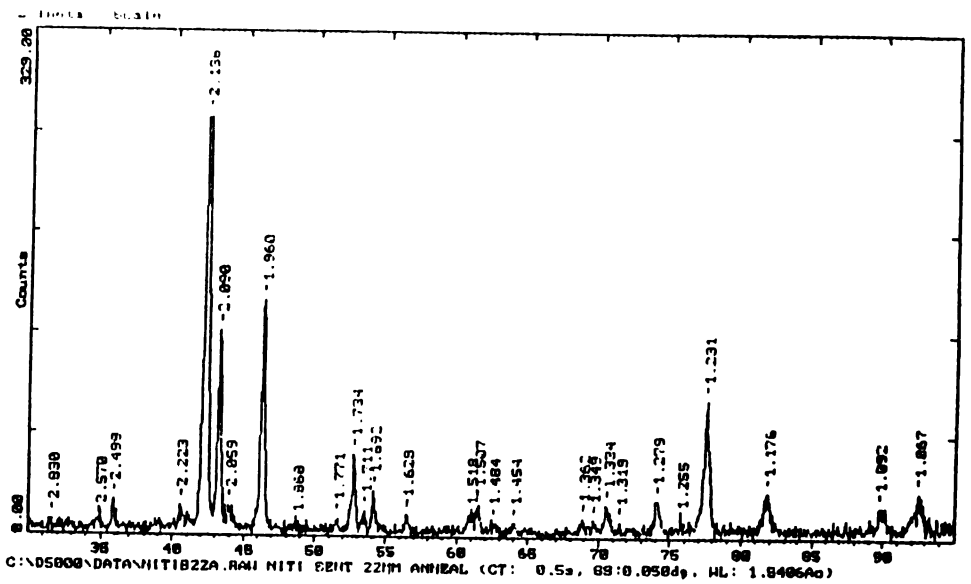

Fig. 5.23b

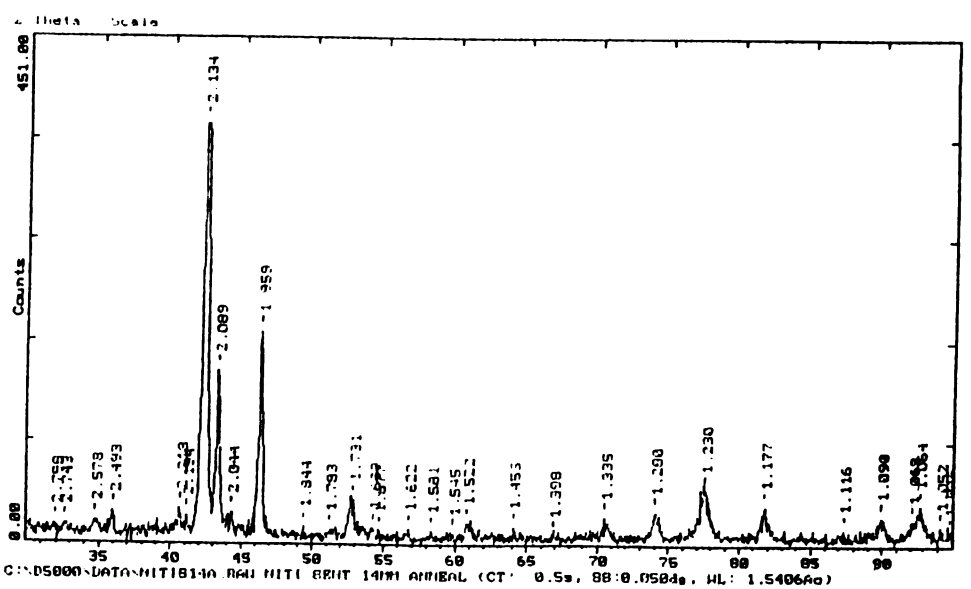

Fig. 5.23c

Figure 5.24, a-c. XRD patterns of Neosentalloy (SM) as-received wires in
a. straight section, 180°,
b. 75° bend,
c. 45° bend.
Temperature at 37°C.

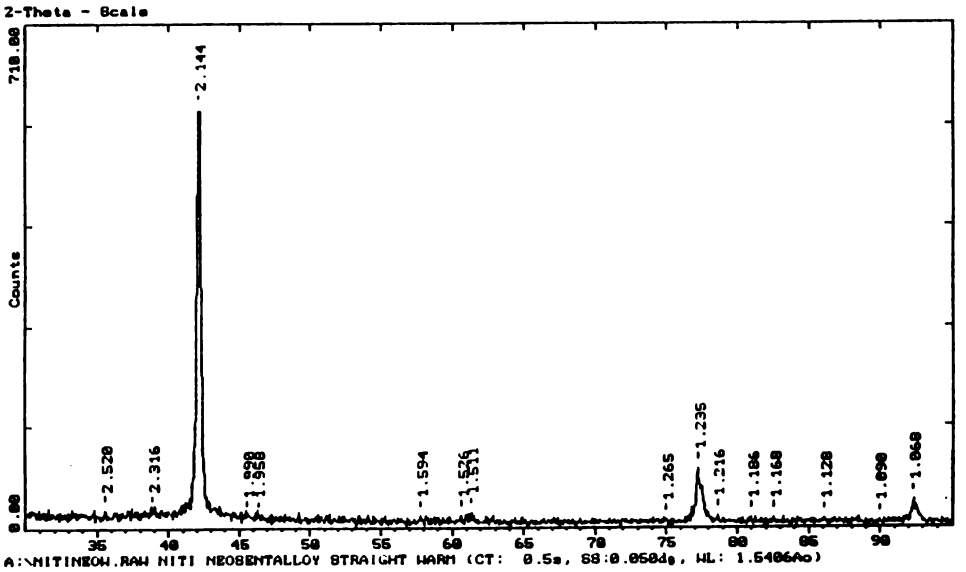

Fig. 5.24a

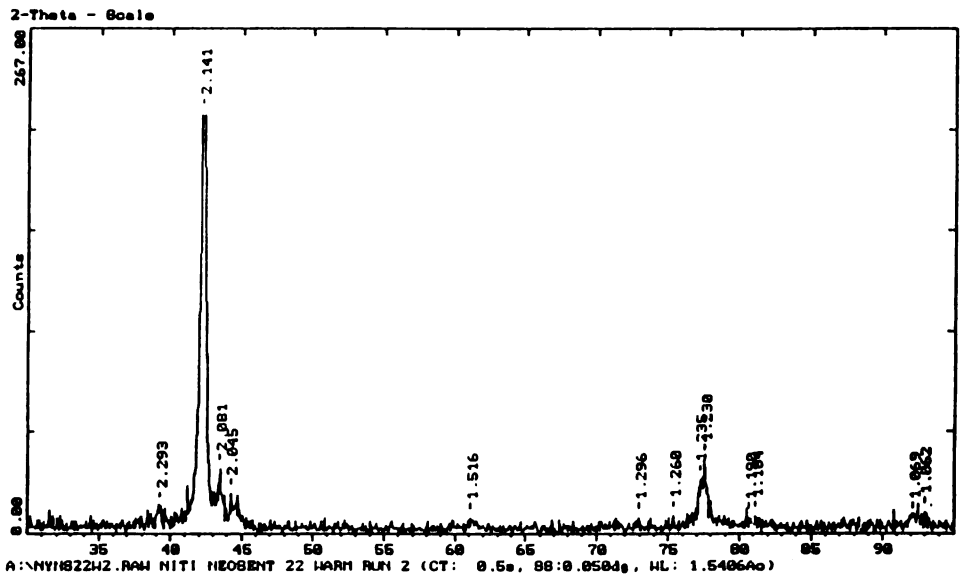

Fig. 5.24b

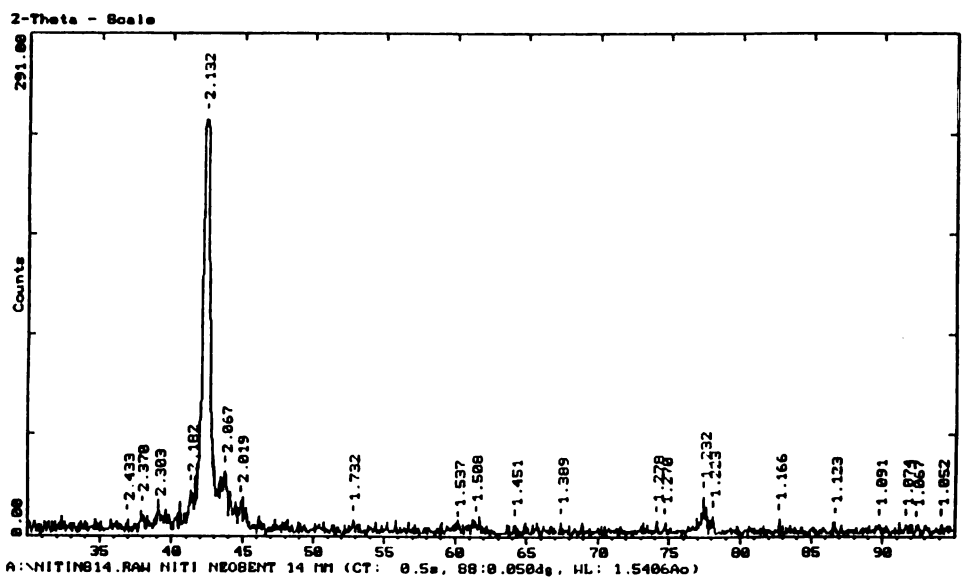

Fig. 5.24c

Figure 5.25, a-c. XRD patterns of Neosentalloy (SM) annealed wires in
a. straight section, 180°,
b. 75° bend,
c. 45° bend.

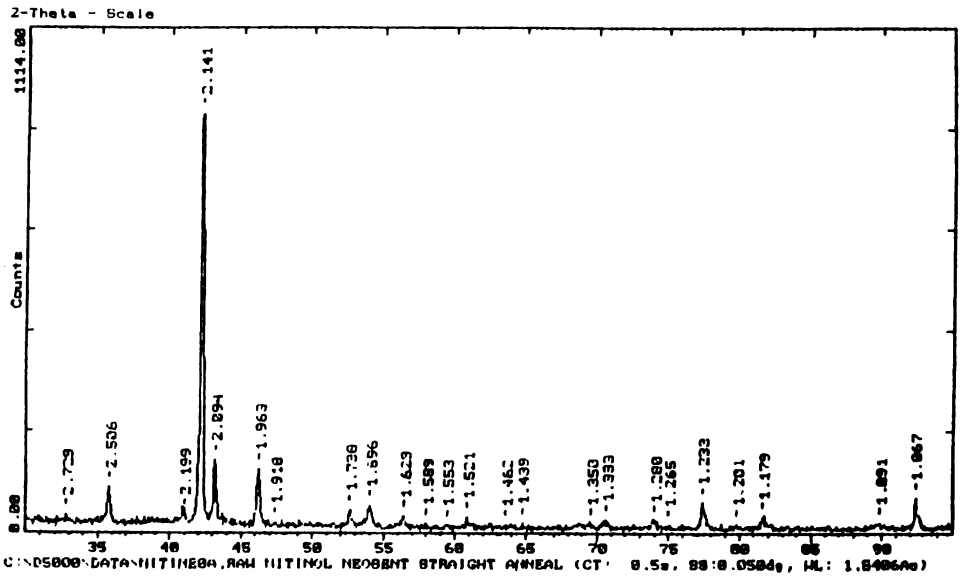

Fig. 5.25a

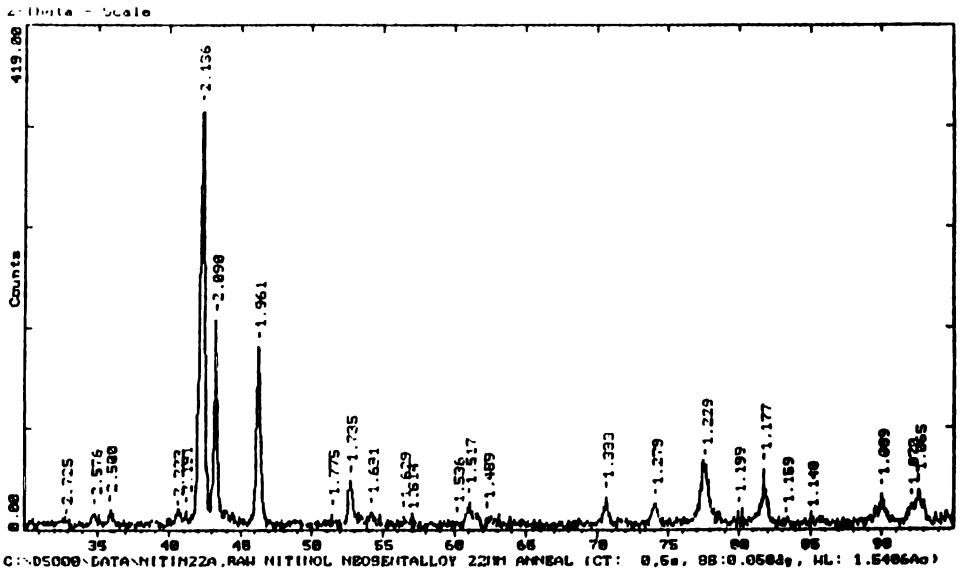

Fig. 5.25b

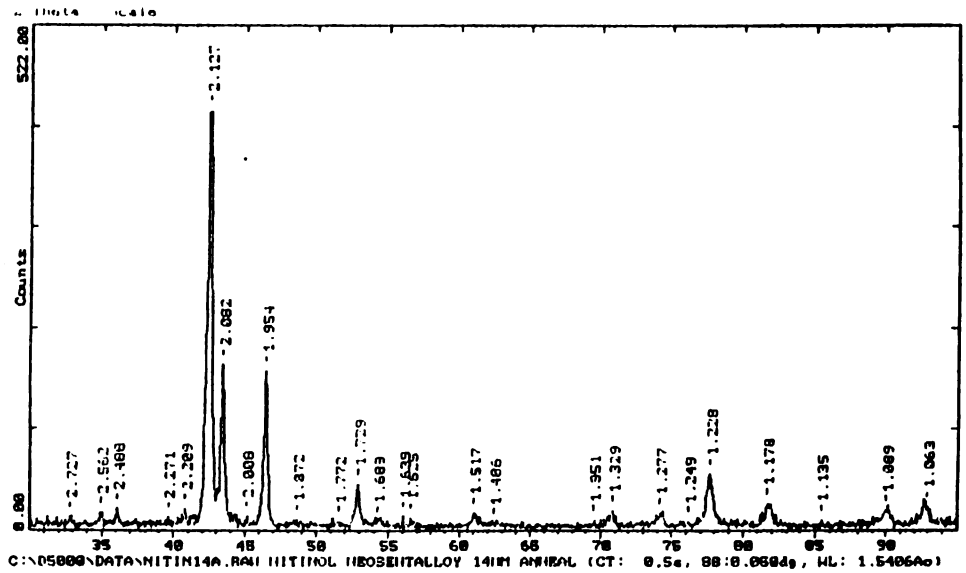

Fig. 5.25c

Figure 5.26, a-c. XRD patterns of Nitinol SE as-received wires in
a. straight section, 180°
b. 75° bend,
c. 45° bend. Temperature at 37°C.

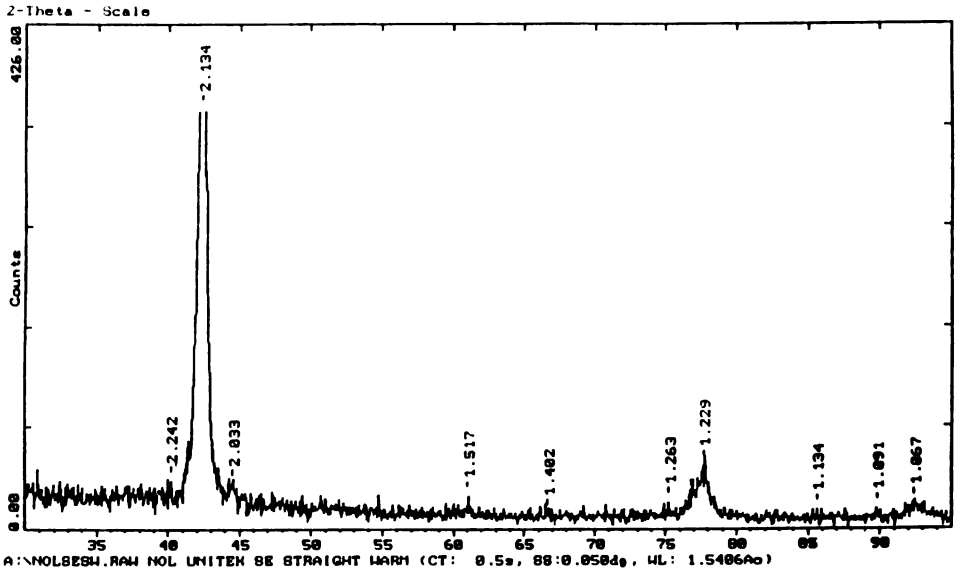

Fig. 5.26a

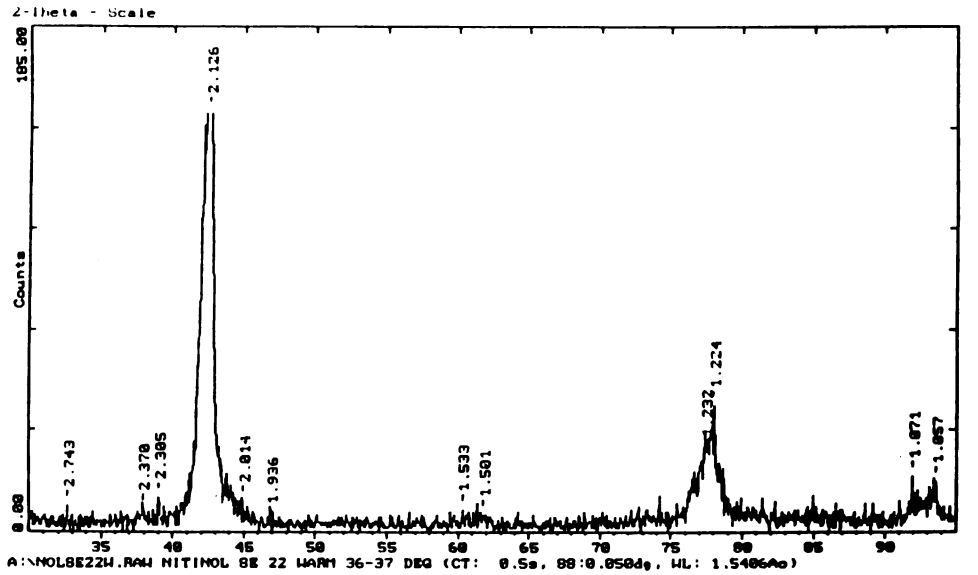

Fig. 5.26b

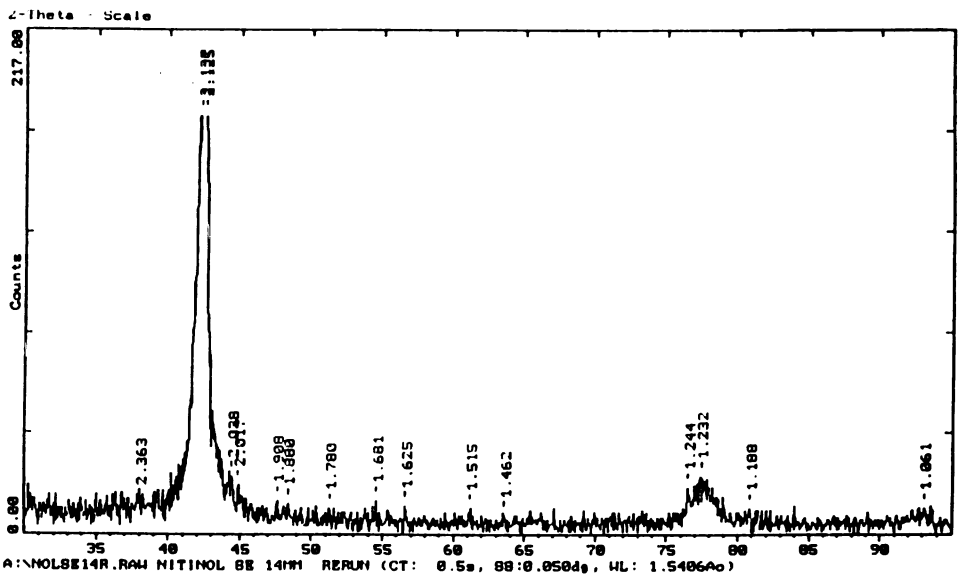

Fig. 5.26c

Figure 5.27, a-c. XRD patterns of Nitinol SE annealed wires in
a. straight section, 180°,
b. 75° bend,
c. 45° bend.

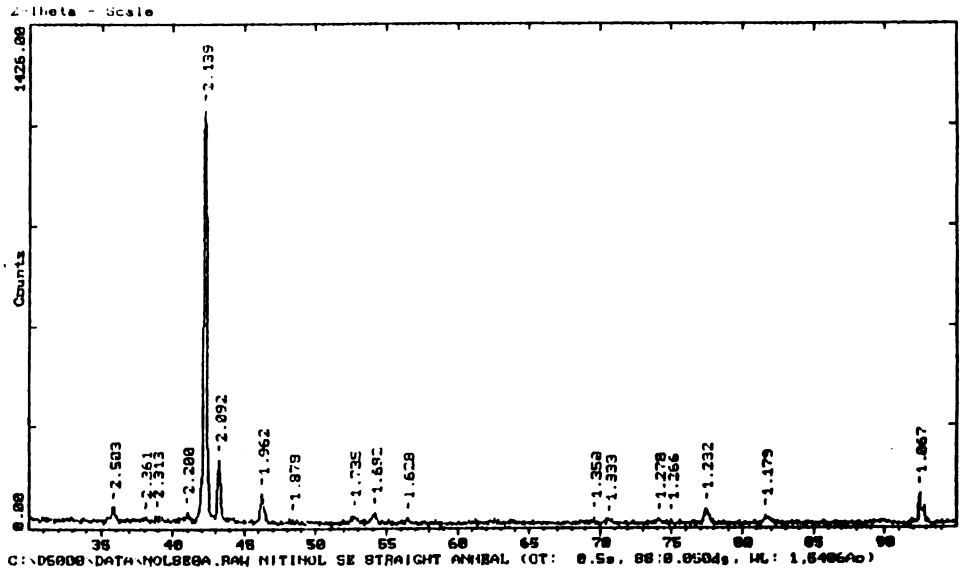

Fig. 5.27a

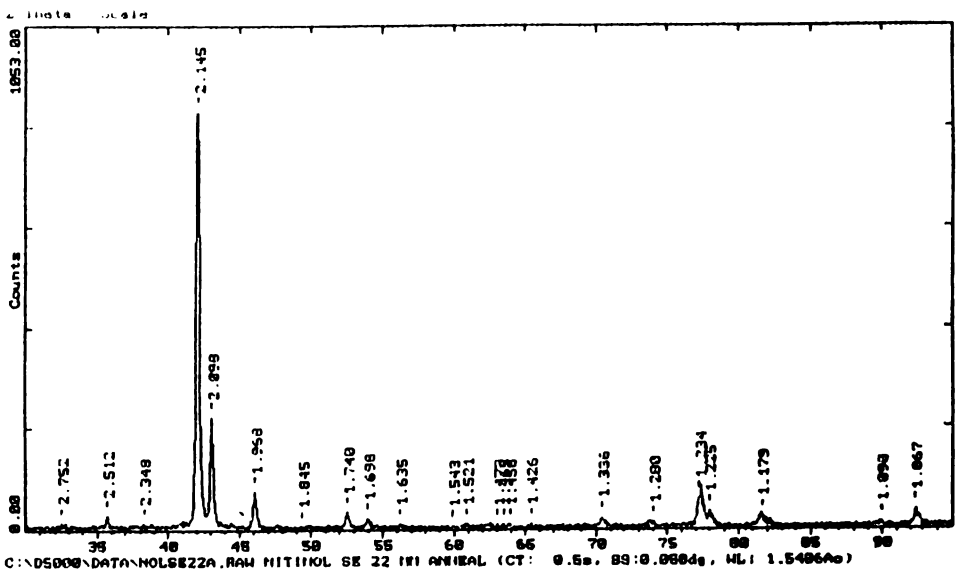

Fig. 5.27b

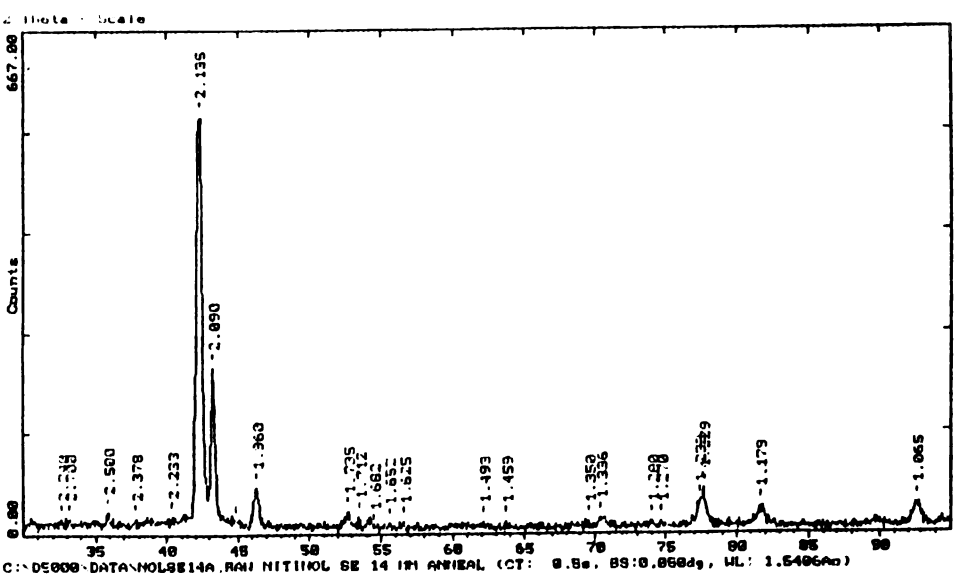

Fig. 5.27c

Figure 5.28, a-c. XRD patterns of Nitinol (SM) as-received wires in
a. straight section, 180°,
b. 75° bend,
c. 45° bend. Temperature at 37°C.

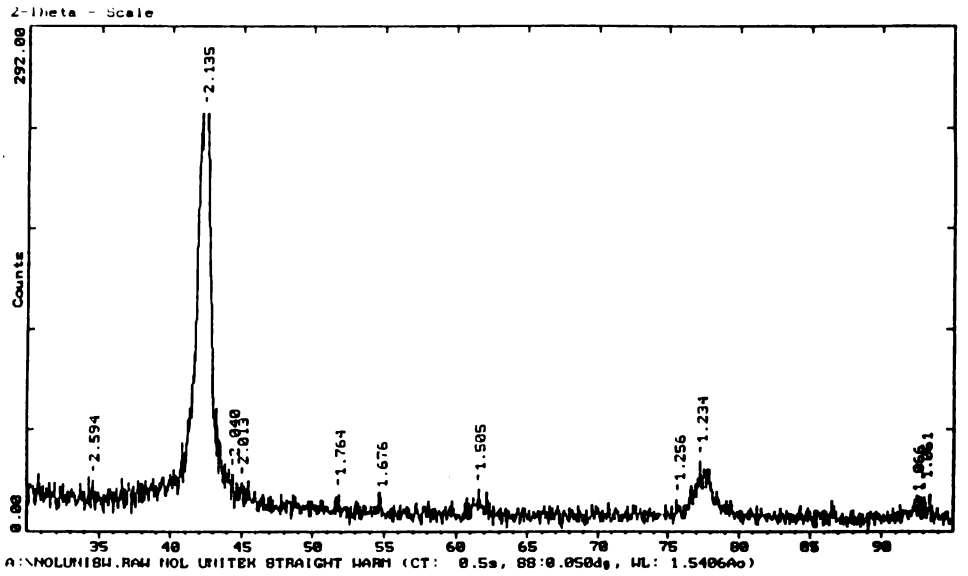

Fig. 5.28a

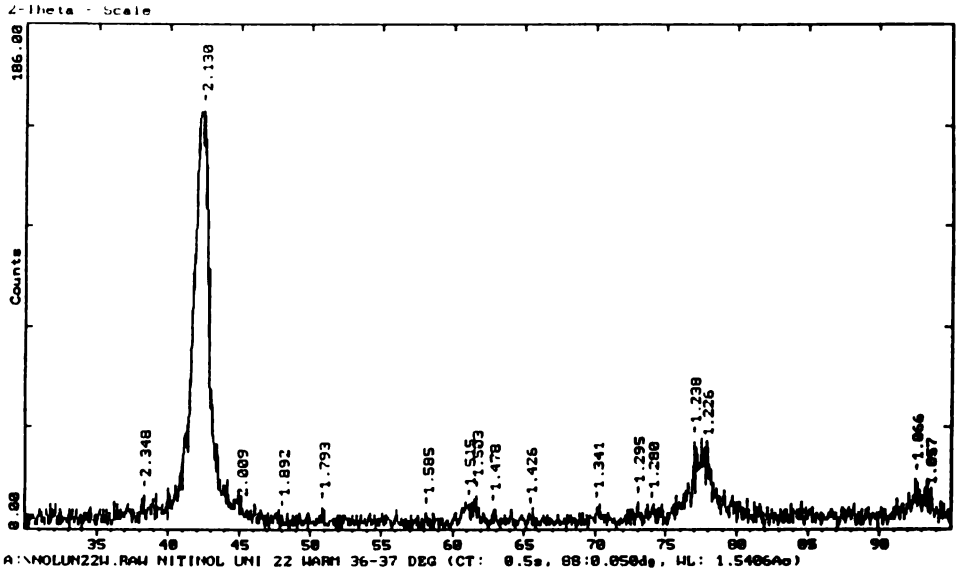

Fig. 5.28b

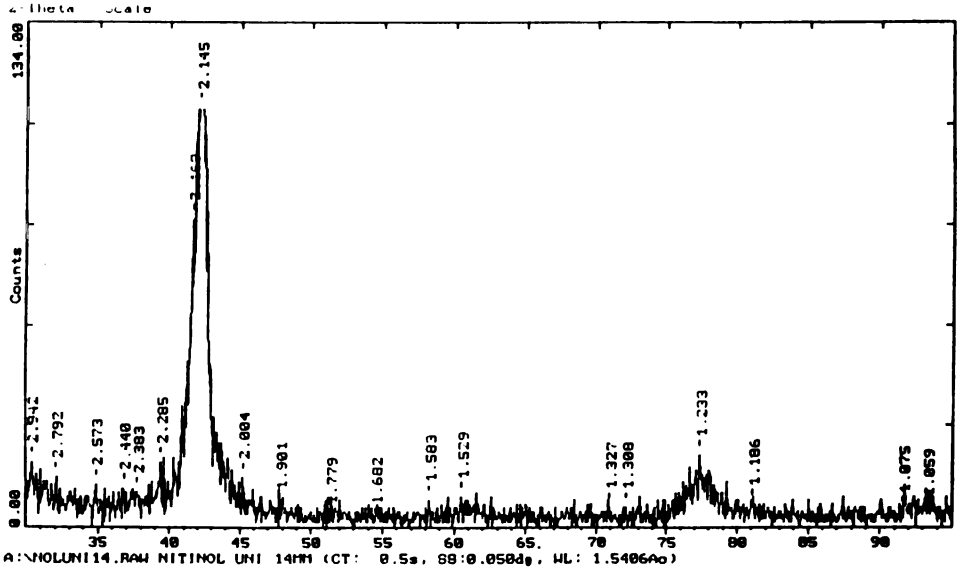

Fig. 5.28c

Figure 5.29, a-c. XRD patterns of Nitinol (SM) annealed wires in
a. straight section, 180°,
b. 75° bend,
c. 45° bend.

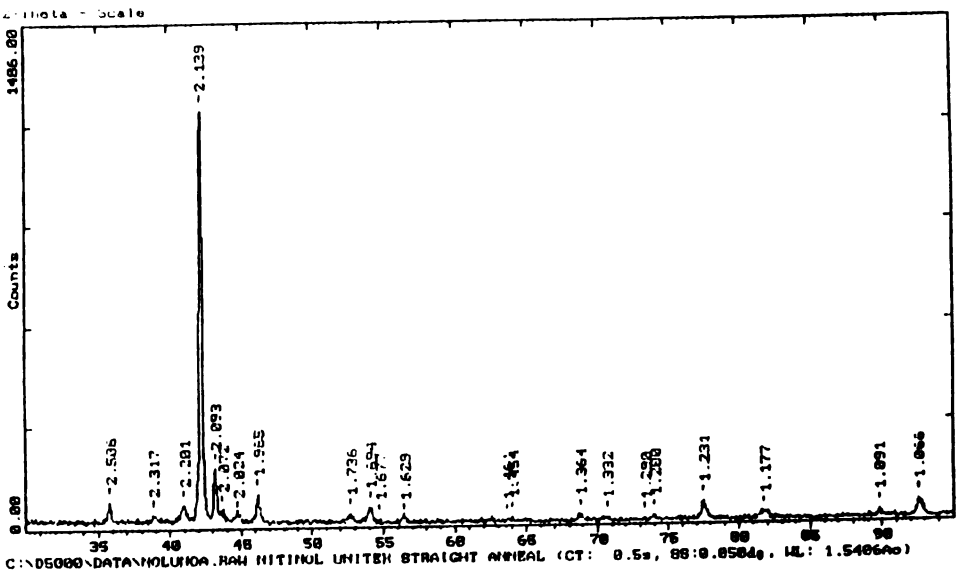

Fig. 5.29a

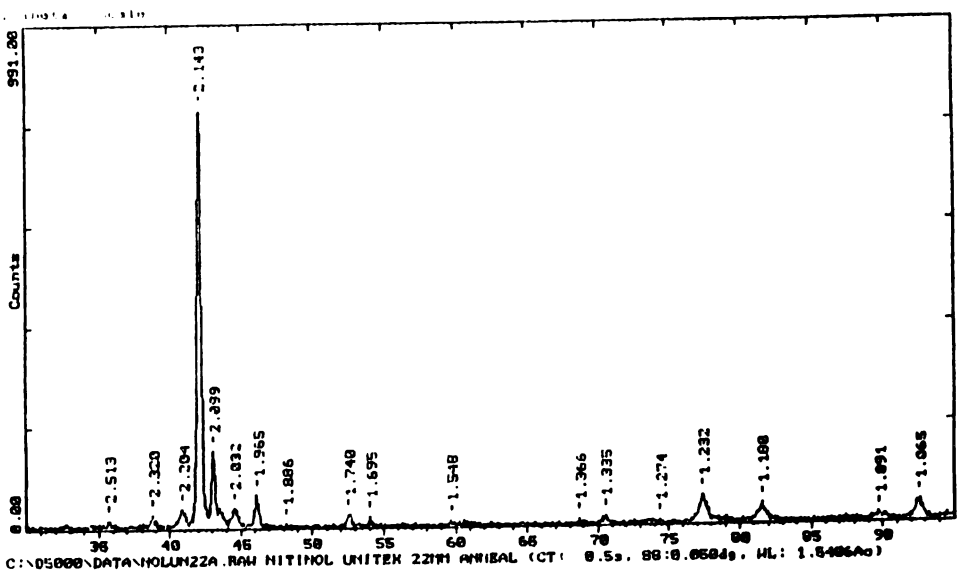

Fig. 5.29b

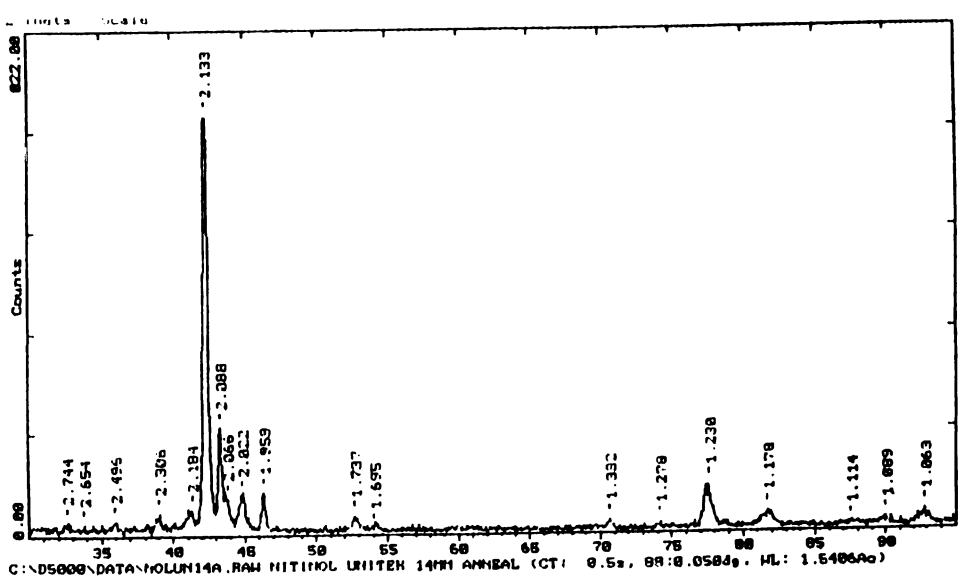

Fig. 5.29c

6. DISCUSSION

6.1 Wire Characterization

When Andreasen introduced Nitinol to orthodontics,[39] he described a work hardened nickel titanium alloy that exhibited shape memory. The wire underwent partial strain recovery after deformation, due to its modulus of elasticity and then complete strain recovery due to the intraoral temperature and the low transition temperature range of the wire (31°C - 45°C). He recognized the property changes associated with the phase transformation and provided the basis for a mechanical characterization of the wires for orthodontics. Although a reliable mechanical characterization of NiTi wires is of clinical significance for the orthodontist, it is important to understand and identify the factors that affect the mechanical behavior. The mechanical properties of NiTi alloys are largely influenced by its stoichiometric composition and its specific thermal and mechanical history.

Although it was difficult to determine the chemical composition of the wires, the Af temperatures of the annealed wires provided a relative determination of nickel content. The experimental data showed the four wires had different Ni compositions. This variation in chemical composition has marked effects on all other physical and mechanical properties, and will dictate how the material responds to subsequent thermomechanical treatments. It is very likely that some, if not all the four wire types were Ni rich. Since the wires are not stoichiometric alloys, they are highly susceptible to precipitation after certain heat treatments. The SE wires, Sentalloy SE and Nitinol SE had a greater nickel content than the SM wires, Neosentalloy SM and Nitinol SM, and subsequently lower Af temperatures. This was determined from the dependence of Af on nickel composition in the Af tests. Although not in agreement with the EDS results, the Af tests were a more reliable measure of nickel content. There were probably other elements besides Ni and Ti. Manufacturers intentionally alloy other elements to manipulate the transformation temperatures. The first NiTi compound, 55-Nitinol, was reported as a ternary compound of NiTiCo.[26] Our EDS studies suggested that Cu and/or Co may be present, although this was not fully explored. The microstructural work suggested a significant oxide content in all the wires. All of these effects will

tend to depress the Ms temperature, and should be reflected in a decreased Af temperature, which would be desirable for SE applications. Although the nickel content varied among the four wire types, there may be other subtle elemental compositional differences between the SE and SM wires. The presence of small quantities of Co, Cr, Mn, Fe have been reported using EDS/EDX.[3]

At ambient temperatures (22°C), the only as-received wire that was completely austenitic was the Nitinol SE (Af = 16°C). Since the other transformation temperatures (Mf, Ms, As) were not determined, the other wires were probably a mixture of both austenite and martensite in the as-received state at room temperature since their respective Af temperatures were greater than 22°C and the hysteresis loop is usually about 20° from Ms to Af. The microstructural analysis at 22°C showed that there was more than one phase present, even in the Nitinol SE, which should be completely austenitic. Characteristic martensite twins were evident in the microstructure of all the as-received wires, indicating that another phase other than austenite was present. The twins could represent either martensite or R-phase. Residual martensite increases the local stress fields, tending to depress the Af temperature. Since Nitinol SE showed the lowest Af among the four wires, it is possible that the twins seen in Nitinol SE were residual martensite, "trapped" by dislocations.[59] The Af temperatures determined in this study were in close agreement with the reported temperatures, and other studies that experimentally determined the Af temperatures.[7,54]

At 37°C, all of the as-received wires should be fully austenitic, since their respective Af temperatures were below 37°C. The x-ray diffraction data of the as-received undeformed wires at 37°C was consistent with this, but small amounts of other phases may have been present. As seen in the diffraction patterns from all wires, clustered around the strongest peak at ≈ 42° 2θ, were other peaks, which may have been martensite, or the R-phase. It is likely that all three phases were present in the as-received wires. Khier et. al[61,62] in studying Nitinol and Nitinol SE, found significantly higher Af temperatures, which would cause alterations in phase contents. They also recognized the R-phase contribution and its likely presence in the as-received wires.[62]

Since the wires contained different phases at 22°C versus 37°C, and the mechanical performance depended on whether the material was tested in its austenitic or martensitic form, the results should be different. The data demonstrated this temperature dependence. As expected, the loading and unloading plateaus were greater at 37°C for all wires since they should be completely austenite (Af < 37°C for all as-received wires), which is stiffer and stronger than martensite. Even the loading and unloading levels of Nitinol SE increased when tested at 37°C, which was a fully austenitic material at 22°C. This increase is due to the dependence of stress on temperature for NiTi alloys. The farther away Td is from the transformation temperatures, the greater the loading and unloading plateau stresses, as dictated by the Clausius-Clapeyron equation.[15,25]

Using the 3-point bend configuration, there were statistically significant differences in the loading and unloading levels between all the wires in the as-received condition, tested at 22°C and 37°C. This supports similar findings of Sachdeva et. al.[63] The difference in loading and unloading at 22°C compared to 37°C for any given wire was also statistically significant and clinically significant. The difference in unloading between 22°C and 37°C was about 50g on average. This amount is enough to intrude the four upper incisors.[64] The hysteresis load drop is also important to consider because between 22°C and 37°C, there may be an increase of up to 100g needed to engage a wire into the bracket. Loads of this magnitude are enough to hinder complete bracket engagement, which may increase the patient's treatment time, cause patient discomfort or even bond failure.

Since it is of interest to examine the wires at 37°C, the discussion will focus on the data at 37°C. All the as-received wires should have superelastic behavior at 37°C and complete shape recovery upon unloading, since by definition, Td > Af. Interestingly enough, the shape memory effect was not utilized in these wires for force delivery, because those wires that were a mixture of phases should revert to austenite at 37°C, before unloading of the wire began. Stress induced martensite

was the primary deformation mechanism involved in all the wires. The shape memory effect would probably be used to facilitate bracket engagement. From the mechanical property testing, two general shapes of the load deflection data emerged. The GAC brand, both Sentalloy (SE) and Neosentalloy (SM), displayed the characteristic flag shaped unloading plateau (similar to Fig. 3.3) that defines superelasticity. At 37°C, the Sentalloy (SE) and the Neosentalloy (SM) wires had similar loading and unloading plateaus and similar shapes in their load deflection curves, indicating that the forces and mechanisms of delivery were the same between the wires. In essence, both the Sentalloy and the Neosentalloy are superelastic wires, reported by the manufacturer to deliver medium ≈ 200g loads. From our mechanical, the load delivery in 3-point bend was slightly less than 200g. The load delivery was fairly consistent as there was little variance between trials. However the Af temperatures of the Sentalloy (SE) versus the Neosentalloy (SM) differed from each other by a few degrees. The microstructure and phase analyses did not show appreciable differences in structure of the as-received wires. Since the Af temperatures of the annealed specimens were markedly and statistically different, the difference between the two wires was likely due to primarily its nickel composition and other small elemental additions as discussed earlier in this section, and secondarily to its processing history. This illustrates how two wires of completely different compositions can be processed to perform similarly.

The second shape of the load deflection data produced by the Nitinol SE and Nitinol (SM) from Unitek displayed a leaf [7] shaped curve (similar to Fig. 3.2) indicative of linear superelasticity.[65] Sachdeva and Miyazaki have classified this as pseudoelasticity,[66] based on Duerig's definition of pseudoelasticity as any nonlinearity during unloading.[15] This unique behavior is not governed by the martensite transformation. Nitinol (SM) is reported as a highly cold worked matrix of twinned and untwinned highly dislocated martensite,[65] with little subsequent heat treatment.[59] Since there is no transformation involved, the mechanical properties are essentially composition and temperature independent. Our data of mechanical performance at 22°C and 37°C supported this temperature independence, showing linear superelasticity/pseudoelasticity at both temperatures. The SM type

from GAC, Neosentalloy (SM) does not have temperature and compositional independence, and is not thought of as linear superelastic as shown in the mechanical performance data and the diffraction data. Sachdeva examined different NiTi wires and found three categories of Af temperatures : <15°C (linear elastic), 15-25°C (superelastic), and >25°C (intermediate form).[63] Jean et. al[67] recognized a need for classification based on the stress required to induce the reverse transformation and presented a similar three category classification. Our data suggests an alternative or sub-classification categorized by both Af temperatures and mechanical properties.

To characterize how the wires were affected by processing, annealed samples of each wire were examined for phase identification, Af, microstructure and mechanical properties, and were compared to the as-received wires. For the Sentalloy (SE), annealing created a lower Af temperature and a less stiff, more ductile metal. Since Td > Af, annealing caused reversion of any martensite to austenite. However, the load deflection data showed a decrease in the loading and unloading plateaus in the annealed wires, illustrating the effect of decreasing the volume fraction of defects from annealing. If there was considerable cold work in the as-received undeformed wire, annealing the undeformed wire would cause sharpening of diffraction peaks and resolution of those peaks that overlap. Annealing actually produced little change in the FWHM between the as-received and annealed wires in the peak at $\approx 42^{\circ}$ 2θ, although the integrated peak intensity did decrease when the wire was annealed. For the Neosentalloy (SM), even though annealing created a higher Af, the load deflection data showed a decrease in the loading and unloading plateaus of the annealed wires. The FWHM slightly decreased, while the integrated peak intensity at 42° 2θ increased. In both the Sentalloy (SE) and Neosentalloy (SM), increases or decreases in Af were paralleled by respective increases or decreases in integrated peak intensities. Since the FWHM did not change between the as-received and annealed Sentalloy (SE) and Neosentalloy (SM) wires, there was little residual cold work in the as-received wires, and the grain orientation and size remained the same.

In contrast, the Unitek brand, both Nitinol SE and Nitinol (SM), displayed different behavior. No values for load delivery were reported by the manufacturer, but from the mechanical testing, both of these wires delivered two times the load of the Sentalloy (SE) and Neosentalloy (SM) wires at 37°C. The Nitinol (SM) delivered the greatest loads at 37°C as compared with all the other wire types. The variance in the load delivery of Nitinol SE was minimal, but marked for the Nitinol (SM). As with the Sentalloy (SE) and Neosentalloy (SM), similar relationships in Af and x-ray peak intensities for the annealed wires were seen in the Nitinol SE and the Nitinol (SM). The Nitinol SE annealed wire showed a decreased integrated peak intensity and a decreased Af as compared to the as-received wire, while the Nitinol (SM) showed an increased peak intensity and increased Af in the annealed wire. The FWHM for both annealed wires markedly decreased, indicating that there was a considerable amount of cold work in the as-received Nitinol (SM) and Nitinol SE wires.

6.2 Extent of the Transformation

This work was a first step in the x-ray diffraction and microstructural characterization of NiTi orthodontic wires in bending. With an emphasis on characterizing phase changes during the transformation, studies have examined either tensile or compressive deformations[50] or thermoelastic conditions.[22,34]

Based on the Af tests, at 37°C any deformation would occur through SIM. At 22°C, the deformation mechanism involves a combination of SIM and martensite twin boundary movement for all the wires except the Nitinol SE. Since Af = 16°C for Nitinol SE, only SIM will be involved. The microstructural work conducted at 22°C on the as-received and annealed wires was supplemented with the diffraction data generated at 37°C for the as-received and annealed wires. While the internal microstructure was examined using microscopy, diffraction will describe the surface of the wire, crystal orientation and quality, so only indirect correlations of the diffraction data and microstructural work were possible. Because x-ray diffraction measures texture, the

inherent surface roughness and preferential grain orientation of the sample cannot be discounted in data interpretation. The surfaces of the wires in the as-received state are heavily textured, the depth of this effect is not known. Furthermore, the drawing effects are so dominant that in bending, the transformation may be obscured because of grain orientation and occur on a much smaller scale than could be detected.

The microstructure and the general phase contents of each wire in the as-received condition were established before structural changes due to deformation could be determined. At 22°C, as expected, the microstructure of all wires appeared multiphase, although austenite was thought to predominate the matrix in the as-received specimens. Diffraction results clearly identified the peaks at ≈ 42° 2θ and 77° 2θ as austenite since the d spacing of these peaks closely correlated to the (110) and (211) planes of austenite, which was in agreement with other studies.[50,62] The difficulty of quantifying austenite because the R-phase and martensite peak overlap the austenite peak was explained earlier and has been recognized.[49,62] The R-phase in as-received orthodontic wires was noted by Leu et. al,[37] and has also been detected in studies of the thermoelastic and stress induced transformation.[22,31-33] Experiments using TEM in temperature controlled conditions have demonstrated the presence of an extra reflection (1/3) identified to be the R-phase. Using diffraction, the R-phase peak was described as a (110) plane from a rhombohedral lattice when a polycrystalline NiTi specimen was heated, then cooled, to ambient temperatures.[29] In this study, the Af temperature tests clearly demonstrate that the R-phase was present during the stress induced transformation produced by bending.

The other phases in the as-received wires appeared to be martensite and oxides. In similar work, Jialiang and Yi described the original microstructure of a 51.6 at% Ni-Ti (Ms = 25°C) as two phase; an ordered parent phase and a smaller second phase of twinned martensite.[68] The twins they identified in the substructure of martensite were very similar in appearance to the twins found in the microstructure of all the as-received wires. Onda et. al[69] characterized the twins in a Ti-

50at% Ni alloy that was fully martensitic at room temperature. Many of the twins observed under the SEM may correspond to the Type II twins described by Onda et. al.[69] Even in the Nitinol SE wire (Af = 16°C), twins were evident in the microstructure at 22°C. These twins could be deformation twins of internally slipped martensite that result from processing,[70] or "trapped" martensite described by Pelton.[59] Either of these structures would influence the Af temperature and the mechanical properties. Filip found that these stable internally slipped martensite contribute to the shape memory effect,[70] seen in cold worked and nickel enriched alloys. His electron diffraction work showed these structures to have equal lattice parameters and symmetry to the twin martensite B19'. From our diffraction data, the FWHM of the as-received and annealed wires showed the as-received wires had much cold work, and so it is possible that these deformation twins were formed through excess cold work. The FWHM of the peak at $\approx 42^\circ 2\theta$ of the as-received wire compared to the annealed wire showed a considerable amount of cold work in the Nitinol SE wire. The composition of the superelastic wires, Nitinol SE and Sentalloy (SE), also suggest that a second phase may be present. The relative compositional determinations from Af tests indicated that the Nitinol SE and Sentalloy (SE) were on the Ni rich side, which would favor Ni precipitates.

As the as-received wires were deformed, significant surface relief effects were noted. Nucleation of martensite could not be identified since individual grains were difficult to localize. As the deformation increased, the microstructures generally showed increased twinning or greater surface effects. This was more evident in the Sentalloy (SE), Neosentalloy (SM), and Nitinol SE wires, and suggested that straining the material produced other phases. The diffraction data corroborated these results as the integrated peak intensity changed under deformation and the other peaks clustered around the austenite peak grew in intensity. The twinning seen on the micrographs was characteristic of martensite, indicating that the new peaks around the austenite peak were martensite. In studying NiTi wires under tensile deformation, Thayer et. al[50] found that under 6% strain, additional peaks formed at $38^\circ 2\theta$ and $44^\circ 2\theta$. They indexed those peaks to a monoclinic

martensite (101), (002), (111), (202), (004). From this study, it generally appeared that qualitatively as the wires were strained, stress-induced martensite formed in proportion to the level of strain.

The 3-point bend tests indicated complete shape recovery was not realized, even at 37°C, when the as-received specimens should have been completely austenitic. The amount of outer fiber strain was not determined in this study, but it must be remembered that tensile strains up to 8% are generally recoverable. Lee et. al[3] studied Nitinol wire in bending, using a similar bending configuration. They calculated that bends smaller than 130° did not show shape recovery, while between 135 - 150°, there was generally 90% shape recovery. Thus they concluded that deformations smaller than 150° bends produced greater than 8% strain in the outer fibers. Pelton et. al[12] found that in 3-point bending of small diameter Nitinol wire, the neutral axis shifted from the middle of the wire, closer to the side of the wire in compression. Since complete shape recovery was not realized from our deformation bending, it is probable that either plastic deformation of martensite occurred on the tensile side of the wire, or that the stresses were large enough to deform austenite. The micrographs showing the structures at 45° and 75° bends may be a combination of twinned martensite, slipped martensite (produced by excessive bending and/or the initial processing) and deformed austenite.

High temperature annealing produced microstructural changes that were reflected in the micrographs of the annealed wires. Both of the annealed SE wire types, Sentalloy SE and Nitinol SE, were primarily austenite since their Td > Af, whereas the annealed SM wire types, Neosentalloy (SM) and Nitinol (SM) were a mixture of martensite and austenite, as suggested by their Af temperatures and the microstructural data. The micrographs of the annealed SE types showed equiaxed austenite grains, the absence of twins, and surface relief effects similar to those that were described by Wayman[49] due to R-phase formation in a NiTiFe alloy. Additionally, the Af tests support the presence of R-phase since R-phase inflections were evident during the

transformations. Thus it is probable that R-phase was seen in the annealed specimens. The Neosentalloy (SM) showed diffuse twins throughout the annealed microstructure, indicating a structure of primarily martensite Td (22°C) < Af (31°C). Identification of the habit plane would verify the predominance of martensite.[71] It is likely that other features were present in the substructure[72], but no other distinguishable regions were observed under the SEM.

While there are reported differences between the martensitic transformation that occurs in the outer and inner fibers of a wire during bending, these differences were not detectable under SEM of the as-received wires. In the clinical situation, it seems that such differences in the extent and mechanism of the transformation would be relevant if large deformations of the wires were used.

6.3 Variability

The variable mechanical performance can be assessed on several levels. This study recognizes three levels of variability. Within one brand, there may be variability among wires from the same package. This is considered as variability within a wire type of the same brand. Several studies have reported the differences among brands of the same type of wire. This is considered as variability within a wire type of different brands. Furthermore there may be potential variability due to the wire type, whether the wire is shape memory or superelastic.

The results of this study showed that within one brand of either the shape memory or superelastic type wire, there was little variability in the mechanical performance. The wires tested for mechanical performance were taken from different packages of the same brand. It was not known if the packages were from different lots. Based on the small variance of three wires tested in 3-point bend, each wire of the same type and same manufacturer, performed consistently, except for the Nitinol (SM) wire. This wire showed the largest range in load delivery with variances up to 60g. To conclusively determine the consistency in performance, which is a quality control issue, examination of more wires, from different packages and different days of production is needed.

Our results support other findings of reproducibility between wires of the same type and manufacturer.

The variability in properties between manufacturers of the same type of wire is remarkable. This has been demonstrated in the orthodontic literature,[7] and was substantiated in this study. Most NiTi wires available to clinicians are not sold as 'SE' or 'SM' wires, but instead as just 'NiTi'. As explained earlier, SE (Figure 3) implies a particular behavior of a constant recovery force during unloading. Not all companies demonstrate this flag shaped curve in loading and unloading of the wire. Since thermomechanical processing procedures to develop or enhance SE have been established,[73] the different loading and unloading recovery forces of wires from different companies is intentional. The GAC (Sentalloy, SE) brand of wires demonstrated this flag shaped superelasticity (Fig. 3.3), which differed from the pseudoelasticity evidenced by the Unitek brand (Nitinol SE). Perhaps more importantly, the unloading plateaus of the Unitek brand, Nitinol SE and Nitinol (SM) were 200 - 300g greater than the unloading plateaus of the GAC brand, Sentalloy SE and Neosentalloy SM.

The wires of the same type, but from different manufacturers were found to be chemically and structurally different. The relative at% of Ni differed between the SM wires and between the SE wires from different companies, which would explain the different Af temperatures between the SM wires and between the SE wires. But other factors besides the at% Ni affect Af and must be considered. Additional elements may have been alloyed into the wires that were could not be definitively detected using our EDS analysis. As discussed earlier, there was a strong suggestion of copper and cobalt present in some of the wire types.

Additionally, the conditions of heat treatment and manufacturing would impart structural changes by the formation of precipitates and defects, alterations in the size and shape of the grains, and preferred orientation of the grains. Because the internal wire structure is so heavily oriented,

precise microstructural and phase analysis of wires in the as-received condition was not possible. SEM examination of the microstructure revealed general differences in the topography within the matrix of each wire type. Defects and twins appeared randomly among the as-received wires of the SM type and the SE type. All wires appeared to have multiphase structures under the microscope at ambient temperatures. At intraoral temperatures, it is expected that most of the structures would also be multiphasic in nature. This was supported by the diffraction experiments, conducted at 37°C, that suggested a predominance of one phase, with smaller amounts of other phases present. These other phases, though difficult to detect, play a paramount role in the distinction between wires of the same type from different manufacturers. SE behavior can be elicited by suppression of the R-phase.[73] The extent to which this is controlled by the various manufacturers probably varies. The shape of the strain-temperature curve from our Af tests indicated that the R-phase was more evident in the Unitek brand Nitinol SE and Nitinol (SM) wires.

In view of the shape memory and superelastic differences, it appeared that the difference within one manufacturer was attributed to both compositional changes and processing alterations. Comparisons of the annealed wires to their as-received counterparts demonstrated the effect of heat treatment on the properties of the NiTi wires. The effects from annealing were very striking and several differences emerged. The Af tests showed that SE wires had higher Ni compositions within each brand and were primarily austenite as shown by diffraction. Thermomechanical treatments are employed to increase transformation temperatures. Inversely, the SM wires had lower nickel compositions, higher transformation temperatures and consist of multiple phases. The intent of subsequent heat treatment was to lower transformation temperatures so that the shape memory and superelastic effects would occur at lower temperatures, e. g. intraoral temperatures.

Finally on a more macroscopic level, there is a difference in the mechanical properties of shape memory versus superelastic wires. There is a clear distinction in their deformation mechanisms, and it would be expected that this would be reflected in their unloading characteristics. Although

this study examined the shape memory and superelastic type wires, only the superelastic effect occurred during simulated testing at 37°C. Since the Af temperatures of both the SE and SM wires were below 30°C, the wires would be primarily austenitic as they were tied into the dentition. The 7°C difference in temperature between intraoral temperature and Af temperature is really a clinically significant difference, because this denotes the difference between the martensitic and austenitic phases.

An explanation for the differences in mechanical properties between SM and SE wires is likely due to their microstructural differences. The difference between the two wire types is reflected in the recoverable strain. Cold worked NiTi has up to 4% recoverable strain, whereas the combination of cold work and annealing or solution treating and aging procedures produce up to 10% recoverable strains in superelasticity.[11] Studies on coldworked NiTi alloys show that SIM mechanism is suppressed and does not contribute to the pseudoelasticity in this state. Extensive cold working can overcome the effects of compositional variations. The dislocations introduced by cold work into the matrix yield permanent deformation and hardening. However, cold work followed by annealing is utilized to create superelastic behavior. Differences between SM and SE alloys may be in the extent of unrelieved cold working. Since cold worked NiTi is composed of highly dislocated martensite, if there are increased dislocations, then perhaps these dislocations would be seen as the many etch pits in the micrographs. The etch pits/voids are a likely combination of dislocations in the matrix and internal oxides. The microscopy results could not be used to support or reject this idea. Quantification of these etch pits/voids would be a useful adjunct to this study since they reflect the processing history of the wire. Between the SM and SE wires, the FWHM were different, but conflicting. The Sentalloy (SE) and Nitinol SE had lower FWHM than their SM counterparts (Neosentalloy SM and Nitinol SM), suggesting less deformation in the SE wires. However as the wires were strained, the FWHM of the Sentalloy (SE) increased over the Neosentalloy (SM), while the FWHM of the Nitinol SE remained lower than the Nitinol (SM).

Qualitatively, there were different concentrations of the defects in the wires, but further tests are necessary to support the relation of the dislocation density to SE/SM differences.

6.4 Clinical Applications

This study suggests simple parameters to aid clinicians in their evaluation of wires. The Af temperature is critical to the performance shape memory materials and the role of the Af temperature should be clearly understood. When the transition temperature range for austenite, As-Af, is above body temperature, a deformed wire remains deformed. The wire feels flimsy and the reverse transformation is never realized. When the As-Af range is too low, the wire is too stiff. These differences will be reflected in the load deflection properties of a wire and so it is important for the clinician to gain a basic understanding of how to interpret load deflection plots.

The clinician should ask the supplier what the Af temperature is and what the general unloading load-deflection characteristics are. The loading and unloading levels, the hysteresis load drop, the extent of shape recovery and the length of the unloading plateau (represents the recoverable displacement) are the most relevant parameters for the clinician. What are the parameters of superelasticity and shape memory for the clinician ? By the strictest definition for superelastic application, the Af should be well below intraoral temperatures, while Md is above intraoral temperatures. This would ensure the constant force delivery upon unloading, as illustrated in Figure 3.3. Not all superelastic wires display the characteristic flag shaped curve and if the clinician uses the wire for constant force delivery then (s)he may not be using the optimal wire.

The shape memory effect has been especially useful in early bracket engagement. Since the wire is probably mostly martensitic, the loads are lower and have less resistance. The clinician could either utilize the shape memory properties for easier bracket engagement, or choose a wire with a narrow hysteresis. Ternary alloy wires with copper will afford the clinician this advantage.[74] Since the variability in bending was small, the general shape of the load-deflection diagram, Af and

the Td in bending would be useful and quick adjuncts for the clinician to evaluate the shape memory/superelastic properties of the wire.

The thermal cycling effects of variable intraoral temperatures from the ingestion of hot and cold foods should be recognized.[63] The desired Af should be a few degrees lower than 37°C, to account for temperature changes during speech and eating.

If the mechanisms of force delivery are different for SE versus SM, then different parameters should be used as guidelines for product selection. Sachdeva et. al[66] have outlined parameters to evaluate SE behavior : stress rate, critical stress for slip, critical stress for inducing martensite transformation, and Af temperature. If the recovery stress is the same in SE and SM mechanisms, then similar guidelines could be used to evaluate SM behavior.

It is widely thought that force constancy is the ideal method of force delivery for orthodontics. Problems arise when forces are excessive and erratic. Stability of tooth position is often questioned when abrupt changes are introduced. It is generally thought that for optimal stability, gradual changes are introduced and allowed to integrate into the patient's own intraoral equilibrium. The NiTi wires have favorable characteristics because they allow this force constancy. Forces are not excessive and are harmonious with the forces generated from the patient's own masticatory musculature and occlusion. For superelastic application, it is therefore suggested that in the initial stage of treatment, low load round wires should be utilized, with an Af near ambient temperatures. In the initial stages of treatment, general alignment is the primary goal. Round SE wires with low unloading loads can achieve this, while providing minimal discomfort to the patient. The next suggested wire that can be inserted would be a rectangular superelastic wire with a low Af. The rectangular cross section would engage the bracket slot more completely to provide third order movement and control. Because of the low Af, the difference between the Td and Af would provide a higher unloading plateau and this would generate the moments needed for

third order movements. Even though the loading plateau also increases, this should not be problematic. Since general alignment has already been accomplished with the initial round SE wire, large deflections are not warranted for bracket engagement of the wire. The load deflection plots of these scenarios are suggested in Figure 6.1.

Figure 6.1. Mechanical Performance for Suggested Use.

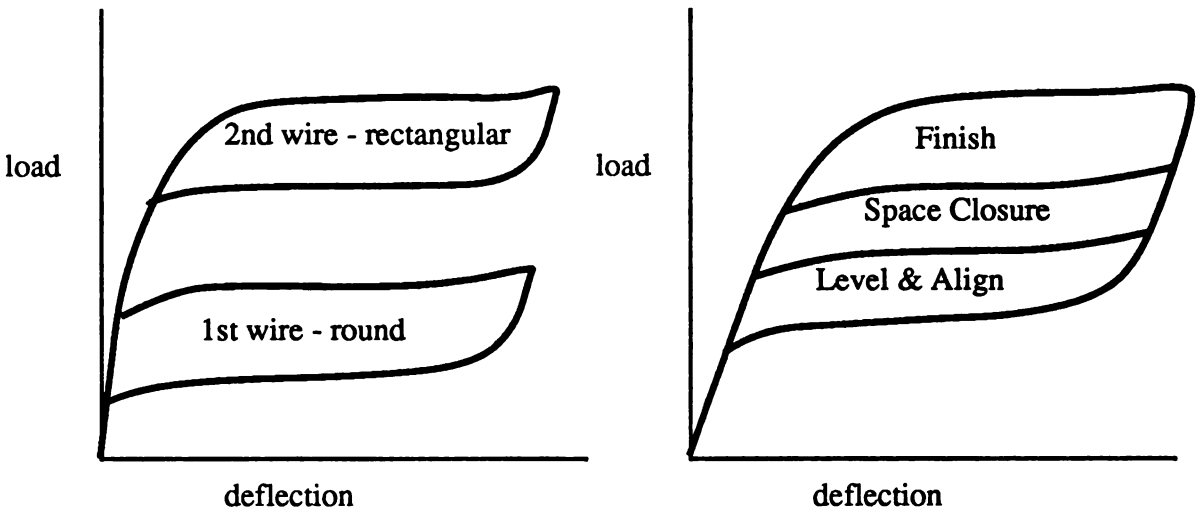

The ideal properties for a SM wire would constitute the following : flexible at room temperature so it can be tied to malpositioned teeth; instantaneously activated by mouth temperatures; clinically apply acceptable forces resulting in tooth movement; once fully activated, the increase in mouth temperature would not produce an increase in force; and the transformation temperature range should be fairly narrow.

Complete shape memory has not been consistently achieved with some SE/SM wires in the clinical setting. It must be remembered that tensile strains up to 8% are recoverable, which is actually quite a large displacement. Recoverable strain in bending has not been determined because of the many confounding variables, i.e. the mode of bending, the length of the span. Some deflections

may actually exceed that which is recoverable. Another possible explanation for reported 'failure'/inactivity of the SM/SE wires is that the unloading stress of the wire may not be enough to achieve tooth movement for that particular patient. Based on the diagnostic classification of skeletal type, the force exerted by the wire may not exceed the patient's intraoral forces of occlusion and musculature. This poses another type of classification for SM/SE usage : wire sequence dictated by the type of mechanics and/or by the patient's skeletal pattern. A final explanation for wire inactivity may be that the Af temperature was too high and so the austenite phase was never reached. Consequently shape recovery was not possible.

In other biomedical applications, the superelastic advantages of NiTi are used to enhance bone healing. The idea of constant force delivery is physiologically and biologically compatible with osteoblastic induction. In many cases fixation is accomplished by rigidly holding bony segments in close approximation so that primary healing occurs. Under movement, the rigid fixation will mechanically lock the segments together as a unit. Small movements are anticipated in the segments, and the type of deformations are not complex, such as those seen in bending or torsion. Problems arise when complex deformations are encountered because of the difference in modulus between the fixation and the bony segments. Due to its mineral density and structure, bone has a low modulus of elasticity, magnitudes lower than that of the metal fixation. When failure occurs, it will generally be at the implant/bone interface. It has been postulated that apparent failure of bone integration or lack of biocompatibility may actually be areas of excess stress concentration. In these instances, NiTi fixation components may be the preferred alternative, since the modulus of the material more closely approximates that of bone, and the resulting stress distribution patterns are largely constant. Additionally, the NiTi material can be fabricated to exert contractile and tensile forces.

7. SUMMARY

The bending, structural and thermal properties of nickel-titanium orthodontic archwires were investigated in order to better understand the martensitic transformation for clinical applications. The shape memory and superelastic type NiTi wires were examined from two different suppliers. Bending behavior using 3-point bend tests was established at ambient temperature (22°C) and intraoral temperature (37°C). Structural characteristics under different degrees of bending deformation were examined using x-ray diffraction and scanning electron microscopy. The transformation temperature, Af, for each wire was established by cycling each wire through a heat bath and recording its deflection recovery. Relative nickel content was determined based on the Af temperatures. As-received and fully annealed wires were studied to differentiate the effects due to thermomechanical processing.

All tests were designed to simulate clinical conditions. The relevant parameters for orthodontics in mechanical testing were defined, and the deformation in bending was designed to simulate intraoral loading conditions.

The following conclusions may be drawn from this investigation :

1. It generally appeared that qualitatively as the wires were strained, stress-induced martensite formed in proportion to the level of strain. X-ray diffraction and electron microscopy analyses provided clear evidence of the transformation.
2. The micrographs and diffraction patterns illustrate that the as-received wire microstructure is multiphase, even though the Af temperature may indicate that the wire should be a single phase.
3. The R-phase was expressed during the transformation and was displayed in the Af temperature plots.
4. The analyses of the heat treated wires illustrates that wires of completely different compositions can be processed to yield similar transformation temperatures. Depending on the application

temperature, the distinction between shape memory and superelastic wires lies in the Af temperature. As observed in the Sentalloy (SE) and Neosentalloy (SM) wires, the difference between the two wire types was 3°C. To alter the transformation temperature a few degrees may require a markedly different manufacturing schedule, which could introduce variability in the performance of the wire for a specific tranformation temperature. However, the load deflection plots and the Af tests showed consistent performance for all the wires except the Nitinol (SM).

5. At 37°C, the wires of the same manufacturer, Sentalloy (SE) and Neosentalloy (SM), showed very similar mechanical performance. The Unitek wires, Nitinol SE and Nitinol (SM), also showed similar load deflection properties at this temperature. However, when compared against manufacturers, the wires displayed different mechanical data. This information should be available to the clinician, as not all NiTi wires of the same cross-sectional dimension will perform the same.
6. The shape memory mechanism is useful for initial bracket engagement, but superelasticity is the mechanism utilized for force delivery and tooth movement.
7. The shape of the load deflection diagram and the Af temperature should give the clinician a general idea of the mechanical performance of the wire. These parameters alone could be sufficient for wire selection. Loading and unloading plateau stresses, and the hysteresis are more specific properties that should be also considered, especially if NiTi wires will be utilized during the later stages of treatment.

Optimal wire selection must be individualized for each patient. As each patient presents with different malocclusions, treatment mechanics will differ according to the desired tooth movements. Understanding and defining the force delivery of the appliances allows the clinician to understand and qualitatively assess the patient's response to applied loads on the teeth.

8. FUTURE STUDIES

This study paves the path for future work in the NiTi field. Depending on the direction, the metallurgical aspects can be examined in greater depth or troubleshooting for clinical problems could be studied. Collaborative work between industry and orthodontic research groups can help solve some of the problems of fabricating different diameter NiTi wires with thorough attention to the thermomechanical history and composition.

Paramount to future development is a better characterization of bending behavior. The results and guidelines presented in this study were based on mechanical data derived from a 3-point bend test that was thought to best represent the clinical loading conditions NiTi wires. However, the 3-point bend is probably not be the best representative test.[14] The actual bending situation was described in Figure 3.6. In this study, it was not possible to replicate this bending situation in the diffractometer and in the SEM chamber so that the microstructural aspects and phase analysis could be examined. Future studies could address these technical difficulties for the design of a sample chamber to study bending deformations. It would also be of considerable interest to explore the clinical limit of recoverable strain in bending. There are currently no guidelines in the literature.

Finally, it would be of considerable interest to all industries that employ NiTi to explore what causes wire fracture. Fractured wires are found occasionally in orthodontics. These studies are merited because of the traumatic effects of aspiration of wire segments. Is fracture related to the mode of deformation, or is it due to defects/phases of the material itself (i.e. the internal oxides, carbides)? Carbides have been localized as nucleation sites for crack propagation,[35] and this idea is worth pursuing. It was previously thought that corrosion caused crack propagation, but studies show it is due to defects and not corrosion of the wire.[75,76] Based on the microstructural and phase analysis of this study, there seemed to be a considerable oxide content in the wires. Examining the oxide content in the wires, perhaps through elemental mapping, would be a useful adjunct to this study.

9. REFERENCES

1. Sachdeva, R., Miyazaki, S., Superelastic NiTi Alloys in Orthodontics. Engineering Aspects of Butterworth-Heinemann, Boston, pp. 452- 469, 1990.

2. Buehler, W. J., Gilfrich, J. V., Wiley, R. C., Effect of low temperature phase changes on the mechanical properties of alloys near composition TiNi. J Appl Physics, 34: 1475- 1477, 1963.

3. Lee, J. H., Park, J. B., Andreasen, G., Lakes, R. S., Thermomechanical study of NiTi alloys. J Biomed Mater, 22: 573- 588, 1988.

4. Khier, S., Brantley, W., Fournelle, R., Structural Characterization of Superelastic NiTi Orthodontic Wire Alloys. J Dent Res, Abs. #1988, 1988.

5. Wasilewski, R. J., "The Shape Memory Effect in TiNi: One Aspect of Stress-assisted Martensitic Transformation ." Shape Memory Effect in Alloys, J. Perkins, ed., Plenum Press, New York, pp. 245- 271, 1975.

6. Yoneyama, T., Doi, H., Hamanaka, H., Okamoto, Y., Mogi, M., Miura, F., Superelasticity and Thermal Behavior of NiTi Alloy Orthodontic Archwires. Dent Mat J, 11: 1- 10, 1992.

7. Chen, R. C., Zhi, Z. Y. F., Arystas, M. G., Advanced Chinese NiTi alloy wire and clinical observations. Angle Orthod, 62: 59- 65, 1992.

8. Reitan, K. Some factors determining the evaluation of forces in orthodontics. Am J Orthod, 43: 32- 45, 1957.

9. Storey, E., Smith, R., Forces in Orthodontics and its Relation to Tooth Movement. Aust J Orthod, 56: 11- 18, 1952.

10. Farz-nia Farrokh, ORMCO/Sybron Corp.: personal communication, 1993.

11. Melton, K. N., NiTi Based Shape Memory Alloys. Engineering Aspects of Shape Memory Alloys. eds. Duerig, T. W., Melton, K. N., Stockel, D., Wayman, C. M., Butterworth-Heinemann, Boston, pp. 21- 35, 1990.

12. Pelton, A. R., Rebelo, N., Duerig, T., Wick, A., Experimental and FEM Analysis of the Bending and Buckling Behavior of Superelastic Tubing. SMST Proceedings, 1994.

13. Petrakis, D., Characterization of Nitinol Material for a Bending Application. ICOMAT '92, pp. 1283- 1288, 1992.

14. Sachdeva, R., Oshida, Y., Farz-nia, F., Miyazaki, S., Load Deflection Characteristics of NiTi Orthodontic Archwires. ICOMAT '92, pp. 1223- 1227, 1992.

15. Wayman, C. M., Duerig, T. W., An Introduction to Martensite and Shape Memory. Engineering Aspects of Shape Memory Alloys. eds. Duerig, T. W., Melton, K. N., Stockel, D., Wayman, C. M., Butterworth-Heinemann, Boston, pp. 3- 26, 1990.

16. Chang, L.C., Read, T. A., Plastic Deformation and Diffusionless Phase Changes in Metals : The Gold-Cadmium Beta Phase. Trans AIME, 191: 47- 52, 1951.

17. Kauffman, G. S., Mayo, I. The Metal with a Memory. Invention and Technology, Fall: 18-25, 1993.

18. Andreasen, G. F., Hilleman, T. B., An Evaluation of 55 cobalt substituted nitinol wires for use in orthodontics. JADA, 821: 1373- 1375, 1971.

19. Andreasen, G., Laboratory and Clinical Analysis of Nitinol Wire. Am J Orthod, 73: 143-151, 1978.

20. Friend, C. M., Mechanism of shape memory. J de Physique IV, C4: 25, 1991.

21. Reed-Hill, R. E., Physical Metallurgy Principles, D. Van Nostrand Co., Cincinnati, pp. 611-657, 1973.

22. Otsuka, K., Sawamura, T., Shimizu, K., Wayman, C. M., Characteristics of the martensitic transformation in TiNi and the memory effect. Metall Trans, 2: 2583- 2588, 1971.

23. Duerig, T., Pelton, A., in press in Titanium Handbook, ASM, 1994.

24. Wayman, C. M., Some Applications of Shape-Memory Alloys. J Met, 32: 129- 137, 1980.

25. Fukanubo, H., Shape Memory Alloys. Gordon and Breach Science Publishers, New York, pp. 1- 114, 1984.

26. Suzuki, Y., On the Formation of Martensite. Mat Sci and Eng, A127: 239-241, 1990.

27. Van Humbeeck, J., Stalmans, R., Chandrasekaran, M., On the Stability of Shape Memory Alloys. Engineering Aspects of Shape Memory Alloys. eds. Duerig, T. W., Melton, K. N., Stockel, D., Wayman, C. M., Butterworth-Heinemann, Boston, pp. 96- 105, 1990.

28. Duerig, T. W., Zadno, G. R., An Engineer's Perspective of Pseudoelasticity. Engineering Aspects of Shape Memory Alloys. eds. Duerig, T. W., Melton, K. N., Stockel, D., Wayman, C. M., Butterworth-Heinemann, Boston, pp. 369- 393, 1990.

29. Jardine, A. P., Ashbee, K. H. G., Bassett, M. J., Effects of Cooling Rate on the Shape Memory Effect Thermodynamics of NiTi . J Mater Sci, 23: 4273- 4281, 1988.

30. Dautovich, D. P., Purdy, G. R., Canadian Met Quart, 4: 129, 1965.

31. Ling, H. C., Kaplow, R., Stress-Induced Shape Changes and Shape Memory in the R and Martensite Transformations in Equiatomic NiTi. Metall Trans A, 12A: 1981- 2111, 1981.

32. Wu, S. K., Wayman, C. M., On the Reciprocal Lattice of the "premartensitic" R-phase in TiNi Shape Memory Alloys. Acta Metall, 37: 2805- 2813, 1989.

33. Tietze, H., Müllner, M., Selgert, P., Assmus, W., The intermediate phase of the shape memory alloy NiTi. J Phys F : Met Phys, 15: 263- 271, 1985.

34. Tietze, H., Müllner, M., Selgert, P., Temperature induced precipitations in the memory alloy NiTi . J Phys D : Appl Phys, 17: 1391- 1398, 1984.

35. Miyazaki, S., Thermal and Stress Cycling Effects. Engineering Aspects of Shape Memory Alloys. eds. Duerig, T. W., Melton, K. N., Stockel, D., Wayman, C. M., Butterworth-Heinemann, Boston, pp. 394- 413, 1990.

36. Otsuka, K., Introduction to the R-Phase Transition. Engineering Aspects of Shape Memory Alloys. eds. Duerig, T. W., Melton, K. N., Stockel, D., Wayman, C. M., Butterworth-Heinemann, Boston, pp. 36- 45, 1990.

37. Leu, L., Fournelle, R., Brantley, W., Ehlert, T., Evidence of R Phase in Superelastic NiTi Orthodontic Wires. J Dent Res., Abs. # 1633, 1990.

38. Proft, J. L., Duerig, T. W., The Mechanical Aspects of Constrained Recovery. Engineering Aspects of Shape Memory Alloys. eds. Duerig, T. W., Melton, K. N., Stockel, D., Wayman, C. M., Butterworth-Heinemann, Boston, pp. 115- 129, 1990.

39. Metals Handbook, American Society for Metal, Metals Park, Ohio, vol. 1, 7, 8, 8th edition, 1973.

40. Suzuki, Y., Fabrication, Characterization, and Applications of the Shape Memory NiTi Alloys. Mater Res Soc, Otsuka and Shimizu, eds., 1989.

41. Suzuki, Y., Horikawa, Thermal Hysteresis in NiTi and NiTiX Alloys and their applications. MRS Proc., 246: 389- 391, 1992.

42. Saburi, T., Komatsu, T., Nenno, S., Watanabe, T. Electron Microscope Observation of the early stages of thermoelastic martensitic transformation in a TiNiCu Alloy. J of Less Common Metals, 118: 217- 226, 1986.

43. Wasilewski, R., The Effect of Applied Stress on the Martensite Transformation in TiNi. Met. Trans., 2A: 2973 - 2981, 1971.

44. Harrison, J. D., Measurable Changes Concomitant with the Shape Memory Effect Transformation. Engineering Aspects of Shape Memory Alloys. eds. Duerig, T. W., Melton, K. N., Stockel, D., Wayman, C. M., Butterworth-Heinemann, Boston, pp. 106- 111, 1990.

45. Cullity, B. D., Elements of X-ray Diffraction. Addison-Wesley Publishing, Menlo Park, CA, pp. 285- 318, 1978.

46. Dwight, A. E., CsCl - Type Equiatomic Phases in Binary Alloys of the Transition Elements. Trans. AIME., 215: 283- 286, 1959.

47. Otsuka, K., Miyazaki, S., Recent Advances in the Crystallography of Martensitic Transformation in Ti-Ni Alloys. Int. Symp. Shape Memory Alloys, pp. 73- 82, 1986.

48. Kudoh, Y., Tokonami, M., Miyazaki, S., Otsuka, K., Crystal Stucture of the Martensite in Ti - 49.2 at% Ni Analyzed by the Single Crystal X-Ray Diffraction Method. Acta Metall., 33: 2049- 2056, 1985.

49. Wayman, C. M., Phase Transformations in NiTi-Type Shape Memory Alloys. Shape Memory Alloys, Guilin, China, pp. 59- 72, 1986.

50. Thayer, T. A., X-Ray Diffraction of Nitinol Orthodontic archwires. Master's Thesis, Univ. Nebraska, 1993.

51. Stoeckel, D., Yu, W., Superelastic Ni-Ti Wires. Wire J Inter, March: 45- 50, 1991.

52. Marshall, G. W. An Introduction to Scanning Election Microscopy. UCSF Dept. of Restorative Materials, pp. 76- 99.

53. Burstone, C. J., Qin, Chinese Ni-Ti Wire - a new orthodontic alloy. Am J Orthod, 87: 445-452, 1985.

54. Lopez, I., Goldberg, A. J., Burstone, C. J., Bending Characteristics of Nitinol wire. Am J Orthod , 75: 569- 575, 1979.

55. Miura, F., Mogi, M., Ohura, Y., Hamanaka, H., The Superelastic Property of the Japanese NiTi Alloy for Use in Orthodontics. Am J Orthod, 90: 1- 10, 1986.

56. Mercier, O., Melton, K. N., Gottardt, R., Kulik, A., Proc. Int. Conf. on Solid-Solid Phase Transformations, pp. 1259- 1263, 1982.

57. Adler, P. H., Yu, W., Pelton, A. R., On the Tensile and Torsional Properties of Pseudoelastic NiTi. Scr. Metall. Mater., 24: 943- 947, 1990.

58. Otsuka, K., Sawamura, T., Shimizu, K., Crystal Structure and Internal Defects of Equiatomic TiNi. Phys. Status Solidi, 5(a): 457- 470, 1971.

59. Pelton, A., personal communication, 1994.

60. Miyazaki, S., Ohmi, Y., Suzuki, Y., Characteristic Deformation and Transformation Pseudoelasticity in Ti-Ni Alloys. J de Physique, C4: 255 - 260, 1982.

61. Khier, S., Brantley, W. A., Fournelle, R. A., Bending Properties of superelastic and nonsuperelastic nickel-titanium orthodontic wires. Am J Orthod, 99: 310- 318, 1988.

62. Khier, S., Structural Characterization, Biomechanical Properties and Potentiodynamic Polarization Behavior of NiTi Orthodontic Wire Alloys. Ph.D. Thesis, Marquette Univ., 1985.

63. Sachdeva, R., Oshida, Y., Mark, J., Fukuyo, S., Miyazaki, S., Thermal, Mechanical and Surface Characterization of Superelastic NiTi. J Dent Res. vol. 70, Abstract #1726, 1991.

64. Burstone, C. J., Deep Overbite Correction by Intrusion. Am J Orthod, 72:1-22, 1977.

65. Zadno, G. R., Duerig, T. W., Linear Superelasticity in Cold-worked NiTi. Engineering Aspects of Shape Memory Alloys. eds. Duerig, T. W., Melton, K. N., Stockel, D., Wayman, C. M., Butterworth-Heinemann, Boston, pp. 414- 419, 1990.

66. Sachdeva, R., Oshida, Y., Farz-nia, F., Miyazaki, S., Systematizing the Use of Ti-Ni Orthodontic Archwires. ICOMAT '92, pp. 1217- 1221, 1992.

67. Jean, R., Lai, H. J., Lin, J. J., Characterization of Ni-Ti Orthodontic Archwires. ICOMAT '92, pp. 1229- 1234, 1992.

68. Jialiang, J., Yi, Z., In Situ Investigation of Stress Induced Transformation in a Superelastic NiTi Alloy. Shape Memory Alloys, Guilin, China, pp. 103-108, 1986.

69. Onda, T., Bando, Y., Ohba, T., Otsuka, K., Electron Microscopy Study of Twins in Martensite in a Ti-50at% Ni Alloy. Mat Trans., JIM, 33: 354- 359, 1992.

70. Filip, P., Mazanec, K., Internally Slipped Martensite in TiNi alloys. Mat Sci Eng, A127: L19-L21, 1990.

71. Wayman, C. M., Martensitic Transformations, Encyclopedia of Materials Science and Engineering. Pergamon Press, Oxford, pp. 2736- 2740, 1986.

72. Nishida, M., Wayman, C. M., Electron Microscopy Studies of Precipitation Processes in Near-Equilibrium TiNi Shape Memory Alloys. Mat Sci Eng, 93: 191- 203, 1987.

73. Suzuki, Y., Tamura, H., Fatigue Properties of Ni-Ti Shape Memory Alloys. Engineering Aspects of Shape Memory Alloys. eds. Duerig, T. W., Melton, K. N., Stockel, D., Wayman, C. M., Butterworth-Heinemann, Boston, pp. 256- 266, 1990.

74. Miyazaki, S., Shiota, I., Otsuka, K., Tamura, H., Effects of Cu Addition on the Mechanical Behavior of Ti-Ni Alloys. MRS Int'l Mtg on Adv Mats, Mat Res Society, 9: 153- 158, 1989.

75. Edie, J. W., Andreasen, G. F., Zaytoun, M. P., Surface Corrosion of Nitinol and Stainless Steel under Clinical Conditions. Angle Orthod, 51: 319- 324, 1991.

76. Schwaninger, B., Sarkar, N. K., Foster, B. E., Effect of Long Term Immersion Corrosion on the Flexural Properties of Nitinol. Am J Orthod, 82: 45- 49, 1982.

For reference

Not to be taken from the room.

632928

3 1378 00632 9281